

Aus dem Institut für Pflanzenernährung und Bodenkunde
der Christian-Albrechts-Universität zu Kiel

Thermal properties in Luvisols under conventional and conservation tillage treatment

Dissertation

zur Erlangung des Doktorgrades

der Agrar- und Ernährungswissenschaften Fakultät

der Christian-Albrechts-Universität zu Kiel

vorgelegt von

Dipl. Ing. Umwelt. **Dorota Agnieszka Dec**

aus Leżajsk, Polen

Kiel, 2006

Dekan: Prof. Dr. Siegfried Wolfram

Erster Berichterstatter: Prof. Dr. Rainer Horn

Zweiter Berichterstatter: Prof. Rainer Duttmann

Tag der mündlichen Prüfung: 20. 07.2006

For my parents, Aneta, Grześ and Sylwia

Content

List of figures	VII
List of tables	XII
Symbols used	XV
1 Introduction	1
2 Literature overview.....	3
2.1 Soil temperature	3
2.2 Heat sources.....	3
2.3 Soil thermal properties.....	4
2.3.1 Heat capacity.....	4
2.3.1.1 Influence of water and air content.....	7
2.3.2 Heat transport in soil.....	8
2.3.2.1 Conduction of heat in soil	8
2.3.2.1.1 Influence of water content	10
2.3.2.1.2 Influence of bulk density and soil structure.....	11
2.3.2.1.3 Influence of temperature.....	13
2.3.2.1.4 Influence of organic substances	13
2.3.2.1.5 Methods for estimating thermal conductivity.....	14
2.3.2.1.5.1 De Vries model	14
2.3.2.1.5.2 Laplace transform	15

2.3.2.1.5.3	Numerical method	15
2.3.2.1.5.4	Statistical –physical model of thermal conductivity in soil	16
2.3.2.1.5.5	Line source method (laboratory method).....	18
2.3.2.1.5.6	Heat pulse method (laboratory method)	18
2.3.3	Thermal diffusivity	19
2.3.3.1	Influence of water content.....	20
2.3.3.2	Influence of bulk density.....	21
2.3.3.3	Estimation of the thermal diffusivity by the Damping Depth method	22
2.4	Thermal regime in soils	25
2.4.1	Sinusoidal character of the temperature development, diurnal and annual temperature variations in the soil.....	26
2.4.1.1	Damping Depth	30
2.4.1.2	Soil-temperature profile.....	31
2.5	Influence of hydraulic properties on thermal soil properties	32
3	Material and methods.....	33
3.1	General description of the experimental field	33
3.1.1	Location	33
3.1.2	Climate.....	33
3.2	Material description	34
3.3	Methods	36

3.3.1	Laboratory measurements.....	36
3.3.1.1	Collection of the soil samples	36
3.3.1.2	Texture determination of the sampled soils	37
3.3.1.3	Determination of organic matter and mineral substances....	38
3.3.1.4	Preparation of the homogenized soil samples	38
3.3.1.4.1	Determination of the Water Retention curve (WRC).....	38
3.3.1.4.2	Determination of the air conductivity	39
3.3.1.4.3	Saturated hydraulic conductivity	40
3.3.1.4.4	Shrinkage	40
3.3.1.5	Determination of the thermal soil properties	40
3.3.1.5.1	Temperature monitoring	41
3.3.1.5.2	Time Domain Reflectometry device.....	41
3.3.2	Field measurements	44
3.3.2.1	Temperature measurements	44
3.3.2.2	Simulation of water content	44
3.3.2.3	Statistical –physical model of thermal conductivity in soil....	47
3.3.2.4	Damping depth method	47
4	Results.....	48
4.1	Thermal properties.....	48
4.1.1	Laboratory measurements.....	48
4.1.1.1	Thermal properties of homogenized material	48

4.1.1.1.1	Soil temperature profiles	48
4.1.1.1.2	Temperature and water content development	49
4.1.1.1.3	Heat properties depending on bulk density	51
4.1.1.1.3.1	Thermal conductivity	51
4.1.1.1.3.2	Heat capacity	52
4.1.1.1.3.3	Thermal diffusivity	53
4.1.1.1.3.4	Thermal diffusivity calculated with the damping depth method	55
4.1.1.2	Undisturbed soil samples	57
4.1.1.2.1	Soil temperature profile	57
4.1.1.2.2	Thermal properties	58
4.1.1.2.2.1	Uncompacted plots	58
4.1.1.2.2.2	Compacted plots	59
4.1.1.2.2.3	Effect of water content on thermal properties of investigated soils.	61
4.1.1.2.2.4	Thermal diffusivity calculated with the damping depth method	66
4.1.2	Field data	69
4.1.2.1	Soil temperature and thermal properties	69
4.1.2.1.1	Calculations with the damping depth method	74
4.2	Hydraulic properties	78
4.2.1	Pore volume and pore size distribution	78

4.2.2	Hydraulic conductivity	79
4.2.2.1	Saturated hydraulic conductivity	79
4.2.2.2	Unsaturated hydraulic conductivity	79
4.2.2.3	Air conductivity measurements.....	80
4.2.2.3.1	Air conductivity	80
4.2.2.3.2	Relationship between air permeability and air-filled porosity	82
4.2.3	Shrinkage	85
4.2.3.1	Development of shrinkage curves	85
4.2.3.2	Shrinkage capacity	86
4.2.3.3	Effect of shrinkage on the volumetric water content	87
5	Discussion.....	89
5.1	Effect of aggregate formation on thermal properties.....	89
5.2	Effect of soil management on soil thermal properties	91
5.3	Effect of soil structure of water retention, hydraulic conductivity and rigidity as the basic for thermal properties	94
5.4	Critical ideas about the applied methods	97
5.4.1	Interpretation of data made by repacked soil samples.....	97
5.4.2	Determination of thermal diffusivity.....	98
6	Conclusions	100
7	Summary.....	102

8 Literature 110

Appendix

List of figures

Figure 2-1	Schema of the radiation balance in the atmosphere- lithosphere system. Radiation at the upper boundary atmosphere = 100. (according to Mason, 1976; cited by Scheffer&Schachtschabel, 2002).	4
Figure 2-2	Unidirectional stationary heat conduction in a homogenous medium. (after Usowicz, 1992).	9
Figure 2-3	Schematic construction of the heat transport mechanism in a three phase porous system. Diagram on the left side shows the microscopic temperature development along the transects A-B (figure on the right side). (after Bachmann et al., 1997).	10
Figure 2-4	Schematic constructions of the thermal conductivity model in soil, a) volumetric unit of soil, b) the system of spheres that form overlapping layers, c) parallel connection in the layers and serial between layers.	17
Figure 2-5	Variation of thermal diffusivity with soil water content, clay content and bulk density for mineral soils. (after Nofziger, 2002).	21
Figure 2-6	Graphical introduction of the damping depth calculation from the a) time shift and b) amplitude ratio.	24
Figure 2-7	Idealized daily fluctuation on surface soil temperature, according to the equation $T=T_{ave}+A_{0\sin}(\omega t/p)$. (after Hillel, 1998).	27
Figure 2-8	Relationship between depths and a) daily and b) annual temperature development. (after Hartge & Horn, 1999).	29
Figure 2-9	Soil-temperature profile showing seasonal variation in a frost free region. (after Hillel, 1998).	31
Figure 3-1	Average yearly temperature and rainfall in 2002, measured for Göttingen. (after www.wetterstation-goettingen.de/klimabericht).	34

Figure 3-2	Arrangement of the experimental field.	35
Figure 3-3	Schematic representation of the shrinkage measurement. (after Dörner, 2005).	40
Figure 3-4	Soil sample with TDR needles, pT 100 thermistors and a heating source.	41
Figure 3-5	Experimental setup: A) TDR device - first and second level multiplexer, delta logger, heat source; A,B)TDR needles, thermistors, and soil sample in PVC cylinder (c), isolation box (a,b) and sensors (d,e).	43
Figure 3-6	Schematic representation of defined boundary conditions for simulation of water content in soil.....	45
Figure 3-7	Rainfall and evapotranspiration (EVP) in 1995 for „Mulch“ from April to September for Göttingen.	46
Figure 4-1	Soil temperature profile from the daily temperature oscillation simulated for homogenized samples; a) first 6 hours correspond to warming phase and b) the next 19 hours to cooling phase. Sample prepared with $d_B = 1,2\text{g/cm}^3$	49
Figure 4-2	Temperature development of simulated daily oscillation for homogenized soil samples with a) $d_B = 1,2$ and b) $d_B = 1,6\text{g/cm}^3$	50
Figure 4-3	Changes in water content during simulation of daily oscillation of temperature for homogenized soil samples with a) $d_B = 1,2$ and b) $1,6\text{g/cm}^3$	50
Figure 4-4	Heat conductivity (λ) of homogenized samples calculated for a bulk density of $d_B = 1,2\text{g/cm}^3$ and measured at two depths: a) 2,5cm and b) 4,5cm.	51
Figure 4-5	Heat conductivity (λ) of homogenized samples calculated for a bulk density of $d_B = 1,6\text{g/cm}^3$ and measured at two depths: a) 2,5cm and b) 4,5cm.	52

Figure 4-6	Volumetric heat capacity (C_v) of homogenized samples calculated for a bulk density of $d_B = 1,2\text{g/cm}^3$ and measured at two depths: a) 2,5cm and b) 4,5cm.	53
Figure 4-7	Volumetric heat capacity (C_v) of homogenized samples calculated for a bulk density of $d_B = 1,6\text{g/cm}^3$ and measured at two depths: a) 2,5cm and b) 4,5cm.	53
Figure 4-8	Thermal diffusivity (D) of homogenized samples calculated for a bulk density of $d_B = 1,2\text{g/cm}^3$ and measured at two depths: a) 2,5cm and b) 4,5cm.	54
Figure 4-9	Thermal diffusivity (D) of homogenized samples calculated for a bulk density of $d_B = 1,6\text{g/cm}^3$ and measured at two depths: a) 2,5cm and b) 4,5cm	55
Figure 4-10	Thermal diffusivities calculated with damping depth method for homogenized soil samples prepared with bulk densities of $1,2\text{g/cm}^3$ and $1,6\text{g/cm}^3$	57
Figure 4-11	Soil temperature profiles from simulation of the daily temperature oscillation for samples taken from the uncompacted conventional tillage treatment; depth a) 0-30cm, b) 30-60cm. First six hours describe the warming phase and the next 21 the cooling phase.	58
Figure 4-12	a) Thermal conductivity (λ), b) volumetric heat capacity (C_v) and c) thermal diffusivity (D) as a function of water content (θ) for samples taken from 0-30cm depth.	62
Figure 4-13	a) Thermal conductivity (λ), b) volumetric heat capacity (C_v) and c) thermal diffusivity (D) as a function of water content (θ) for samples taken from 30-60cm depth.	63
Figure 4-14	Relationship between damping depths (d) calculated from the phase shift and the amplitude ratio for: a) uncompacted (M_{uc}, P_{uc}), c)	

compacted (Mc, Pc) plots from 0-30cm, and b) uncompacted, d) compacted plots from 30-60cm.....	67
Figure 4-15 Thermal diffusivity calculated with damping depth method for samples taken from Muc, Puc and depth of a) 0-30cm, b) 30-60cm.	68
Figure 4-16 Thermal diffusivity calculated with damping depth method for samples taken from Mc, Pc and depth of a) 0-30cm, b) 30-60cm.	69
Figure 4-17 Temperature at 5 and 15cm depth under „Mulch“ treatment from April to July 1995.	70
Figure 4-18 Water content development in the field from April to September 1995, for a) „Mulch“ (M) and b) „Plough“ (P) at depths of 5cm and 15cm.	71
Figure 4-19 Thermal conductivity calculated for the field data from April to September 1995; a) „Mulch“ (M) and b) „Plough“ (P).	73
Figure 4-20 Volumetric heat capacity calculated from the field data from April to September 1995; a) „Mulch“ (M) and b) „Plough“ (P).	73
Figure 4-21 Thermal diffusivity calculated from the field data from April to September 1995; a) „Mulch“ (M) and b) „Plough“ (P).	74
Figure 4-22 Correlation between damping depths (d) calculated from phase shift and amplitude ratio for „Mulch“ and „Plough“ in 1995 and 1997-2000.	75
Figure 4-23 Thermal diffusivity calculated with the damping depth method for „Mulch“ and „Plough“ in 1995 and 1997-2000.	76
Figure 4-24 Saturated hydraulic conductivity (k_f) for three bulk density (d_B) values (1,2-1,4-1,6g/cm ³) for „Mulch“ (M) and „Plough“ (P).	79
Figure 4-25 Simulated unsaturated hydraulic conductivity (k_u) for three bulk densities for a) „Plough“ (P); b) „Mulch“ (M).	80

-
- Figure 4-26 Air conductivity (k_i) for samples taken at different depths from „Mulch“ (M) and „Plough“ (P); k_i at a) -60hPa and b) -150hPa. Samples were collected from big cylinders (850 cm³) with an initial bulk density of 1,4 g/cm³. 81
- Figure 4-27 Air conductivity (k_i) measured at -500hPa. Samples taken at different depths from „Mulch“ (M) were collected from big cylinders (850 cm³) with an initial bulk density of 1,4 g/cm³. 81
- Figure 4-28 Air conductivity (k_i) of homogenized material depending on bulk density (d_B) and matric potential. 82
- Figure 4-29 Relationship between air permeability (k_a) and air-filled porosity (ϵ_a) depending on the bulk density for samples taken from „Plough“. 84
- Figure 4-30 Shrinkage curves for disturbed samples from a) „Plough“ (P) and b) „Mulch“ (M) for three bulk densities (d_{BI}) of 1,2; 1,4 and 1,6g/cm³. The error bars show the standard error (n=4). 86
- Figure 4-31 Shrinkage capacity for homogenized samples prepared from „Plough“ (P) and „Mulch“ (M) for three bulk densities (d_B): 1,2; 1,4; 1,6g/cm³. 87
- Figure 4-32 Effect of shrinkage on volumetric water content. a) „Plough“ (P) and b) „Mulch“ (M) at three bulk densities (1,2; 1,4; 1,6g/cm³). The dashed line represents the situation for a soil assumed as a rigid body. 88

List of tables

Table 2-1	Specific heat capacity (c) and heat conductivity (λ) of different soil components. ^{a)} Bolt et al., (1965) cited by Hartge and Horn (1999); ^{b)} Lang (1878) cited by Scheffer&Schachtschabel (2002).	7
Table 2-2	Differences in heat capacities in relation to the degree of saturation for two types of soil materials. (after Scheffer&Schachtschabel, 2002).	7
Table 3-1	Characterization of the Tschernosem-Parabraunerde (after Pälchen, 1996 or AG Boden, 1994).	34
Table 3-2	Sampled soil horizons, characteristic and number of used cylinders for determining properties as: thermal diffusivity (D), thermal conductivity (λ), heat capacity (C_v), shrinkage, water retention curve (WRC), saturated water conductivity (k_f) and air permeability (k_i) from the investigated tillage treatments.....	37
Table 3-3	Properties of the soil samples.	38
Table 4-1	Thermal diffusivity values calculated from the amplitude ratio and the phase shift damping depths. Calculations made for homogenized soil sample prepared with bulk density of $1,2\text{g/cm}^3$	56
Table 4-2	Thermal diffusivity values calculated from the amplitude ratio and the phase shift damping depths. Calculations made for homogenized soil sample prepared with bulk density of $1,6\text{g/cm}^3$	56
Table 4-3	Measured (T and θ) and calculated (λ , C_v , D) properties for uncompacted samples taken from „Mulch“ and „Plough“ and depths of 0-30cm and 30-60cm.	59

Table 4-4	Measured (T and θ) and calculated (λ , C_v , D) properties for compacted samples taken from „Mulch“ and „Plough“ and depths of 0-30cm and 30-60cm.	60
Table 4-5	Regression parameters ($y=ax+b$) of the relationship between volumetric water content and thermal conductivity in „Mulch“ (M) and „Plough“ (P) before (uc) and after (c) compaction. In addition homogenized samples with $d_B=1,2$ and $1,6\text{g/cm}^3$ were analysed.	64
Table 4-6	Regression parameters ($y=ax+b$) of the relationship between volumetric water content and heat capacity in „Mulch“ (M) and „Plough“ (P) before (uc) and after (c) compaction. In addition homogenized samples with $d_B=1,2$ and $1,6\text{g/cm}^3$ were analysed.	64
Table 4-7	Regression parameters ($y=ax+b$) of the relationship between volumetric water content and thermal diffusivity in „Mulch“ (M) and „Plough“ (P) before (uc) and after (c) compaction. In addition homogenized samples with $d_B=1,2$ and $1,6\text{g/cm}^3$ were analysed.	65
Table 4-8	Thermal conductivity (λ) and volumetric heat capacity (C_v) in „Mulch“ (M) and „Plough“ (P), plots before (uc) and after (c) compaction at 0-30cm depth (the cardinal letters mean the difference between uc and c plots, and small letters differences between treatments by significant level of $p<0,05$).	65
Table 4-9	Bulk density for „Mulch“ and „Plough“ calculated from the WRC of samples taken from 12-16cm (the cardinal letters mean the difference between uncompacted (uc) and compacted (c) plots, and small letters the differences between treatments by significant level of $p<0,05$) (data taken from Fazekas, 2005).	66
Table 4-10	Distribution of coarse pores for „Mulch“ and „Plough“ calculated from the WRC of samples taken from 12-16cm (the cardinal letters mean the difference between uncompacted (uc) and compacted (c) plots, the small letters	

define differences between treatments by significant level of $p < 0,05$) (data taken from Fazekas, 2005).....	66
Table 4-11 Maximal and minimal values of volumetric water content (θ), thermal conductivity (λ), volumetric heat capacity (C_v) and thermal diffusivity (D) calculated from field data (average daily values), measured for „Mulch“ and „Plough“ at 5 and 15cm during April- July 1995,1997-2000.	72
Table 4-12 Bulk density, total porosity (TP), water content at saturation (θ_s) and pore size distribution (PSD) determined from the water retention curve for “Mulch” (M) and “Plough” (P).....	78
Table 4-13 Regression parameters and coefficients for the relationship between air conductivity (k_i) and bulk density (d_B).	82
Table 4-14 K_1 -value (k_a/ε_a) determined at -60hPa for „Mulch“ and „Plough“.	83
Table 4-15 K_1 (k_a/ε_a) depending on bulk density and matric potential.....	83
Table 4-16 Regression parameters and blocked porosities (ε_b) depending on bulk density (d_B).	84

Appendix

Appendix A General minimum (T_{\min}) and maximum (T_{\max}) temperature, months with maximal temperature and amplitude in these periods (Ampl_{\max}), average temperature (T_{av}) in the remaining period and average amplitude (Ampl_{av}) in this time period. Presented values are for years 1995, 1997-2000; in months April- August. I

Appendix B Temperature at 5 and 15cm depth under „Mulch“ treatment from April to July 1995. II

Appendix C a) Thermal conductivity (λ), b) volumetric heat capacity (C_v) and c) thermal diffusivity (D) as a function of water content (θ) for samples prepared from homogenized material and bulk density 1,2g/cm III

Symbols used

Latin figures and literal

%	Percent
\varnothing	Diameter [cm]
a	gaseous phase [-]
A	cross-sectional area of the soil samples [cm ²]
A_{mpl}	temperature amplitude [°C]
$A_{\text{mpl}z_1/z_2}$	amplitude of the temperature wave at depths z_1 and z_2 [°C]
$A_{\text{mpl}0}$	amplitude of the soil surface temperature fluctuation [°C]
c	- specific heat capacity [J/gK]
C_v	volumetric heat capacity [J/cm ³ K]
°C	temperature unit (Celsius degree)
cm	length unit (centimeter)
cm ²	area unit (square centimeter)
cm ³	volume unit (cubic centimeter)
D	thermal diffusivity [m ² /s]
d	damping depth [cm]
d_B	bulk density [g/cm ³]
$d\theta$	relative water content difference [cm ³ /cm ³]
d.F.	density of solid phase [g/cm ³]
E_{plant}	plant transpiration [mm/d]
ET_o	grass reference transpiration [mm/d]
EVP	evapotranspiration [cm]
F	area of the soil sample [cm ²]

FLM	first level multiplexer
g	acceleration due to gravity [m/s^2]
g/cm^3	unit of bulk density
h_0	pressure height at the beginning of the measurement [cm]
h_1	1) pressure height at the end of the measurement [cm] 2) reference point for estimation of the soil shrinkage
h_2	height of the soil for estimation of the soil shrinkage [mm]
ha	Hectare
K	temperature unit (Kelvin degree)
K_1	continuity parameter [$\mu m^2 * 10^2$]
k_c	population coefficient [-]
k_a	air permeability [μm^2]
k_f	saturated hydraulic conductivity [cm/s]
k_l	air conductivity [cm/s]
k_u	unsaturated hydraulic conductivity [cm/s]
L	length [cm] specific transpiration heat [$(J/cm^2)/mm$]
l	distance of the flow length [mm]
M	„Mulch“
Mc	„Mulch“ compacted (wheeled)
Muc	„Mulch“ uncompacted (unwheeled)
m	mineral matter [-]
mm	length unit (millimetre), or rainfall amount
n	1) van Genuchten parameter [-] 2) replication [-]

o	organic matter [-]
U	relative air humidity [%]
P	period of one harmonic oscillation [sec] „Plough“
P _c	„Plough“ compacted (wheeled)
P _{uc}	„Plough“ uncompacted (unwheeled)
PSD	pore size distribution [%]
q _h	heat flux density [J/cm ² s]
s	solid phase [-]
SLM	second level multiplexer
T	temperature [°]
t	time [sec]
TDR	Time Domain Reflectometry
w	liquid phase [-]
WRC	water retention curve
- oS	without shrinkage correction
- mS	with shrinkage correction
pF	logarithm of the water suction in hPa
x	vertical distance [cm]
z	investigated depth [cm]
∫	volume fraction of component

Greek literal

α	van Genuchten parameter [-]
ε_a	air filled porosity [cm^3/cm^3]
ε_b	blocked porosities [%vol]
θ	volumetric water content [cm^3/cm^3]
θ_R	residual water content [cm^3/cm^3]
θ_s	volumetric water content at saturation [cm^3/cm^3]
θ_{rs}	θ of rigid soil [cm^3/cm^3]
π	Pi
ρ	particle density [g/cm^3]
ρ_i	air pressure [kg/m^3]
λ	thermal conductivity [W/mK]
γ	constant of the psychrometer [hPa/K]
φ_0	phase constant
Φ	phase shift of the temperature wave [sec]
$\omega t_1; \omega t_2$	radial frequencies at times t_1 and t_2 [sec]
Ψ_m	water tension (matric potential) [hPa]

1 Introduction

Soil temperature varies with time and space, as well as with land use systems and gas emissions and affects also the global change. Thermal properties are of main importance for the determination of rates and directions of soil physical, chemical and biological processes as well as for energy and mass exchange with the atmosphere. Temperature governs also evaporation, aeration, and biological processes, such as the uptake of nutrients and water by roots, the decomposition of organic matter by microbes, the germination of seeds and seedling emergence. Thus, growth strongly depends on the temperature regime.

Soil temperature shows a pronounced fluctuation with time and soil depth. These changes are propagated into the soil profile depending on the heat capacity, thermal diffusivity and heat conductivity, the rates, however, are affected by soil properties varying in time and space. Hence the quantitative formulation and prediction of the soil thermal regime can be an important issue. Tillage has a strong influence on soil temperature. Ploughing changes the structure of the upper part of the soil and makes its structure looser and less continuous than the deeper parts. The more complete rigid soil aggregates become rearranged the greater remains the macroporosity, but this is not equivalent with the heat transfer in soils. If the new pores are air filled the heat conductivity, volumetric heat capacity and according to these factors the thermal diffusivity decrease. In this sense also the soil hydraulic properties depend on soil compaction, as a result of tillage treatment and should be linked to soil thermal properties. Investigations from last few years showed that as a consequence of subsoil compaction the emission of nitrous oxide, a strong greenhouse gas, increases. Despite the fact that its evaluation is not completely recognised, it was found that it ranges from 1 to 50 kg N per hectare annually. It has been found that it depends on soil oxygen status but also on physical parameters such as soil temperature (Hillel, 1998; Zawadzki et al., 1999).

Regarding the facts mentioned above, the aim of this work was to:

- assess how far soil management systems (conventional and conservation) and compaction can influence the soil thermal regime and thermal properties (thermal conductivity, heat capacity and thermal diffusivity)
- compare the soil thermal properties of undisturbed and disturbed soil samples prepared by different bulk densities and determined by two different methods (damping depth and statistical-physical model)
- determine the effect of bulk density on soil shrinkage and pore functioning (k_f , k_u , k_l) relating them to soil thermal properties.

2 Literature overview

2.1 Soil temperature

Physical, chemical, and biological processes which occur in soils are influenced by soil temperature. Biological processes such as the uptake of nutrients and water by roots, the decomposition of organic matter by microbes and the germination of seeds are strongly affected by soil temperature. The rate of some processes increases by more than double for each 10°C increase in temperature. Physical processes such as water movement and soil drying can also be strongly influenced by temperature (Hillel, 1998; Kowalik, 2004).

The soil temperature fluctuations with depth are propagated into the soil profile and depend on the heat capacity, the thermal diffusivity and the heat conductance. Therefore the determination of these properties can be an important issue. Beyond theoretical prediction, the possibility of optimizing the thermal regime requires basic knowledge of the processes and the environmental and soil parameters determining their rates. The soil parameters, which allow information about the soil thermal regime, include the specific heat capacity, thermal conductivity, and thermal diffusivity. These parameters are strongly affected by the bulk density and water content. Internal sources and sinks of heat also play an important role in the soil thermal regime (Campbell, 1985; de Vries, 1996; Bachmann et al., 1997).

2.2 Heat sources

The sun's radiation is the primary source of heat coming into the soil. The heat circulation constitutes a closed circuit i.e.: the radiation coming from the sun and finally returns to the atmosphere. Figure 2-1 shows the radiation balance and their percentage proportions (Scheffer&Schachtschabel, 2002).

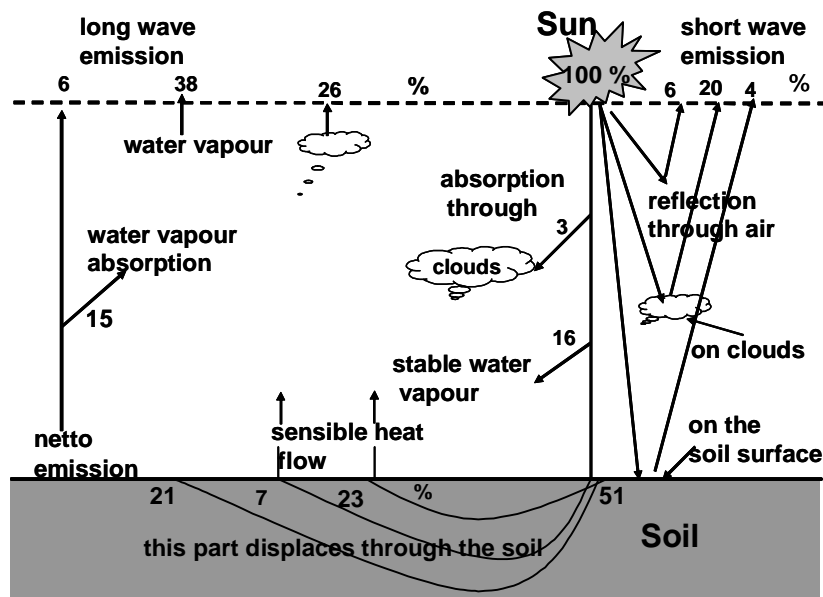


Figure 2-1 Schema of the radiation balance in the atmosphere- lithosphere system. Radiation at the upper boundary atmosphere = 100. (according to Mason, 1976; cited by Scheffer&Schachtschabel, 2002).

2.3 Soil thermal properties

The main soil thermal properties are heat capacity, thermal conductivity and thermal diffusivity. These properties govern the thermal state of the soil, their ability and the rate of warming, cooling and storage of heat.

2.3.1 Heat capacity

Heat capacity is the property of a body to store heat during warming of that body and it is equal to the ratio between the heat adsorbed through the body and the increment of temperature. It is defined as the amount of the heat needed to raise the temperature of a unit of a substance by one degree (°C or K) (Hillel, 1998; Kowalik, 1999). If the heat capacity is related to a specific soil volume it is denoted as C_v [$\text{J}/\text{cm}^3\text{K}$] and defined as the product of the particular density (ρ) and the specific heat (c) per unit mass:

$$C_v = c \cdot \rho$$

Equation 2-1

Soils are three phase systems composed of a solid (mineral and organic constituents), liquid and gaseous phase. Each component has its own specific heat capacity. Therefore, the value of volumetric heat capacity C_v can be estimated by summing up the heat capacities of the soil components, weighed according to their volume fractions (Keith, 1991; de Vries, 1996; Hillel, 1998), as follows:

$$C_v = \sum_i s_i C_{s_i} + \sum_w C_w + \sum_a C_a \quad \text{Equation 2-2}$$

where:

- \sum_i = volume fraction of each phase: solid (s), liquid (w) and air (a)
- i = number of solid components (minerals and organic matter)
- C_v = volumetric heat capacity [$\text{J}/\text{cm}^3\text{K}$]
- s = solid phase
- w = liquid phase
- a = gaseous phase

Specific heat capacities of individual soil phases are calculated as the product of the particular density and the specific heat capacity:

$$C_s = c_s \cdot \rho_s \quad \text{Equation 2-3}$$

$$C_w = c_w \cdot \rho_w$$

$$C_a = c_a \cdot \rho_a$$

where:

- $C_{s,w,a}$ = specific heat capacity of each phase: solid (s), water (w) and air(a) [$\text{J}/\text{cm}^3\text{K}$]
- $c_{s,w,a}$ = specific heat of each phase: solid (s), water (w) and air(a) [J/gK]
- $\rho_{s,w,a}$ = particular density of each phase: solid (s), water (w) and air(a) [g/cm^3]

Table 2-1 informs about some thermal properties of different soil constituents. Most of the soil minerals have nearly the same values of density and heat capacity. Since it is difficult to separate the different components of the soil

organic matter they are gathered into a single constituent (with an average density of $1,3\text{g/cm}^3$ or $1,3\text{Mg/m}^3$ and an average heat capacity of $2,5 \cdot 10^6 \text{J/m}^3\text{K}$) (Hillel, 1998). The specific heat capacity of the air phase is smaller than the capacities of the liquid and solid phase. Therefore, the contribution of the specific heat capacity of the gaseous phase of the soil can generally be neglected (Bachmann et al., 1997; Hillel, 1998; Kowalik, 1999; Peth, 2004).

Thus, equation 2-2 can be simplified as follows:

$$C_v = \int m C_m + \int o C_o + \int w C_w \quad \text{Equation 2-4}$$

where:

m = mineral matter
o = organic matter
w = water

In moist soils the heat capacity depends on the volumetric water content (θ), the content of mineral (m) and organic (o) matter and the bulk density (d_B) (Hanks and Ashcroft, 1980). Therefore, the equation 2-4 can be also written as follows:

$$C_v = d_B \cdot c_s + \theta \cdot c_f = d_B \cdot c_s + 4,19 \cdot \theta \quad \text{Equation 2-5}$$

where the value of 4,19 corresponds to specific heat capacity of water (Table 2-1). If we consider the values of specific heat capacities for mineral and organic matter, shown in Table 2-1, we can write:

$$C_v = 1,94 \cdot \int m + 2,51 \cdot \int o + 4,19 \cdot \int w \quad \text{Equation 2-6}$$

Table 2-1 Specific heat capacity (c) and heat conductivity (λ) of different soil components. ^{a)}Bolt et al., (1965) cited by Hartge and Horn (1999); ^{b)}Lang (1878) cited by Scheffer&Schachtschabel (2002).

Soil components	Specific heat capacity c	Thermal conductivity λ
	[J/gK]	[J/cmsK]
air	$1,3 \cdot 10^{-3}$ ^{a)}	$2,5 \cdot 10^{-4}$ ^{a)}
water	4,19 ^{b)}	$5,7 \cdot 10^{-3}$ ^{a)}
ice	1,88 (0°C) ^{b)}	$2,2 \cdot 10^{-2}$ ^{a)}
quartz	2,13 ^{b)}	$8,8 \cdot 10^{-2}$ ^{a)}
clay	2,1 ^{a)}	$2,9 \cdot 10^{-2}$ ^{a)}
humus	2,34 ^{b)}	$2,5 \cdot 10^{-3}$ ^{a)}

2.3.1.1 Influence of water and air content

Thermal behaviour of soil is strongly influenced by changes in water content. Differences in heat capacities, related to changes in water content, for mineral soil (2% organic matter) and peat soil (60% organic matter) are summarized in Table 2-2.

Table 2-2 Differences in heat capacities in relation to the degree of saturation for two types of soil materials. (after Scheffer&Schachtschabel, 2002).

Material	Water content θ	Volumetric heat capacity C_v
	[cm ³ /cm ³]	[J/cm ³ K]
quartz	0	1,26 – 1,67
	0,2	1,67 – 2,5
	0,4	2,5 – 3,3
peat	0	0,08 – 0,42
	0,4	1,67 – 2,1
	0,8	3,35 – 3,77

If peat soils dry out, the volumetric heat capacity decreases despite of the relative high capacity value of the organic matter due to the low amount of solid fraction (80% porosity). On the other hand, undrained peat has the highest values for the heat capacity. From this relationship the low temperatures of the

soils lying close to air layers can be explained through the undrained peat or the corresponding water surfaces. Some changes in the water content, due to drainage, influence not only the air- and water balance, but also the heat balance of the soil (Bachmann et al., 1997). Soil-loosening and/or compaction influence the volume fraction of the phases (air, water and solid) and the orientation of the solid particles and enclosed voids of the soil. Consequently, the volumetric heat capacity with a corresponding interface to the atmosphere or free water is affected as well. Equation 2-4 shows that the heat capacity increases linearly with increasing water content (de Vries, 1996; Hartge and Horn, 1999; Ochsner et al., 2001).

During freezing two factors influence the volumetric heat capacity: the volumetric fraction of the water and the values of volumetric heat capacity for water and ice. Due to the phase-change of the water, from fluid to solid phase, the value of heat capacity is reduced from 4,19 MJ/m³K to 1,88 MJ/m³K (below 0°C) while the volumetric fraction of the water increases at about 9%.

2.3.2 Heat transport in soil

2.3.2.1 Conduction of heat in soil

Conduction, defined as the ability of the soil to conduct the heat, is the primary mechanism of the heat movement in the soil. Fourier (1822) described this process with the following equation (Fourier's law):

$$q_h = -\lambda \frac{dT}{dx} \quad \text{Equation 2-7}$$

where:

q_h	=	heat flux density [J/cm ² s]
λ	=	thermal conductivity [W/mK]
T	=	temperature [K]
x	=	vertical distance [cm]

Equation 2-7 applies to the heat flow in the vertical direction (Figure 2-2) but it is easily generalized to three dimensions by adding conductivities and temperature gradients in the x, y and z directions. The negative sign defines the direction of the heat transport as opposite to the temperature gradient i.e.: heat flows from regions of higher potential (higher temperature) to regions of lower potential (lower temperature).

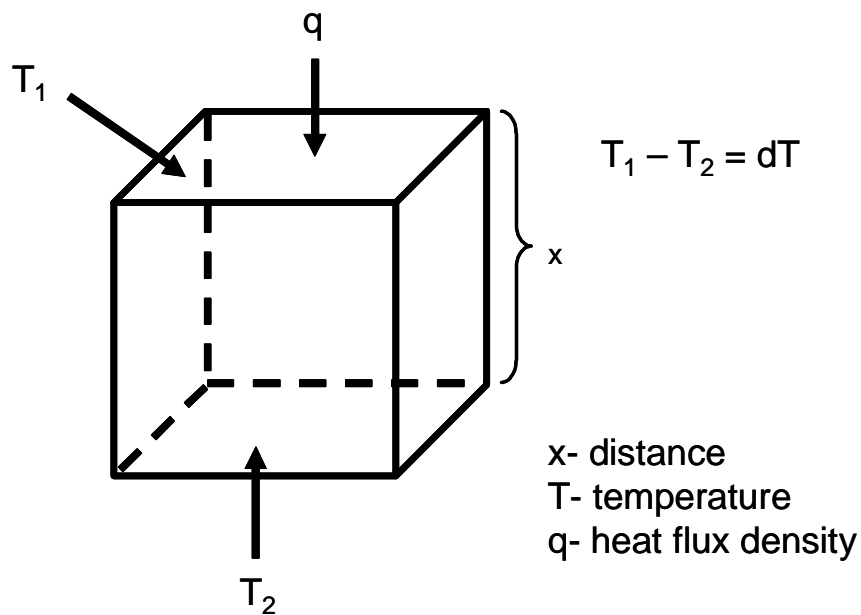


Figure 2-2 Unidirectional stationary heat conduction in a homogenous medium. (after Usowicz, 1992).

Factors, affecting thermal conductivity, are the same as those that affect the volumetric heat capacity, but their relative effects vary. Therefore, the variation in λ is greater than that of C_v . Thus, the thermal conductivity can not be related to soil components in a similar manner as it is possible for the heat capacity. The reason is that the elements transmitting the heat in the soil are arranged to each other parallel and in series. The total thermal conductivity arises from the spatial arrangement of the particles and grains of the solid phase, which have a high conductivity and can be connected by a less conductive liquid or gaseous phase (about 0,02 W/mK) (Kowalik, 1999).

2.3.2.1.1 Influence of water content

The permeability coefficients of soils are smaller than those of minerals and other solid materials because of the limited areas of the contact points in a granular soil matrix. For an air dried soil the air filled pore space acts as an insulator, due to its low thermal conductivity and results in very pronounced temperature gradients. Water at field capacity form a circular meniscus around the contact points of the mineral soil particles, whereby the heat energy can be transferred from grain to grain through the water bridges (De Vries, 1996) and therefore results in a greater heat flow (Figure 2-3). Especially the formation of the menisci results in an increase of thermal conductivity which can even exceed 100 percent in sand with a high content of quartz (Bachmann et al., 1997; Scheffer&Schachtschabel, 2002). The higher the water content, the lower is the increase of the conducting cross-section with a unit of water because the menisci have larger radii, and impede the thermal conductivity (Hanks and Ashcroft, 1980; Hartge and Horn, 1999).

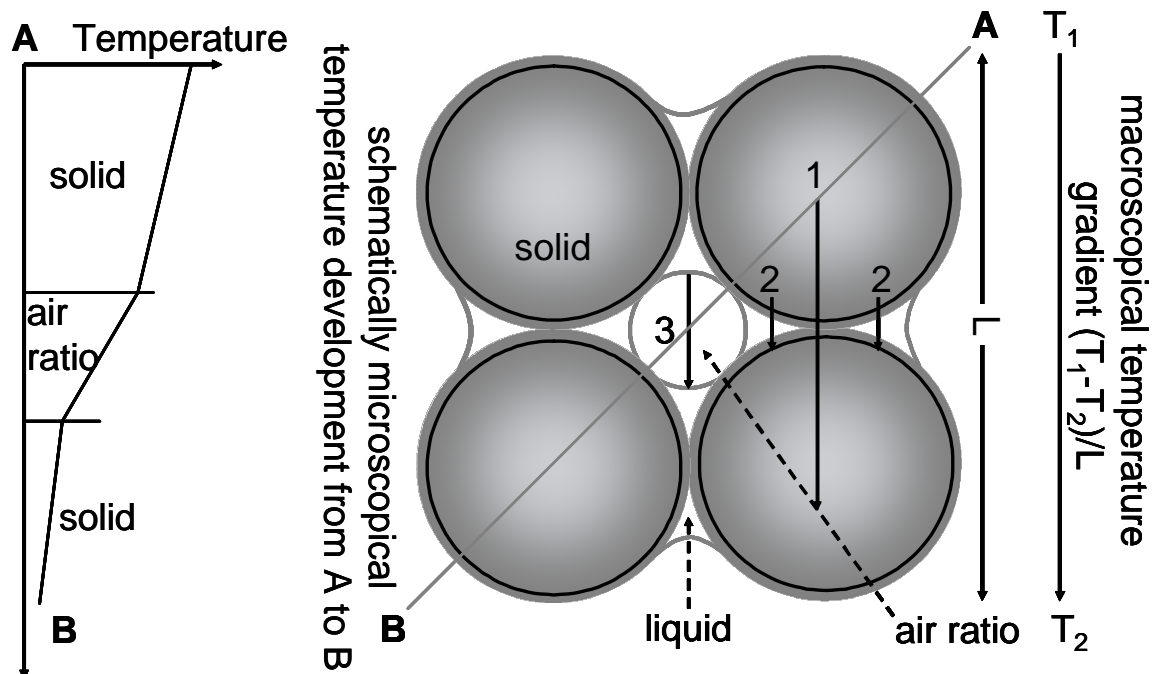


Figure 2-3 Schematic construction of the heat transport mechanism in a three phase porous system. Diagram on the left side shows the microscopic temperature development along the transects A-B (figure on the right side). (after Bachmann et al., 1997).

From the above described dependencies, it can be concluded that the thermal conductivity depends strongly on the geometrical arrangement of particles, water and air as well as on soil structure and water content.

The influence of soil structure and with it the spatial arrangement of water in between is so strong, that the changes in thermal conductivity depend upon the soil moisture-tension rather than on the water content (Schulte in Walde et al., 1976). Abu-Hamdeh and Redder (2000) investigated two soil types (sandy and clay loam) in a wide temperature range. They found out, that the water content has no effect on permeability by sorption and by desorption of the samples (samples prepared with the same water content).

Horton et al., (2001) determined the influence of water repellency on thermal soil properties. In these investigations the thermal conductivity, presented as a function of the saturation degree, was described as a fitted polynomial second-order curve. They found out that the thermal conductivity is higher in wettable than in water-repellent soils and these differences became larger with increasing degree of saturation. Thus, with increasing hydrophobicity the heat transport in unsaturated soils through the water menisci decreases with decreasing amount of water, which is located in the edges between the contact points of the solid phase. Involved in this process might be the formation of macroscopic liquid domains in hydrophobic media and, correspondingly, the formation of relatively dry areas, which may reduce the heat conduction.

2.3.2.1.2 Influence of bulk density and soil structure

Thermal properties are generally related to soil structure. With increasing bulk density (d_B) increases the amount and the number of the grain contacts in between well conducting minerals per unit volume while the air volume, with low thermal conductivity and heat capacity decreases. This circumstance results in an increase in thermal conductivity, which, however, as a rule is not linear and depends on the inflection of the curve ($\lambda = f(d_B)$), the gravimetric water content and its arrangement in the pore space. In sandy soils the thermal conductivity

increase progressively with increasing density while in fine textured soils this increase is much smaller (Bachmann et al., 1997). Generally, the differences in soil texture caused by the specific combinations of density and water content tend to intensify thermal conductivity with increasing soil density. Nidal et al., (2000) investigated four soils and calculated that sandy soils have a higher thermal conductivity compared to clayey and loamy soils at all investigated densities and water contents. This increase, in sand and sandy loam soil was also rapid and varies with density increment. In clay and clay loam soil this increase was rapid with the first increase in bulk density, however, a further increase in bulk density caused only a slight increase in thermal conductivity.

Beside the bulk density, the soil structure and composition also influences the thermal conductivity (Anandakumar et al., 2001). In undisturbed soils this property was greater than in disturbed soils, apparently due to the different distribution and geometry of water menisci (Arshad and Azzoz, 1996). Soil aggregates play also an important role in the heat conduction in the soil. Hadas (1997) presents a decrease in thermal conductivity with increasing diameter of the aggregates because the number of overall contact points between aggregates decreases with increasing diameter. This thermal property is also influenced by roughness, arrangement and shape of the aggregates (i.e.: packages from the angular aggregates have higher thermal conductivity as round aggregates) (Hadas, 1997). Investigations about thermal properties of aggregates (made by Kaune et al., in 1993) result in a high thermal conductivity in aggregated silty loam soil than in a corresponding soil with lower degree of aggregation. This effect was caused by a more intense transport of latent heat. In addition Kaune et al., (1993) pointed out that in the first 10cm depth of a silty soil about 51% of the heat transfer occurs through vapour flow. However, the influence of soil structure on soil thermal properties is not well understood and requires further investigations.

2.3.2.1.3 Influence of temperature

In partly saturated soils at water contents identical to those at the permanent wilting point (relative air humidity equals 100%) the temperature differences cause variable local water vapour density in the pore space. Consequently, the equilibrium movements caused the condensation at cold and evaporation at warm fluid-gaseous interfaces (Bachmann et al., 1997). This process overlaps with the heat conduction which occurred in granular structure and the fluid phase. The energy transport in form of the latent heat takes place from higher to lower temperatures, while during the condensation of the water vapour at the cold ends of the transport distance, a heat amount of $2,5 \cdot 10^6$ J/kg of condensed water vapour (at 0°C) will be released.

2.3.2.1.4 Influence of organic substances

In comparison to other soil components organic matter has a very low thermal conductivity ($2,2 \cdot 10^{-2}$ J/cmsK) if compared e.g.: to quartz ($8,8 \cdot 10^{-2}$ J/cmsK) (Table 2-1). In natural soils, the organic matter content within the soil profile varies insignificantly (about 1%) with time and is in relative equilibrium with the climate, amount and type of produced biomass as well as with the level of biological activity occurring in the soil (Wierenga, 1968; Abu-Hamdeh et al., 2000). The quartz content, however, is mostly constant with depth and therefore changes in thermal conductivity with soil depth are caused primarily by variations in soil water content and porosity (Wierenga, 1968). Furthermore, changes in soil matter components ought to be included. Bachmann et al., (1997) postulated that the creation of organic matter widely influences thermal storage in soils. Investigations about the influence of organic matter on soil thermal properties were carried out by Abu-Hamdeh et al., (2000). They showed that the thermal conductivity decreases with increasing content of organic matter. Literature regarding this field of research is rare because, as mentioned above, the organic matter content in the soil is relatively stable and varies only very slightly.

2.3.2.1.5 Methods for estimating thermal conductivity

2.3.2.1.5.1 De Vries model

The de Vries model (de Vries, 1996) is based on the application to a granular medium of potential theory. This model considers the soil as a granular material, which consists of two substances (continuous medium: water for moist and air for dry soil) with defined volume fraction (x_0) and thermal conductivity (λ_0) in which granules with defined volume fraction ($x_1= 1-x_0$) and thermal conductivity (λ_1) are dispersed. The thermal conductivity of such system is calculated as the weighed average of the conductivities of the various components as follows:

$$\lambda = \frac{\sum_{i=1}^n k_i \lambda_i x_i}{\sum_{i=1}^n k_i x_i} \quad \text{Equation 2-8}$$

where:

- n = number of components [-]
- λ_i = thermal conductivity of each components [W/mK]
- x_i = volume fraction of each components [-]

Volumes of k_i are calculated from:

$$k_i = \frac{1}{3} \sum_{i=1}^n \left[1 + \left(\frac{\lambda_i}{\lambda_0} - 1 \right) g_i \right]^{-1} \quad \text{Equation 2-9}$$

where:

- g_i = shape factors for i -th components granules considered as ellipsoids

2.3.2.1.5.2 Laplace transform

The Laplace transform method is based on the numerical integration of the Laplace transformation of the heat conduction equation in soil. This method assumes the relationship describing the surface soil temperature as a boundary condition (Hadas, 1968; Asrar and Kenemasu 1983; Usowicz, 2001) and is defined by following equation:

$$\frac{d^2 L[T(z,t)]}{dt} = \frac{s}{\alpha} L[T(z,t)] = 0 \quad \text{Equation 2-10}$$

where the Laplace transformation is given by (equation 2-11):

$$L[T(z,t)] = \int_0^{\infty} T(z,t) \exp(-st) dt \quad \text{Equation 2-11}$$

with:

$s \geq 5.0 / t_{\max}$ = Laplace transformation parameter [-]

t_{\max} = maximum duration of the measurement [sec]

The transformation is used to determine the thermal diffusivity (D) of the material, while the volumetric heat capacity (C_v) is measured or calculated using equation 2-6. Thus, the thermal conductivity is determined from the relation between the thermal diffusivity and the heat capacity as shows equation 2-12:

$$\lambda = D \cdot C_v \quad \text{Equation 2-12}$$

2.3.2.1.5.3 Numerical method

This numerical method (Wierenga et al., 1969; Hanks et al., 1971; Hanks, 1980; Sikora and Kossowski, 1993) is based on the solution of one dimensional heat conduction equation (equation 2-13) in finite-difference form:

$$\frac{T_{i,j} - T_{i,j-1}}{\Delta T} = D \frac{T_{i-1,j-1} - 2T_{i,j-1} + T_{i+1,j-1}}{(\Delta z)^2} \quad \text{Equation 2-13}$$

where:

T	=	soil temperature [°C]
i, j	=	indices of depth z [cm]
t	=	time [sec]
D	=	thermal diffusivity [cm ² /s]

2.3.2.1.5.4 Statistical –physical model of thermal conductivity in soil

To determine soil thermal properties the statistical-physical model compiled by Usowicz (1991, 1992 and 2002) was used. This model is based on terms of the heat resistance (Ohm's and Fourier's laws), both laws of Kirchhoff, and the polynomial distribution (equation 2-15). With this model the heat capacity, thermal conductivity and thermal diffusivity can be calculated. In this model the volumetric unit of the soil consists of solid particles, water and air and is treated as a system made up of the elementary geometric figures (in this case spheres) which form overlapping layers (Figure 2-4 b). Connections between layers of the spheres and the layer between neighboring spheres are represented by the serial and parallel connections of thermal resistors, respectively (Figure 2-4 c). The average value of the thermal conductivity (equation 2-14) is estimated by comparison of resultant resistance of the system, with consideration of all possible configurations of particle connections together with a mean thermal resistance of a given soil volume unit (Usowicz, 1992, 2000). The thermal capacity and diffusivity were calculated with empirical formulas given in chapter 2.3.1 and 2.3.2.

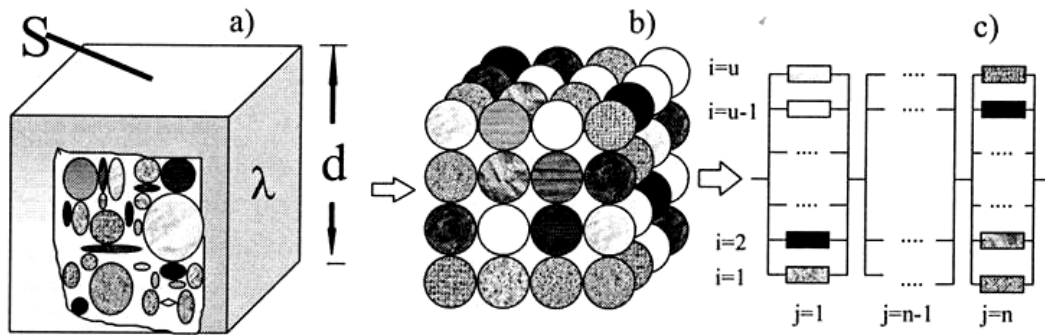


Figure 2-4 Schematic constructions of the thermal conductivity model in soil, a) volumetric unit of soil, b) the system of spheres that form overlapping layers, c) parallel connection in the layers and serial between layers.

$$\lambda = \frac{4\pi}{u \sum_{j=1}^L \frac{P(x_1, \dots, x_{kj})}{x_1 \lambda_1(T) r_1 + \dots + x_{kj} \lambda_k(T) r_k}} \quad \text{Equation 2-14}$$

where:

u = number of parallel connections of soil particles treated as thermal resistors

L = number of all possible combinations of particle configuration

x_1, x_2, \dots, x_k = number of particles of individual particles of a soil with thermal conductivity $\lambda_1, \lambda_2, \dots, \lambda_k$

$\lambda_1, \lambda_2, \dots, \lambda_k$ = thermal conductivities of the soil individual particles [W/mK]

r_1, r_2, \dots, r_k = particle radii

$P(x_{ij})$ = probability of occurrence of a given soil particle configuration

$$\sum_{i=1}^k x_{ii} = u, \quad j = 1, 2, \dots, L$$

Probability of occurrence is calculated from the polynomial distribution:

$$P(x_1, \dots, x_{k,j}) = \frac{u!}{x_{1,j}! \dots x_{k,j}!} \int_1^{x_{1,j}} \dots \int_k^{x_{k,j}} \quad \text{Equation 2-15}$$

The condition: $\sum_{j=1}^L P(X = x_j) = 1$ must also be fulfilled. The probability of

selecting a given soil particle f_i , $i = s, c, g$, in a single trial was determined

based on fundamental physical soil properties. In this case f_s , f_c and f_g are the contents of individual materials and organic matter – $f_s = 1 - \phi$, liquid - $f_c = \theta$ and air - $f_g = \phi - \theta$ in a unit of volume, ϕ – soil porosity (Usovicz, 2001).

2.3.2.1.5.5 Line source method (laboratory method)

The line heat source is a thin heating wire, which constitutes a heating element and a thermocouple. When the probe is inserted into the soil, a known amount of energy is supplied to the probe during a short time interval. Increase in the soil temperature caused by applying current is measured with the thermocouple in the probe and then the thermal conductivity (λ) can be expressed as a function of the temperature change with time (Jaeger and Sass, 1964) (equation 2-16):

$$\lambda = \frac{I^2 R \ln t_2 / t_1}{4\pi(T_2 - T_1)} \quad \text{Equation 2-16}$$

where:

- I = current of the heater probe [amp]
- R = resistance of the heater probe [ohms/cm]
- t = time [sec]
- T = temperature of the probe [°C]

Finally, the value of thermal conductivity in this method is calculated from relation between $\ln t$ and T and equation 2-16 (Janse and Borel, 1965; Wierenga et al., 1969; Bachmann, 1997).

2.3.2.1.5.6 Heat pulse method (laboratory method)

This method is based on the application of a heat pulse to a line source and the analysis of the temperature response at the line source or at some distance from the line source (Wierenga et al., 1969; Campbell et al., 1991; Keith et al., 1993; Bristow et al., 1994; Bachmann et al., 1997). The line source consists of a heat probe of finite length, which contains an electrical heater, and a

thermocouple located at the centre of the probe. Heat is generated in the probe by applying a constant energy through the heating wire for some specified time period. The heat pulse device consists of three needle probes mounted parallel to provide a heater, sensor and reference probe.

2.3.3 Thermal diffusivity

The experimental determination of the thermal conductivity is difficult, therefore this property is often calculated with the aid of temperature differences as a function of time (t) and depths ($z_1; z_2$) with distance, Δz . Written as a partial differential equation, the time-dependent change of the heat amount ($C_v \cdot dT/dt$) in a defined volume element corresponds to the sum of the heat flow $q_h(z)$ in and out of the volume element through the border, which is described by the following equation 2-17:

$$C_v \frac{dT}{dt} = \frac{d}{dz} q_h = -\lambda \frac{d^2 T}{dz^2} \quad \text{Equation 2-17}$$

transformation results in:

$$\frac{dT}{dt} = \frac{\lambda}{C_v} \frac{d^2 T}{dz^2} = D \frac{d^2 T}{dz^2} \quad \text{Equation 2-18}$$

where D denotes the thermal diffusivity and can be defined as follows:

$$D = \frac{\lambda}{C_v} \quad \text{Equation 2-19}$$

Equation 2-18 can be also applied to the penetration of frost into soil or to the attenuation of heat under a very hot soil surface (Bohne, 2005). Equation 2-19 shows that the thermal diffusivity is the ratio of the thermal conductivity to the heat capacity.

Thermal diffusivity defines the ability of the soil to equalize the temperature in all locations (depth, distance) (Usowicz, 2002) and therefore determines the rate of

heating or cooling accompanying a given temperature of the profile (Arshad and Azzoz, 1996).

2.3.3.1 Influence of water content

Similar to the heat capacity and thermal conductivity, thermal diffusivity also depends on the water content which, among other factors, has the greatest influence on that property (Arshad, 1996; Tyson, 2001; Usowicz, 2005). Thermal conductivity and volumetric heat capacity (λ and C_v) increase with increasing water content. When a dry soil will be saturated the thermal conductivity increases more intensely than does the heat capacity. After exceeding some characteristic values of water content, this phenomenon is inverted (Arshad and Azooz, 1996; Hartge and Horn, 1999; Scheffer and Schachtschabel, 2002). In moist soils the heat capacity increases linear with increasing water content, while a further increase of the water content results in a reduced increase of thermal conductivity. Thus, the thermal diffusivity after reaching some maximum value (volumetric water content between 8-20%) (Arshad and Azooz, 1996), starts to decrease gradually (Potter et al., 1985) (Figure 2-5) with continuously increasing water content (Bachmann et al., 1997; Hillel, 1998; Nofziger, 2002; Usowicz, 2002, 2005). Thermal diffusivity at a water tension of -1000hPa (1 bar) reaches their maximum value between $1 \cdot 10^{-3}$ and $7 \cdot 10^{-3} \text{cm}^2/\text{s}$ (Kohnke, 1968). Mineral soils show maximum diffusivity at relatively low (16-18vol%) water contents (Fuhrer, 2000). Wierenga et al., (1969) investigated the thermal diffusivity for non-irrigated and irrigated plots. They observed that in non-irrigated plots, the variation in thermal diffusivity with depth was more marked. Irrigation caused uniform water distribution in the soil and thus minor thermal diffusivity variations.

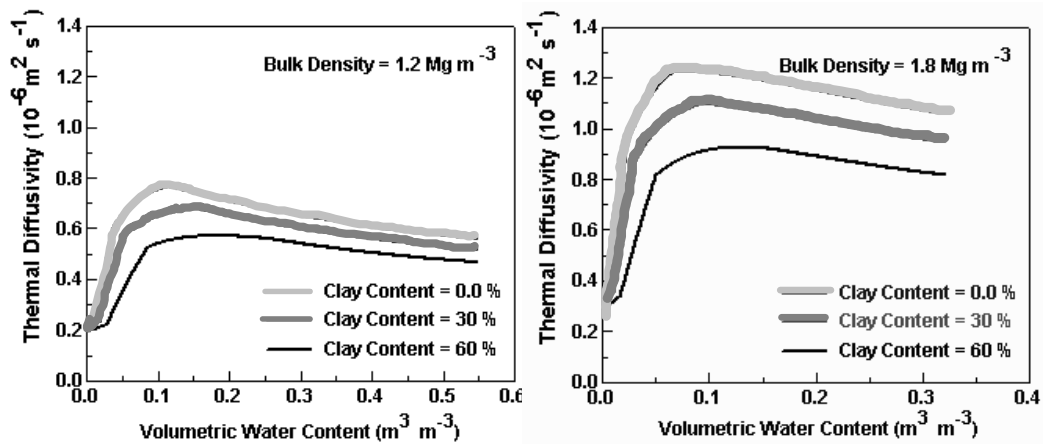


Figure 2-5 Variation of thermal diffusivity with soil water content, clay content and bulk density for mineral soils. (after Nofziger, 2002).

2.3.3.2 Influence of bulk density

Generally, thermal diffusivity increases with increasing bulk density. However, this relationship is weaker than that with water content (Figure 2-5). Tyson, (2001) investigated four soil types and pointed out that the thermal diffusivity increases with increasing bulk density with the exception of the driest samples of the silt loam soil. Hay et al., (1978) observed higher thermal diffusivity in a direct-drilled barley field than in a plowed field during the growing season. These effects were explained by the higher bulk density and stone content in the direct-drilled plots and by the differences in moisture content between these treatments. In contrast, investigations made by Arshad and Azooz (1996) show greater D in conventional than in no-tillage treatment. This phenomenon was related to the greater volumetric heat capacity, relative to the thermal conductivity (Johnsons et al., 1985; Anandakumar et al., 2001) of the wetter no-tillage treatments (higher loosening of soil in conventional tillage increases surface roughness and potential evaporation) (Allmaras et al., 1972), as well as to the increasing aggregate stability, organic matter and water storage capacity under no-tillage treatment.

2.3.3.3 Estimation of the thermal diffusivity by the Damping Depth method

The main assumption of this method is the harmonic development of the temperature changes during daily or yearly cycles. If this condition is fulfilled the damping depth (d) (described in chapter 2.4.1.1) can be calculated from the phase shift and the amplitude ratio of the temperature wave (Chacko and Renuka, 2002). Temperature measurements in at least two depths (Wierenga et al., 1969; Elimoel et al., 2004; Peth, 2004) are needed. The harmonic development of the daily changed temperature profiles occurs by some short-time temperature variations. This method can be applied if the days are sunny and clear (Wierenga et al., 1982) and when the temperature maximum or other arbitrary characteristic values of the temperature wave reaches depth z_1 in the time t_1 (equation 2-20) and depth z_2 in time t_2 (equation 2-21) :

$$\omega t_1 + \varphi_0 - \frac{z_1}{d} = \frac{\pi}{2} \quad \text{Equation 2-20}$$

$$\omega t_2 + \varphi_0 - \frac{z_2}{d} = \frac{\pi}{2} \quad \text{Equation 2-21}$$

where:

$t_1; t_2$ = times at which the wave reach the max value at depths z_1 and z_2
[sec]

$\omega t_1; \omega t_2$ = radial frequencies at times t_1 and t_2

φ_0 = phase constant; $\varphi_0 = -\omega t_0$

$z_1; z_2$ = investigated depths [cm]

d = damping depth [cm]

$$\rightarrow \omega t_1 + \varphi_0 - \frac{z_1}{d} = \omega t_2 + \varphi_0 - \frac{z_2}{d} \quad \text{Equation 2-22}$$

Transformation of equation 2-22 results in following equation 2-23:

$$d = \frac{1}{\omega} \cdot \frac{(z_1 - z_2)}{(t_1 - t_2)} = \frac{P}{2\pi} \cdot \frac{(z_1 - z_2)}{(t_1 - t_2)} \quad \text{Equation 2-23}$$

where:

P = period of one harmonic oscillation [sec]

The damping depth can be estimated graphically as the dependence between investigated depths and the time in which the temperature wave reaches their maximum temperature (T) (Figure 2-6). The raising of the received line multiplied by the reciprocal value of the oscillation frequency $1/\omega$ yields the damping depth from the phase shift (Figure 2-6a). The calculation of the damping depth from the amplitude ratio method is similar, however, in the phase shift, instead of time, the natural logarithm of the amplitudes is plotted versus the investigated depths (Figure 2-6b). Damping depth can be read directly from the slope of the line. This method is described by the following equation 2-24:

$$d_{\text{amplitude}} = \frac{(z_1 - z_2)}{\ln|A_{\text{mpl}z_1}| - \ln|A_{\text{mpl}z_2}|} = \frac{(z_1 - z_2)}{\ln \left| \frac{A_{\text{mpl}z_1}}{A_{\text{mpl}z_2}} \right|} \quad \text{Equation 2-24}$$

where:

$A_{\text{mpl}z_1}$; $A_{\text{mpl}z_2}$ = amplitude of the temperature wave at depths z_1 and z_2 [°C]

Generally it is assumed that the daily average amplitude is constant with time. Under in situ conditions, however, this value is not constant and therefore in the equation 2-24 this value is taken as an annual average of the daily amplitude (Elimoel, 2004).

If the changes in soil water content with depth are considerable, or when the temperature wave shows no periodic behaviour, the sinusoidal function (equations 2-23 and 2-24) can not be used (Wierenga et al., 1968; Chacko, 2002).

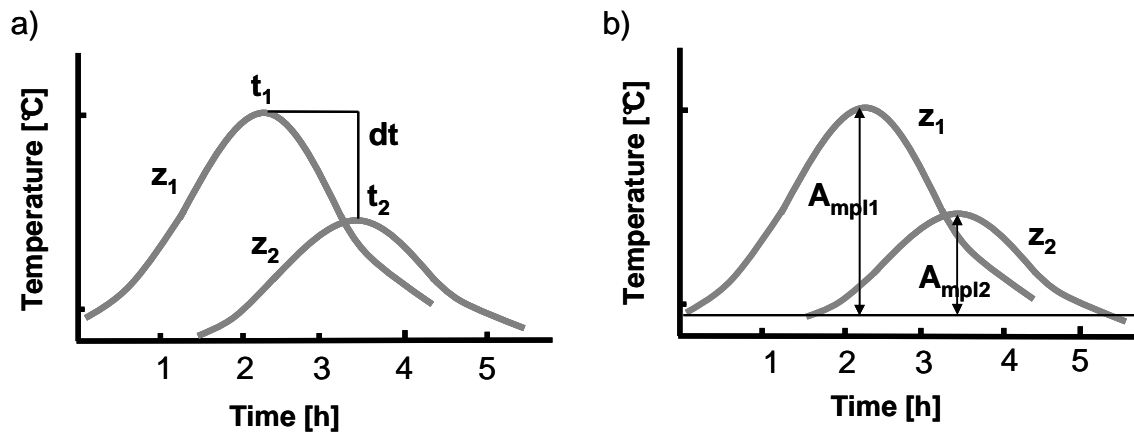


Figure 2-6 Graphical introduction of the damping depth calculation from the a) time shift and b) amplitude ratio.

If the values of the damping depths estimated from the phase shift and amplitude ratio method are similar, the thermal diffusivity can be calculated from the transformed equation (2-23) as follows:

$$D = \left(\frac{\pi}{P} \right) d^2 \quad \text{Equation 2-25}$$

where d is the average value estimated from amplitude and phase shift damping depth. If the values of the damping depths are very different the application of this equation is not allowed.

If the soil is assumed as a homogenous body, the thermal diffusivity can be calculated from field data (for different depths) by using already defined equations. Under natural conditions, thermal properties vary within the soil profile caused by different water content conditions and soil-layering. Derivation of the analytical equation for a two or more layered soil was presented by van Wijk and Derksen (1996). For a two layered soil profile these equations are defined as:

$$T_1 = T_A + A_1 e^{-z/d_1} \cdot \sin\left(\omega t - \frac{z}{d_1} + \phi_1\right) + A_2 e^{-z/d_2} \cdot \sin\left(\omega t + \frac{z}{d_2} + \phi_2\right) \quad \text{Equation 2-26}$$

for the upper layer $0 \leq z \leq b$, and

$$T_2 = T_A + A_d e^{-(z-b)/d_2} \cdot \sin\left(\omega t - \frac{(z-b)}{d_2} + \varphi_2\right) \quad \text{Equation 2-27}$$

for the lower layer $z \leq b$

where:

$A_1; A_1''$ = amplitudes of both temperature waves of the upper border ($z=0$) [°C]

A_d = amplitude of the upper border of the lower layer ($z=d$) [°C]

φ = phase constant of the respective layer (1/2 - upper/lower layer)

d = damping depth of the respective layer (1/2 - upper/lower layer) [cm]

For the smooth transfer at the layer border from these equations the same heat flows have to be calculated. The amplitudes and phase constants execute these conditions and are calculated from the damping depths of the thickness of the upper layer and the amplitude and phase constants of the temperature variations on the soil surface (Peth, 2004).

2.4 Thermal regime in soils

Variations in soil temperature are the consequences of meteorological changes acting on the soil-plant-atmosphere interface, caused by the regular and periodic succession of days and nights and of summers and winters. These cycles can be disturbed by the irregular processes happening in the atmosphere. Also the geographical location, soil management, vegetative cover or their lack, soil properties, depth and meteorological changes (especially changes related to water content (Bohne, 2005)) influence the thermal regime of the soil (de Vries, 1996; Campbell, 1998; Hillel, 1998; Hartge and Horn, 1999; Kowalik, 1999; Zawadzki et al., 1999).

2.4.1 Sinusoidal character of the temperature development, diurnal and annual temperature variations in the soil

The mathematical description of the natural fluctuation of the thermal regime includes the temperature changes at the soil surface e.g.: as a consequence of heating during the day and cooling during the night. The temperature development can be defined as a variable in time in accordance with the harmonic sinusoidal function around an average value (Figure 2-7) (Kluitenberg and Horton, 2000; Kowalik, 1999). In nature the temperature development varies differently at each soil depth (Hasan and Zinke, 1964; Hillel, 1998). In the mathematical description, however, the average temperature is considered to be the same for all depths. If at time $t=0$ the surface is at the average temperature, it can be described by the following equation:

$$T(0;t) = T_{ave} + A_0 \sin \omega t \quad \text{Equation 2-28}$$

where:

- $T(0,t)$ = temperature at depth $z=0$ (soil surface) as a function of time t [°C]
- T_{ave} = average temperature of the soil surface [°C]
- A_0 = amplitude of the soil surface temperature fluctuation (range from T_{max} or T_{min} to the T_{ave}) [°C]
- ω = radial frequency (2π times the actual frequency. In diurnal variation, the period is $24h = 86,400$ sec, so $\omega = 7,27 \cdot 10^{-5}/\text{sec}$)

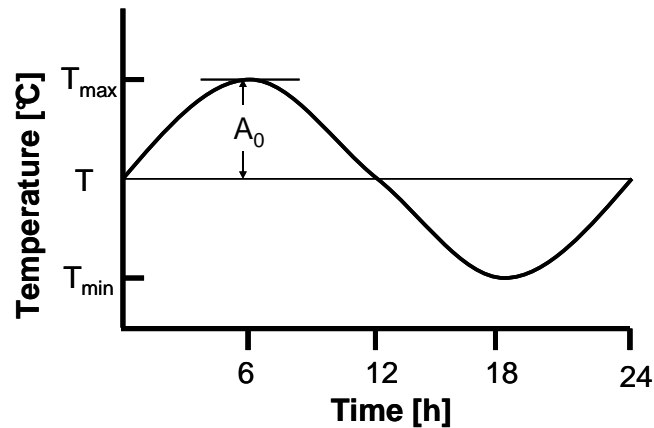


Figure 2-7 Idealized daily fluctuation on surface soil temperature, according to the equation $T=T_{ave}+A_0\sin(\omega t/p)$. (after Hillel, 1998).

Equation 2-28 is valid for the boundary conditions $z=0$. Van Wijk (1996) defined conditions for other depths ($z=\infty$), where temperature is constant and equal to T_{ave} , through the equation:

$$T(z;t) = T_{ave} + A_z \sin[\omega t + \Phi(z)] \quad \text{Equation 2-29}$$

where:

$T(z;t)$ = temperature at depth z as a function of time t [°C]

T_{ave} = average temperature of the soil profile [°C]

A_z = temperature amplitude at depth z [°C]

T_{ave} = average temperature of the surface (as well as of the profile) [°C]

ω = radial frequency ($\omega= 7,27 \cdot 10^{-5}/\text{sec}$)

Φ = phase shift of the temperature wave [sec]

The resultant effect of the changes in inflow of energy to the regular surface, running of the energy and mass exchange processes at that surface, as well as the flow and accumulation of heat in the soil profile are represented by the changes of the soil temperature with time and depth. The soil temperature changes are characterized by the natural periodicity in diurnal and annual cycles, as a response to the radiation or heat flux, which are reaching the soil (Zawadzki et al., 1999).

In conditions of the free inflow of sun radiation to the soil surface and by the right proportion of days and nights the pattern of the temperature development on the soil surface depicts a sinusoidal character. In principle, the highest temperatures and temperature fluctuations are observed in the first centimetres at the soil surface. The amplitude of the temperature fluctuations become smaller with increasing depth (Hasan and Zinke, 1964) and finally disappear at some depth. The depth, at which the amplitude of the temperature fluctuations decreases to the fraction of $1/e$ ($e = 2,718$) of the amplitude on the soil surface (A_0), is called the damping depth (precise description is presented in chapter 2.4.1.1 (see also Kluitenberg and Horton, 1990; Hillel, 1998; Bachmann et al., 1997).

Temperature variations present daily, weekly, monthly and annual cycles. These cycles present different amplitudes and frequencies as shown in Figure 2-8 a, b. Some long-term investigations demonstrated that the daily soil fluctuations of the temperature in the soil disappear after some centimetres whereas the annual fluctuations attain the level of the meter scale. Daily cycles are more influenced by the changes in atmospheric conditions than annual cycles – even in short periods e.g.: clouds cause the decrease of temperature in the top soil layer. The longer the period of these changes persists the deeper is the penetration of the temperature wave (Bachmann et al., 1997).

Besides the decrease of the daily fluctuations with increasing depth, a daily shift of the temperature changes in relation to the soil surface temperature also occurs. This phenomenon can be observed at the time when the extreme temperature appears at particular depths. The maximum temperatures at the soil surface appear mostly 1-2 hours after midday, whereas in the lower part of the tilled horizon (depth 20-25 cm) it is appropriate 5-6 hours delayed (Zawadzki et al., 1999). Similar delays are also observed for the minimal daily temperatures. Near to the soil surface they occur in the early morning and later with increasing soil depth. The consequence of the differences in the daily developments of the soil temperature at the individual depths is the differentiation and equalization of their value in the soil profile. This

phenomenon appears twice during a twenty-four hour period and alternately, the differentiation of the temperature (before the midday and during the night) and the equalization (in the morning and in the evening). The magnitude of the vertical temperature differentiation at the soil surface (topsoil) without the plant cover can reach few degrees in the afternoon during sunny summer days.

The annual temperature development (Figure 2-8) shows similar character with the diurnal cycle i.e.: periodicity of changes, decrease of the fluctuations of the amplitude with depth, variability and equalization of the temperature in the soil profile. These characteristics of the temperature development in soils are influenced by the thermal properties related to the type of the soil, moisture conditions, human management and also the presence and kind of plant shields. Nevertheless, the daily development depends on the climate conditions during the day of investigations and the season of the year, while the annual development depends on the prevailing climate in the examined area (Zawadzki et al., 1999).

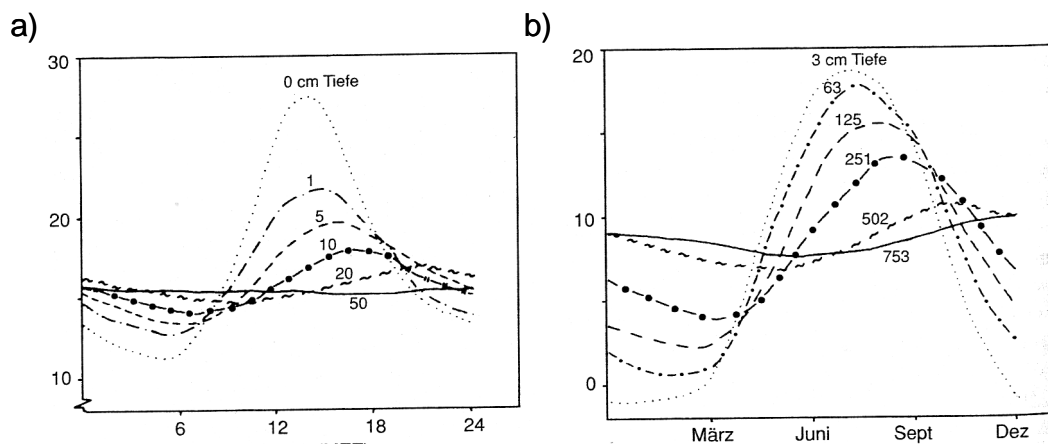


Figure 2-8 Relationship between depths and a) daily and b) annual temperature development. (after Hartge & Horn, 1999).

2.4.1.1 Damping Depth

The depth at which the amplitude decreases to the fraction of $1/e$ of the amplitude on the soil surface (A_0) is called the damping depth, whereby $e = 2,718$ ($1/2,718 = 0,37$) is the base of the natural logarithms.

Damping depth (d) can be described with the following equation:

$$d = \sqrt{\frac{D \cdot P}{\pi}} \quad \text{Equation 2-30}$$

where:

D = thermal diffusivity [cm^2/sec]

P = period of the harmonic oscillation [sec]

The physical reason for the damping of the temperature waves with depth is the heat absorption or release along the path of heat propagation, when the temperature of the conducting soil increases or decreases, respectively. The damping depth depends on the specific heat conductance for a defined soil type, their actual physical state (Zawadzki et al., 1999) and also on the period of the temperature fluctuations (Hillel, 1998). Bachmann et al., (1997) and Hillel (1998) said that the annual temperature fluctuations are transferred into the soil even with $(365)^{1/2}$ i.e.: the damping depth is 19 times larger than the diurnal high-frequent wave, also for the soil with the same values of thermal properties. Campbell (1985) measured this value for a mineral soil and observed diurnal damping depths of 10-15cm and annual of 2-3m. Van Wijk and de Vries (1996) pointed out the damping depth for a soil with $D = 5,23 \cdot 10^{-3} [\text{cm}^2/\text{s}]$ and obtained $d = 12\text{cm}$ for the diurnal temperature fluctuation and $d = 2,29\text{m}$ for the annual fluctuation. These investigations show that the temperature at around 30cm depth remains almost constant over a diurnal cycle and the temperature at a depth of 5-6m remains almost constant over an annual cycle. The typical penetration depths of the temperature wave are measurable down to $z = 3d$. According to Bachmann et al., (1997) the daily fluctuation can be about 0,5m, while the annual one is more than 10m.

2.4.1.2 Soil-temperature profile

If the heat state is not the same in the whole soil profile, temperature changes occur and induce heat movement. This state is normal for soils because the isothermal state is an exception (Hartge and Horn, 1999). The heat flux during daily temperature cycles can assume two directions. During the day it flows from the warm soil surface to their deeper layers and results in positive values. At night it assumes the opposite direction, when the soil surface, as a consequence of the coolness, has a lower temperature than the lower parts, which results in negative values (Figure 2-9). Zawadzki et al., (1999) stated that the change of the heat flux direction at the soil surface takes place in the morning (mostly 2-3 hours after sunrise) and in the evening. With respect to the time remained to transmit the heat resulting in warming or cooling the following depths, the two- directional flow of the heat can take place (in late morning hours, in the evening and at the beginning of the night). The highest temporary values (positive and negative) and the greatest heat fluctuations are therefore observed close to the soil surface (Zawadzki et al., 1999; Hillel, 1998; De Vries, 1996; Kowalik, 1999).

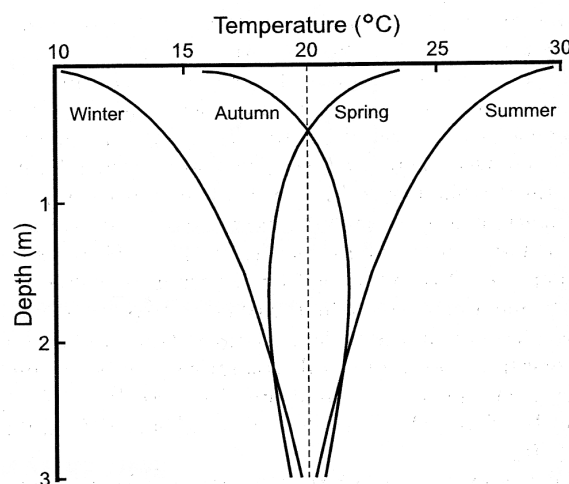


Figure 2-9 Soil-temperature profile showing seasonal variation in a frost free region. (after Hillel, 1998).

2.5 Influence of hydraulic properties on thermal soil properties

Soil water regime influences the soil thermal properties (Hasan et al., 1964; de Vries, 1996; Ochsner et al., 2001). Therefore, the measurement of hydraulic properties describing the behaviour of the water in a three-phase soil system is needed to better understand the thermal processes in soils. Under saturated conditions soils are good heat conductors, because water transmits heat well (Lang et al., 1878; Bachmann et al., 1997; Hillel, 1998; Scheffer&Schachtschabel, 2002). With increasing dehydration (amount of the air filled pores increases), the process of heat conduction is retarded.

Many authors reported the influence of bulk density on hydraulic (Richard et al., 2001; Dexter, 2004) soil properties. Horn and Baumgartl (1999), Hartge & Horn, (1999) reported that with d_B increase the amount of contact points between particles increase heat capacity, as well as in the consequence also the thermal conductivity and thermal diffusivity (Hopmans and Dane, 1986; Nidal et al., 2000). Thus also soil compaction influences the soil thermal regime.

Pore size distribution as well as the continuity of the porous system decides about the ability of soils to lead water/air and, consequently heat. Other authors such as Ehlers (1973), Parker (1982), Ahuja et al., (1998) and Hartge & Horn (1999) said that decrease in the volume of macropores and in the continuity of the pores can therefore cause bad growth conditions for plants.

3 Material and methods

3.1 General description of the experimental field

3.1.1 Location

The research field is located in Harste / Niedersachsen; about 8km north of Göttingen where the Institute of Sugar Beet Research (IFZ) carries out long-term experiments on the effects of tillage on crop yield. This field has been analysed since 1991 for experiments and started in 1992 with two tillage treatments – conservation and conventional. The experimental field is situated 150m above N.N. in a slightly undulating area.

3.1.2 Climate

Göttingen is situated at the transition from the maritime to the continental climate. The climate in Göttingen in winter is temperately cold and in summer temperately warm. The average yearly temperature is about 8,8°C and the amplitude reaches 17,4°C. The warmest month is July (average temperature ≈17,1°C) while the coldest is January (average temperature ≈0,3°C). The yearly rainfall amounts to about 602mm. Figure 3-1 shows the annual pattern of temperature and rainfalls in 2002, measured for Göttingen. June (81,3mm) and February (39,1mm) are the wettest and the driest months, respectively. The relative air humidity is about 77,3% and the air pressure reaches 1015,9hPa. The maximum duration of sunshine is 4464 hours.

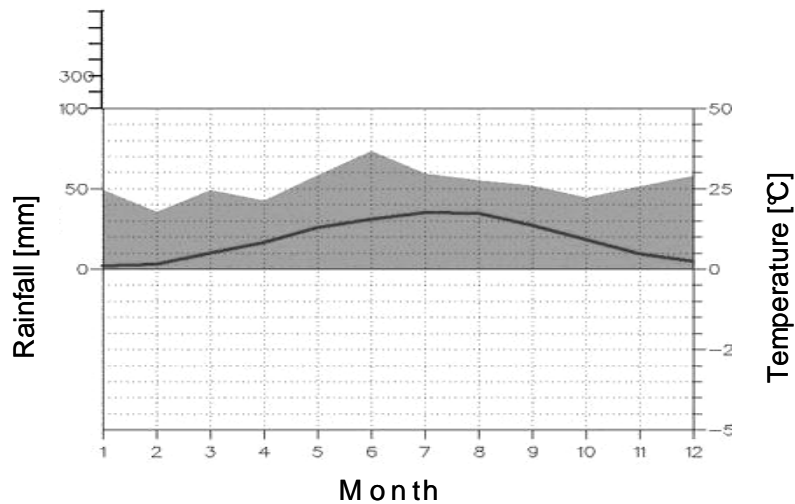


Figure 3-1 Average yearly temperature and rainfall in 2002, measured for Göttingen. (after www.wetterstation-goettingen.de/klimabericht).

3.2 Material description

The soil type is a Tschernosem-Parabraunerde derived from loess. Some physical properties of the soil profile are shown in Table 3-1. There are changes in the soil texture which are the consequence of the clay eluviation from the higher (A_{xh}-A_l) to the lower (A_{xh}-B_t) parts of the soil profile. The humus content decreases with increasing depth.

Table 3-1 Characterization of the Tschernosem-Parabraunerde (after Pälchen, 1996 or AG Boden, 1994).

Depth [cm]	0 - 30	30 - 50	50 - 60
Horizon	A _{xp}	A _{xh} - A _l	A _{xh} - (B _t)
Soil texture	Ut ₃	Ut _{3/4}	Ut ₄
Humus	h ₃	h ₂	h ₁
Structure	crumb/polyhedral	platy	platy/polyhedral

The experimental field is divided into 3 parts. In each segment of the experimental field a culture rotation was conducted as follows: sugar beet,

winter wheat and winter barley. Each segment of the experimental field has 4 replications (Figure 3-2). The whole field is about 4,5ha large, 100m wide and 450m long. A part of each replication is divided into two tillage treatments. The tillage treatment in fixed parcels varied between conservation (later denoted as „Mulch“) and conventional treatment (later denoted as „Plough“). „Mulch“ defines the treatment when the soil is loosened with a field cultivator to a depth of 8-10cm, while „Plough“ means ploughing to 30cm. Before 1992 the whole field was ploughed down to 30cm depth. Therefore, until today there is a hard plough pan on the whole field.

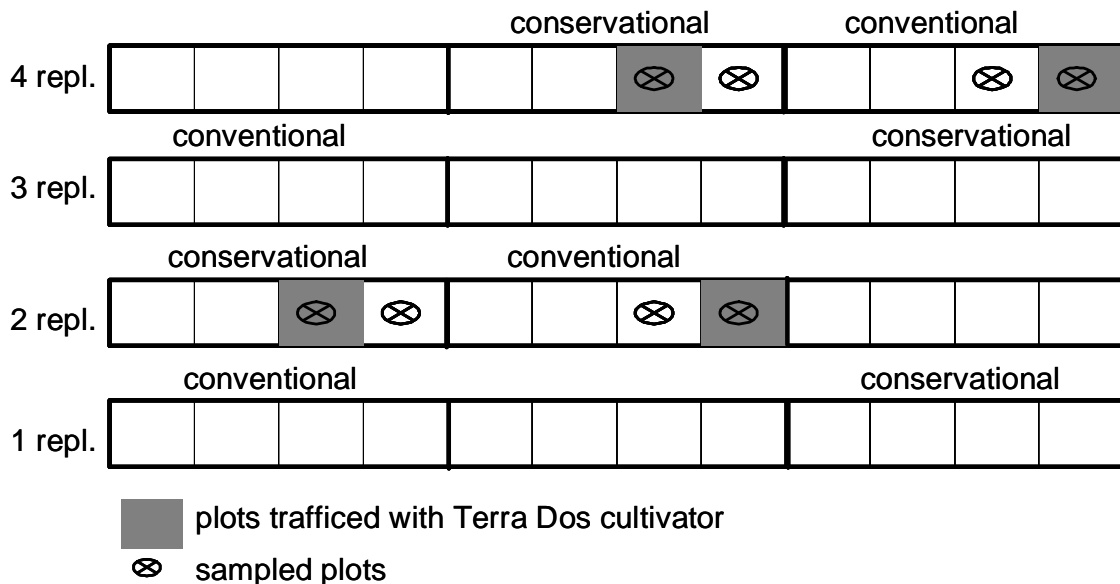


Figure 3-2 Arrangement of the experimental field.

Some of the chosen plots under conservation and conventional treatments were additionally wheeled for the first time only ones with a “Holmer Terra Dos” (weight of the half loaded machine 35- 40Mg¹) (marked as “c”) to describe the effect of the wheeling during the harvesting on some hydraulic and thermal properties of the soil. Those treatments have been carried out only ones in 2003. The plots not wheeled with Holmer Terra Dos are depicted as the control parcels and are later labelled as uncompacted surfaces (marked as “uc”).

¹ Later denoted compacted field and marked as “c”

3.3 Methods

3.3.1 Laboratory measurements

3.3.1.1 Collection of the soil samples

Undisturbed soil samples were taken with PVC cylinders at two depths of the conventional and conservation tillage treatments (see also Table 3-2). Disturbed soil samples were also obtained from the same depths in plastic bags to determine some basic physical and chemical properties.

The sampling took place in November 2002. Disturbed and undisturbed soil samples were taken from the “replication 2” and the “replication 4” to determine some physical and thermal soil properties of the two tillage treatments („Mulch“ and „Plough“) before and after compaction. For description of the tillage treatments the following notation was used:

- Muc for „Mulch“ before wheeling
- Mc for „Mulch“ after wheeling
- Puc for „Plough“ before wheeling
- Pc for „Plough“ after wheeling

The sampled soil horizons and the analysed parameters are summarized in Table 3-2.

Table 3-2 Sampled soil horizons, characteristic and number of used cylinders for determining properties as: thermal diffusivity (D), thermal conductivity (λ), heat capacity (Cv), shrinkage, water retention curve (WRC), saturated water conductivity (k_f) and air permeability (k_i) from the investigated tillage treatments.

Tillage treatment	2, 4 „Mulch“		2, 4 „Plough“		Volume [cm ³]
	0 - 30	30 - 60	0 - 30	30 - 60	
Depth [cm]	Axp	Axh-AI/Axh-(Bt)	Axp	Axh-AI/Axh-(Bt)	
Horizon					
D	4	4	4	4	~ 8505
λ	4	4	4	4	~ 8505
Cv	4	4	4	4	~ 8505
Shrinkage ²	4	4	4	4	100
WRC ²	4	4	4	4	100
k_f ²	6	6	6	6	100
k_i ²	4	4	4	4	100

The determination of the thermal properties was carried out on a greater soil samples (h=30cm, Ø=19cm), which were taken from the field. The homogenized material was refilled according to the site specific properties. Other physical properties were determined on small samples prepared from homogenized material.

3.3.1.2 Texture determination of the sampled soils

The disturbed soil samples were air-dried, grounded and sieved (2mm). To achieve a total dispersion of the soil samples the fine fraction was treated with pyrophosphate and the organic matter was destroyed using H₂O₂.

Fractions smaller than 630, 200 and 100µm were determined by sieving, and

² Measurements made for soil samples with homogenized (disturbed) material. Samples prepared with bulk densities of 1,2- 1,4- 1,6 g/cm³.

the fractions smaller than $63\mu\text{m}$ were analysed by the sedimentation method (Hartge and Horn, 1989).

3.3.1.3 Determination of organic matter and mineral substances

To determine the organic matter content and the amount of C_{org} in the investigated soils the calorimetric method and the Scheibler-analysis were used. The precise description of this method is presented in Scheffer and Schachtchabel (2002).

3.3.1.4 Preparation of the homogenized soil samples

For the determination of the total porosity, bulk density and pore size distribution homogenized soil samples were prepared from homogenized material (Table3-3). The sieved soil ($< 2\text{mm}$) was carefully mixed with water to get a 20% gravimetric water content. To ensure uniform bulk densities, the soil was packed into cylinders at carefully controlled densities by means of a "Load frame" device.

Table3-3 Properties of the soil samples.

Homogenized material	
Aggregate size [mm]	< 2
Bulk density [g/cm^3]	1,2 - 1,4 - 1,6
Initial water content [v/v]	20%

3.3.1.4.1 Determination of the Water Retention curve (WRC)

Water Retention Curve was determined at different water suctions. The samples were drained between -10 till -30hPa on sand tanks. The drainage of the samples at water tensions of -60, -150, -300 and -500hPa occurred on ceramic plates. At each water suction, when the samples attained equilibrium

with the applied vacuum, the gravimetric water content was measured. After the last equilibration (at -500hPa) the samples were saturated again and the saturated hydraulic conductivity (k_f) was measured. After the k_f measurement the samples were dried in an oven at 105 °C for 16 hours. From the dried soil, the bulk density was calculated and the volumetric water content for each soil water tension was determined. To measure the water content at -15000hPa air pressure was applied (Hartge and Horn 1989).

The water retention curve was fitted with the van Genuchten equation with the RETC Software (van Genuchten et al., 1991) and the parameters θ_S , θ_R , α and n were determined from equation 3-1 as follows:

$$\theta(\Psi_m) = \theta_R + \frac{\theta_S - \theta_R}{\left[1 + (\alpha \cdot \Psi_m)^n\right]^m} \quad \text{Equation 3-1}$$

where:

- θ = water content [cm^3/cm^3]
- Ψ_m = water tension (matric potential) [hPa]
- θ_S = water content at saturation [cm^3/cm^3]
- θ_R = residual water content [cm^3/cm^3]
- α, n, m = empirical parameter for the description of the curve [-]

The air-filled porosity, defined as the difference between the total porosity (d.F. value = $2,63\text{g}/\text{cm}^3$) and the measured volumetric water content, was determined at the same water tension (-60hPa) as for the air permeability measurements.

3.3.1.4.2 Determination of the air conductivity

The air conductivity (k_i) was measured at water tensions of -60, -150, -300 and -500hPa. The measuring device is described in detail by Peth (2004). The measurement occurs at a constant gradient of 1hPa and the air flows against gravitation. Calculations were made after Kmoch and Hanus (1965).

3.3.1.4.3 Saturated hydraulic conductivity

The saturated hydraulic conductivity (k_f) was measured under instationary conditions (Hauben Permeameter) (Hartge and Horn, 1989).

3.3.1.4.4 Shrinkage

During the determination of the WRC the shrinkage of the homogenized samples was also measured.

The vertical shrinkage of the soil was measured at 6 defined points (1 in the middle and 5 on the sides) to correct the volumetric water content (Figure 3-3). A similar method was used by Peng et al., (2005) and Dörner (2005).

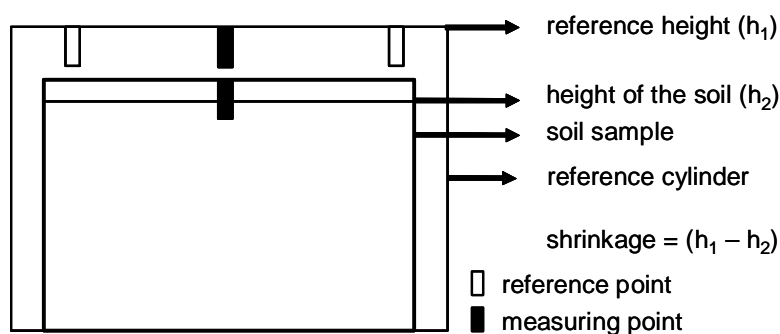


Figure 3-3 Schematic representation of the shrinkage measurement. (after Dörner, 2005).

3.3.1.5 Determination of the thermal soil properties

Heat conductivity (λ), heat capacity (C_v) and thermal diffusivity (D) were determined both for homogenized as well as for undisturbed soil material. Disturbed soil samples were prepared under controlled conditions (with the Load Frame device) to ensure uniform bulk densities of 1,2 and 1,6g/cm³. To minimize the influence of external factors, cylinders were wrapped with isolations and then sensors for measuring water content (TDR needle from *Fa. Easy Test, Ltd., Poland*) and temperature (pT 100 thermistors) were put into the soil at defined depths (Figure 3-4). A heating lamp, fixed above the samples,

was used to heat the soil from the surface.

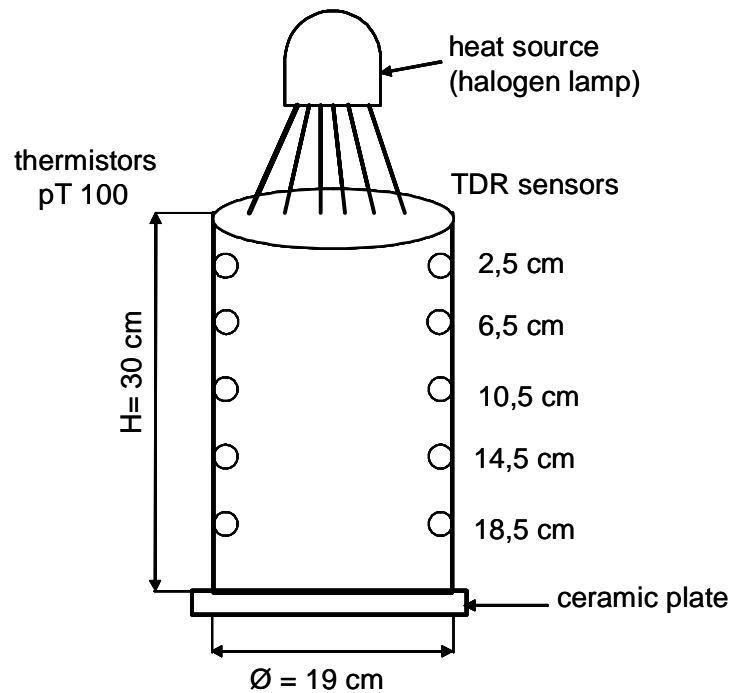


Figure 3-4 Soil sample with TDR needles, pT 100 thermistors and a heating source.

3.3.1.5.1 Temperature monitoring

The measurement consists of two phases: warming phase - the intensity of the applied heat increases (seven steps) and the cooling phase - heat intensity decreases (next seven steps). Each step takes 30 minutes, and the whole monitoring about 25 hours. The intensity of heat at the soil surface from the heating lamp was manually controlled (the heating lamp was shifted up and down). Lateron, a power box dimmer was additionally used to improve the precision of the experiment.

3.3.1.5.2 Time Domain Reflectometry device

The TDR device (Figure 3-5) allows the measurement of the volumetric water content with a defined time velocity. This device is composed of three parts: the main box, the multiplexer (first and second level) and the TDR needles. Each

second level multiplexer box is connected with 6 needles, which measure the water content within a time-space of 30 minutes. The TDR needle measures the apparent dielectric constant of the soil surrounding a waveguide. The propagation velocity (v) of an electromagnetic wave along a transmission line (waveguide) of length L , embedded in the soil, is determined from the time-response of the system to a pulse generated by the TDR cable tester. The propagation velocity is a function of the soil bulk dielectric constant. A change in the dielectric constant is a response at each change in water content.

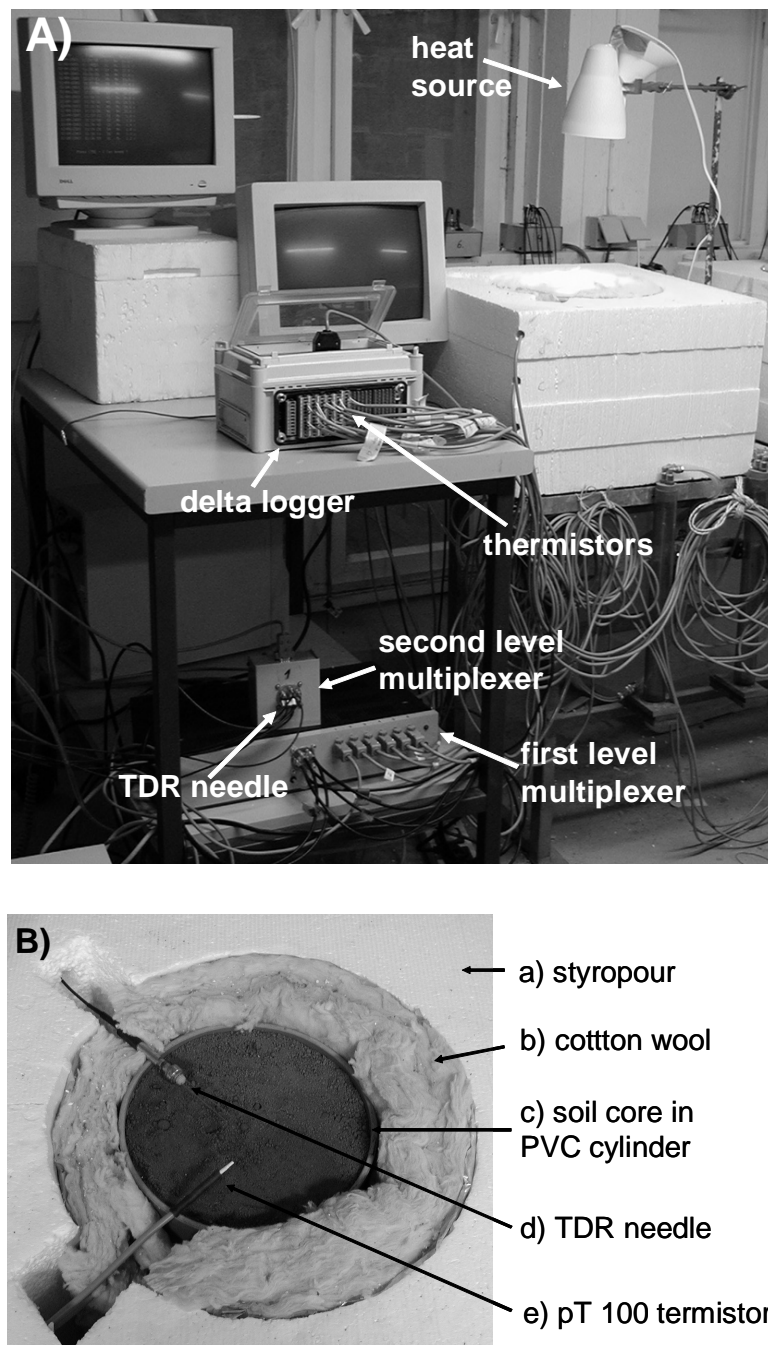


Figure 3-5 Experimental setup: A) TDR device - first and second level multiplexer, delta logger, heat source; A,B) TDR needles, thermistors, and soil sample in PVC cylinder (c), isolation box (a,b) and sensors (d,e).

3.3.2 Field measurements

3.3.2.1 Temperature measurements

The soil temperature on the experimental field was measured by the Institute of Sugar Beet Research (IFZ) in Göttingen. The measurements took place in 1995, and between 1997-2000 at two depths: 5cm and 15cm. During these years the crop rotation was sugar beet and cereals. The temperature measurements were carried out from April to September each year. During the harvesting the equipment was taken away from the field. From these data the thermal diffusivity based on the damping depth method was calculated. Thermal properties like heat capacity, thermal conductivity and thermal diffusivity were derived from a statistical–physical model (both methods described in chapters 2.3.2.1.5.4 and 2.3.3.3).

3.3.2.2 Simulation of water content

To interpret the thermal diffusivity of the soil, both: temperature and water content are required. However, water content was not measured in the field. To circumvent this problem the one dimensional (1D) water flow was simulated with Hydrus-1D (Šimůnek, 2003). To simulate the changes in the water content, the soil horizons and the hydraulic properties of the horizons are needed. For that purpose the WRC and k_f , measured on undisturbed samples, were used (data taken from Fazekas, 2005). The boundary conditions were defined as follows (Figure 3-6):

- length of the soil profile: 3m
- top: atmospheric conditions (rainfall and evapotranspiration)
- bottom: ground water level ($\Psi_m \approx 0\text{hPa}$)

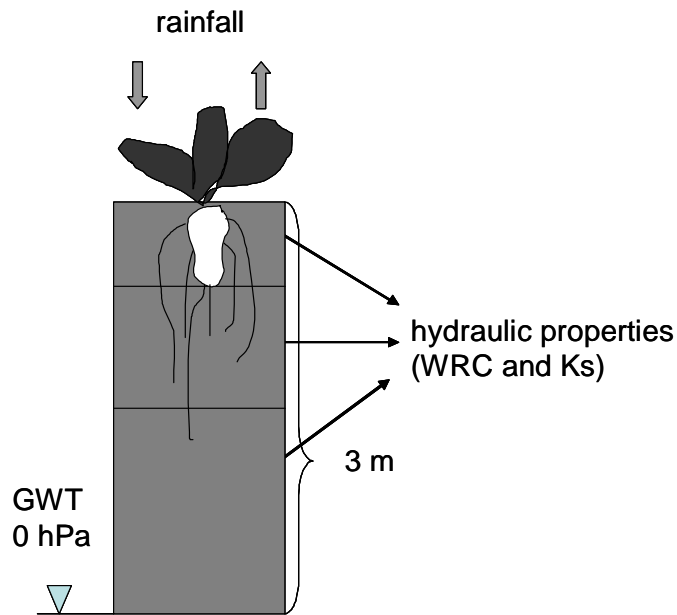


Figure 3-6 Schematic representation of defined boundary conditions for simulation of water content in soil.

The “Grass reference Transpiration” proposed by Allen (cited by DVWK, 1996) was used to estimate evapotranspiration (EVP):

$$ET_o = \frac{s}{s + \gamma * (1 + 0,34 + v_2)} * \left(\frac{R_n}{L} + \left(\frac{e_s(T)}{s} * \frac{\gamma + 3,75}{T + 273} \right) * t * v_2 \left(1 - \frac{U}{100} \right) \right) \text{Equation 3-2}$$

where:

ET_o = grass reference transpiration [mm/d]

s = increase of the saturation vapour pressure curve [hPa/k]

γ = constant of the psychrometer [hPa/K]

R_n = radiation balance [J/cm²]

L = specific transpiration heat [(J/cm²)/mm]

t = time [day]

v_2 = wind velocity [m/s]

U = relative air humidity [%]

This method is an application of the Penman- Monteith -relationship described by Allen et al., (1994) and depends on the water content, plant types and plant

development. This method is recommended by FAO- standard and is imperative for the grass population (the whole year) if the height is 0,12m by absence of the water pressure. The plant cover is defined by soil crop coefficients (k_c). Those coefficients differ for the growth phases of the population and their values range between 0,5 and 1,5. The calculation of the coefficient for the sugar beet is as follow:

$$E_{plant} = ET_o \cdot k_c \quad \text{Equation 3-3}$$

where:

E_{plant} = plant transpiration [mm/d]

k_c = population coefficient [-]

The required data have been taken from the “Deutsche Wetterdienst” for the weather station located next to the experimental field. The corresponding plant transpiration coefficients for the sugar beet have been taken from DVWK (1996).

Figure 3-7 shows the climatic conditions from January till December 1995.

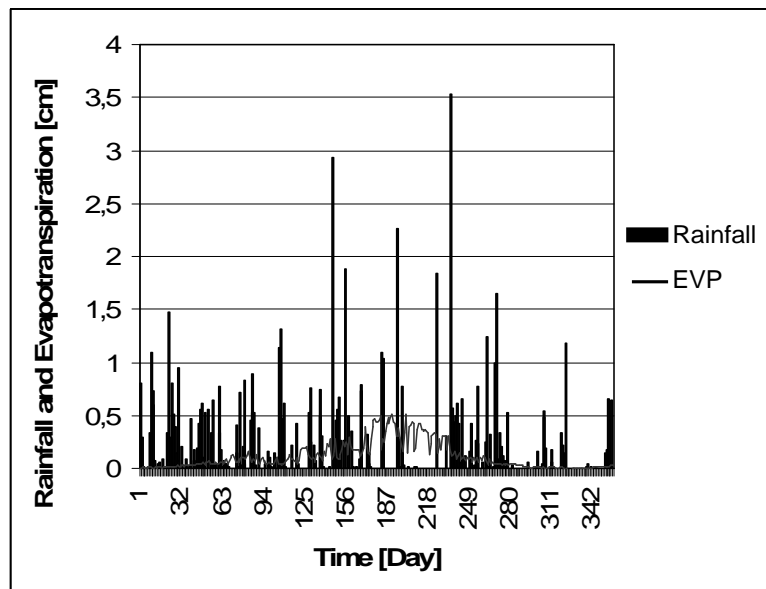


Figure 3-7 Rainfall and evapotranspiration (EVP) in 1995 for „Mulch“ from April to September for Göttingen.

3.3.2.3 Statistical –physical model of thermal conductivity in soil

To determine the investigated thermal properties like thermal conductivity, heat capacity and thermal diffusivity, the statistical-physical model was used for undisturbed soil samples taken in the field and the bulk density values were determined (see also chapter 2.3.2.1.5.4). The values vary between 1,50g/cm³ for uncompacted and 1,55g/cm³ for compacted samples. Additionally, the effect of different bulk densities on soil thermal properties (on samples from homogenized material) was investigated. For samples prepared with $d_B=1,2\text{g/cm}^3$ calculations were made additionally for bulk densities of 1,4 and 1,6g/cm³, and for samples prepared with 1,6g/cm³ calculations were made also by bulk densities of 1,2 and 1,4g/cm³.

3.3.2.4 Damping depth method

Thermal diffusivity was calculated by the damping depth method (Hanks et al., 1980; Usowicz, 2001; Renuka, 2002). The precise description of that model is presented in chapter 2.3.3.3.

4 Results

4.1 Thermal properties

4.1.1 Laboratory measurements

Laboratory investigations were performed at disturbed (homogenized material, <2mm) and undisturbed (soil cores) soil samples. The results will be presented in the following order: (i) disturbed soil samples with bulk densities (d_B) of 1,2 and 1,6g/cm³, (ii) soil cores from uncompacted and compacted plots, (iii) field data.

4.1.1.1 Thermal properties of homogenized material

4.1.1.1.1 Soil temperature profiles

Figure 4-1 shows soil temperature profiles in a soil sample with d_B of 1,2g/cm³ obtained from the daily temperature oscillation simulated in the laboratory. The measurement takes 25 hours. The first 6 hours (Figure 4-1 a) correspond to the warming and the next 19 hours (Figure 4-1 b) to the cooling phase (samples were left for the night). During the investigated time, the intensity of applied heat is absorbed by the soil which warms the ground surface more than the layers beneath. Therefore, the velocity of the temperature changes in the soil decreases with increasing depth. With temperature increase the gradients get steeper; the opposite was assessed during the cooling of samples.

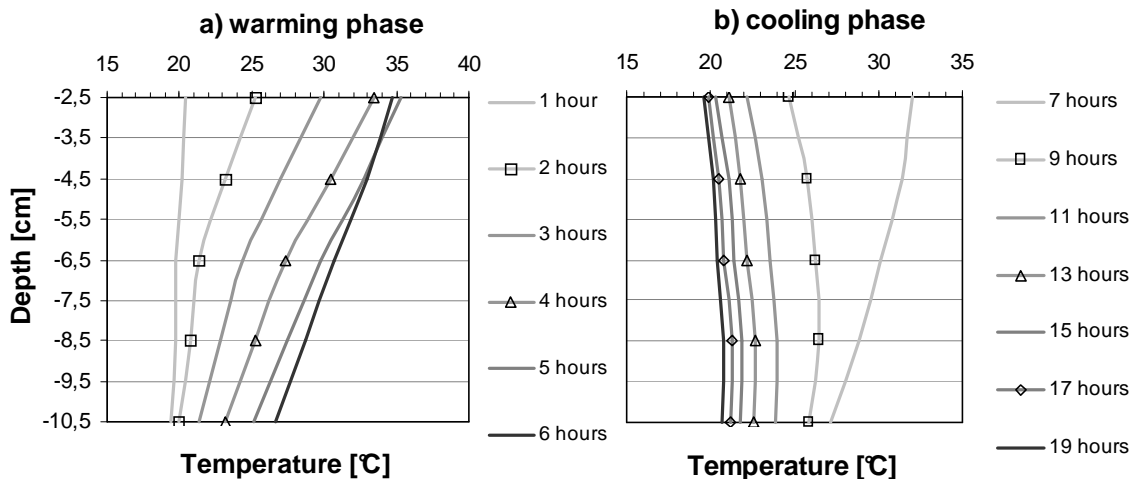


Figure 4-1 Soil temperature profile from the daily temperature oscillation simulated for homogenized samples; a) first 6 hours correspond to warming phase and b) the next 19 hours to cooling phase. Sample prepared with $d_B = 1,2\text{g/cm}^3$.

4.1.1.1.2 Temperature and water content development

To calculate thermal properties of investigated soils the daily temperature oscillation was simulated. Figure 4-2 shows that the temperature amplitude in first investigated depth (2,5cm) for $1,2\text{g/cm}^3$ is $16\text{-}17^\circ\text{C}$ and for $1,6\text{g/cm}^3$ $14\text{-}18^\circ\text{C}$. The maximum temperature occurs in samples with lower d_B , where the soil temperature wave penetrates to the last depth of 10,5cm with amplitudes of approximately 8°C . For $d_B=1,6\text{g/cm}^3$ the temperature development at 8,5cm and 10,5cm was almost the same. The amplitude decrease of the soil temperature wave with depth (between 2,5-4,5 and 4,5-8,5cm) was almost 5°C and then decreased. For both samples it is noticed that the temperature amplitude decreases with increasing depth. In the cycles of heating and cooling the temperature in soil samples increases and decreases according to the intensity of the applied heat. Reactions at the shallower depths are more visible and stronger. With increasing soil depth the time shift to reach the depth dependent maximum temperature increases.

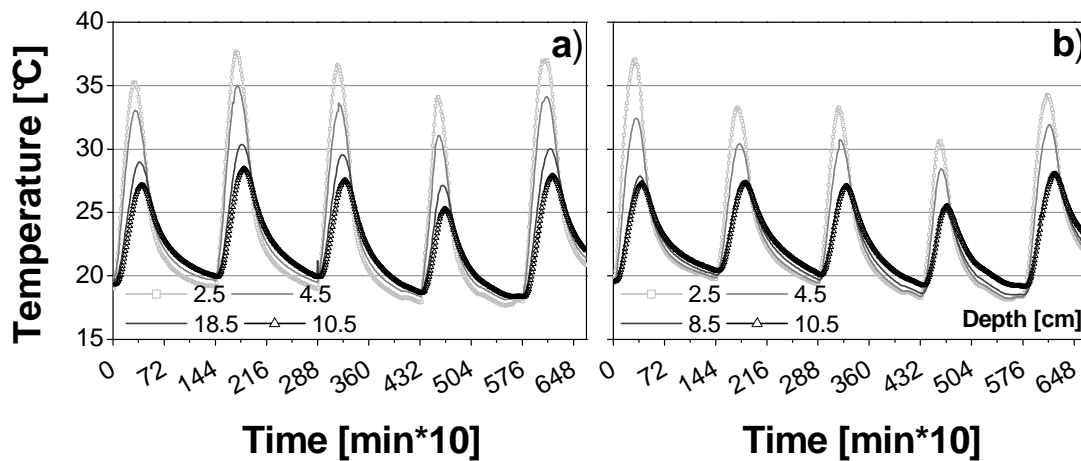


Figure 4-2 Temperature development of simulated daily oscillation for homogenized soil samples with a) $d_B=1,2$ and b) $d_B=1,6\text{g/cm}^3$.

The initial water content measured with TDR for $1,2\text{g/cm}^3$ is approximately 15vol% and for $1,6\text{g/cm}^3$ almost 29vol% (Figure 4-3). The water loss decreases with increasing depth and is the highest at depth of 2,5cm where the temperature (Figure 4-2 a,b) reaches the highest values as well. At a d_B value of $1,2\text{g/cm}^3$ the total water loss at 2,5cm is approximately 15vol% followed by 2,0vol% at 10,5cm. By higher $d_B=1,6\text{g/cm}^3$ (Figure 4-3 b) first depth (2,5cm) loses 3,4vol% and the last (10,5cm) 1,8vol%.

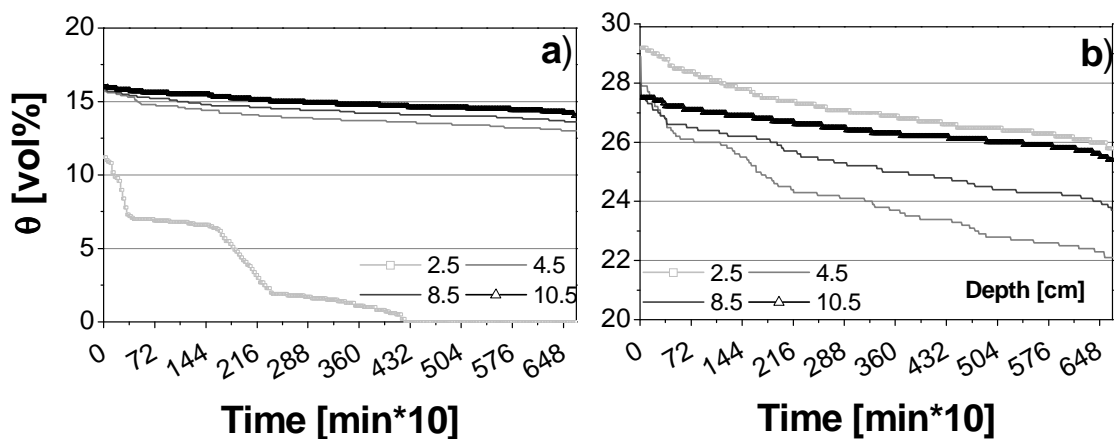


Figure 4-3 Changes in water content during simulation of daily oscillation of temperature for homogenized soil samples with a) $d_B=1,2$ and b) $1,6\text{g/cm}^3$.

4.1.1.1.3 Heat properties depending on bulk density

In order to describe the effect of bulk density on soil thermal properties, results (θ and T) derived from homogenized samples were used to simulate the thermal conductivity, heat capacity and thermal diffusivity for different bulk densities.

4.1.1.1.3.1 Thermal conductivity

The thermal conductivity decreases with decreasing water content. For $d_B=1,2\text{g/cm}^3$ (Figure 4-4) the greatest decrease of λ is observed during the heating phase at the first and the cooling phase at the second day when the water loss (Figure 4-3 a) was the highest as well. Generally, thermal conductivity increases with increasing water content- at first rapidly and then gradually (rise of water content and bulk density enlarges the surface or contact points conducting the heat). This phenomenon is visible in Figure 4-4 b) where the water content is higher in comparison to 2,5cm depth. Decrease of thermal conductivity became smaller with depth increase, as a consequence of the smaller decrease of water content. It is proportional to the d_B increase (λ increases about 0,2 W/mK per 0,2g/cm³ increase). This difference, however, becomes smaller with decreasing water content.

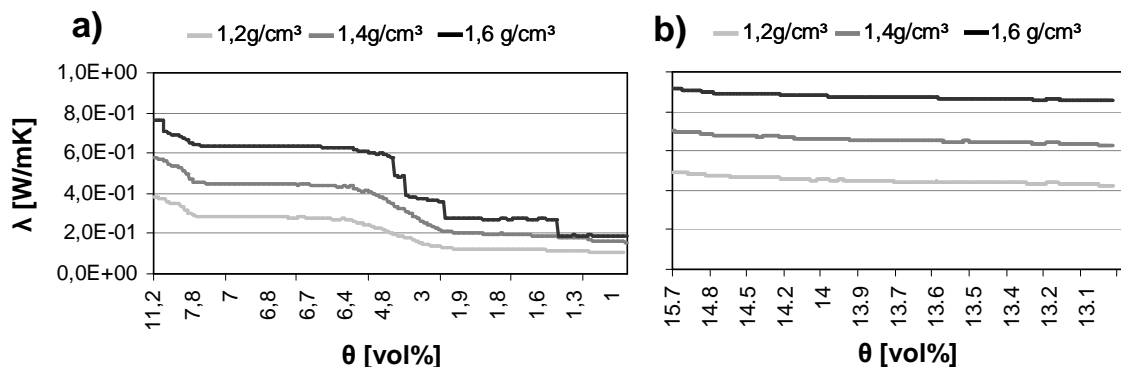


Figure 4-4 Heat conductivity (λ) of homogenized samples calculated for a bulk density of $d_B=1,2\text{g/cm}^3$ and measured at two depths: a) 2,5cm and b) 4,5cm.

At bulk density of $1,6\text{g/cm}^3$ water loss is lower than at $d_B=1,2\text{g/cm}^3$ and therefore the decrease of thermal conductivity is smaller as well (Figure 4-5). The λ decrease during the simulation for singular d_B values ($1,2-1,4-1,6\text{g/cm}^3$) becomes smaller with increasing bulk density. The depth of $4,5\text{cm}$ shows a higher water loss, and correspondingly to that the decrease of λ is higher as well.

Comparing the decrease of thermal conductivity with the total decrease of water content it is remarkable that the highest decrease of λ occurs at lower values (range) of θ (e.g.: at θ of $13-15,7\%$ λ decreases by about $0,08\text{ W/mK}$ while at θ of $22-29\%$ λ decreases only by $0,058\text{ W/mK}$). The highest decrease of λ is observed at $4,5\text{cm}$ at $d_B=1,2\text{g/cm}^3$ where also the volumetric water loss is highest.

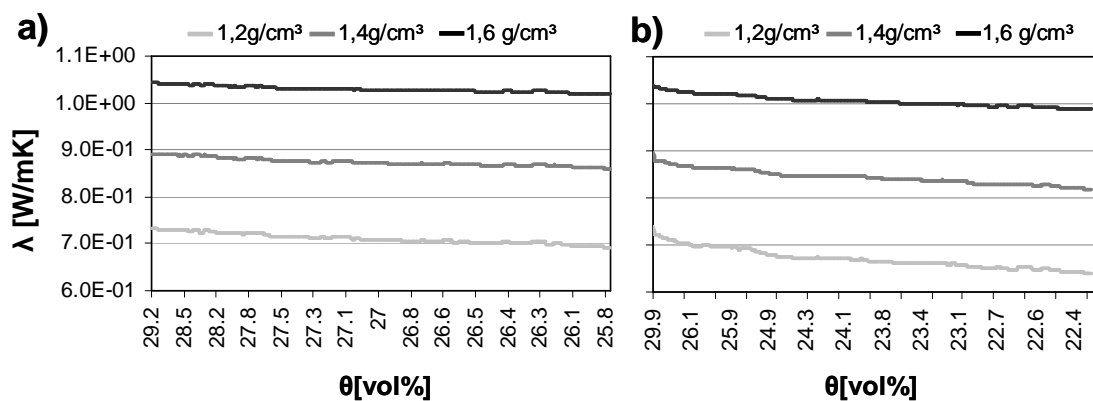


Figure 4-5 Heat conductivity (λ) of homogenized samples calculated for a bulk density of $d_B=1,6\text{g/cm}^3$ and measured at two depths: a) $2,5\text{cm}$ and b) $4,5\text{cm}$.

4.1.1.1.3.2 Heat capacity

Due to evaporation the soil water content (θ) decreases with time. Because the amount of organic substance is constant, the volumetric heat capacity (C_v) depends only on θ and decreases with their decrease as well. At $4,5\text{cm}$ depth where the water loss is lower than at the upper depth also C_v reaches lower values in samples prepared with $d_B=1,2\text{g/cm}^3$ (Figure 4-6). By $d_B=1,6\text{g/cm}^3$

(Figure 4-7), however, this depth indicated the highest decrease of C_v according to the θ change. Visible is also that C_v increases with increasing bulk density what is caused by the rise of the contact points between soil particles leading the heat. This increase in C_v at higher d_B is approximately $0,15 \cdot 10^6 \text{ J/m}^3\text{K}$ per $0,2\text{g/cm}^3$.

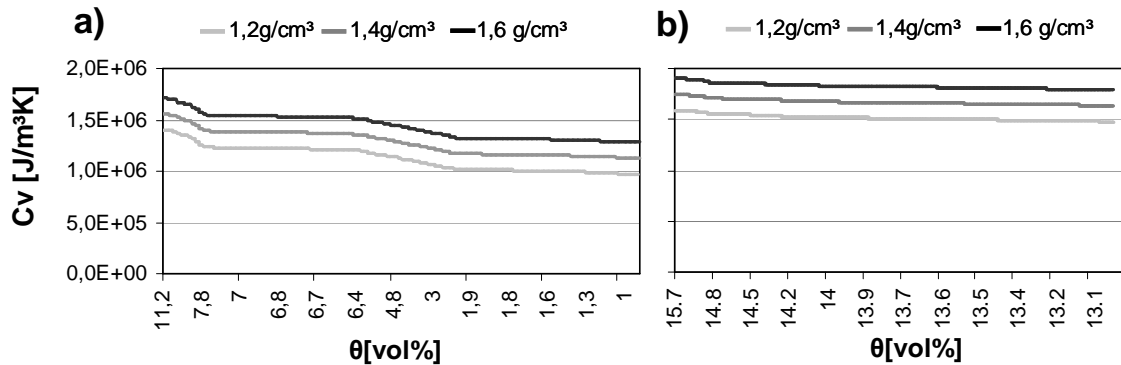


Figure 4-6 Volumetric heat capacity (C_v) of homogenized samples calculated for a bulk density of $d_B=1,2\text{g/cm}^3$ and measured at two depths: a) 2,5cm and b) 4,5cm.

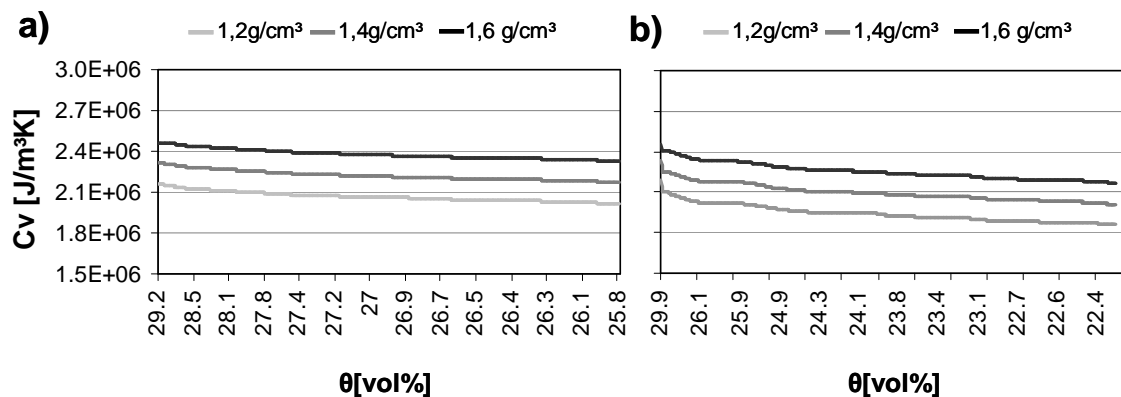


Figure 4-7 Volumetric heat capacity (C_v) of homogenized samples calculated for a bulk density of $d_B=1,6\text{g/cm}^3$ and measured at two depths: a) 2,5cm and b) 4,5cm.

4.1.1.1.3.3 Thermal diffusivity

Thermal diffusivity depends on the magnitude of θ (increases with increasing θ , but after exceeding of approximately 20vol% it starts to decline); it shows two different behaviours. In samples prepared with $d_B=1,2\text{g/cm}^3$ thermal diffusivity

decreases (Figure 4-8) ($\theta=11,2\text{vol}\%$) and with $d_B=1,6\text{g}/\text{cm}^3$ (Figure 4-9) ($\theta=29,2\text{vol}\%$) it increases with increasing θ . Corresponding to the θ changes, the greatest variations of D were observed at 2,5cm depth in samples with $d_B=1,2\text{g}/\text{cm}^3$ (Figure 4-8 a). At 4,5cm as well as in samples prepared with $d_B=1,6\text{g}/\text{cm}^3$ these changes are uniform.

Presented results show that thermal diffusivity is also affected by bulk density and increases (Figure 4-8 a, b) or decreases (Figure 4-9 a, b) according to their changes. In samples with lower d_B , the difference in D at 2,5cm depth becomes smaller with decreasing θ due to different d_B , while at 4,5cm at almost constant θ it stays relatively constant. At higher bulk density ($d_B=1,6\text{g}/\text{cm}^3$; Figure 4-9 b) it is visible that the range of D changes is smaller with decreasing d_B .

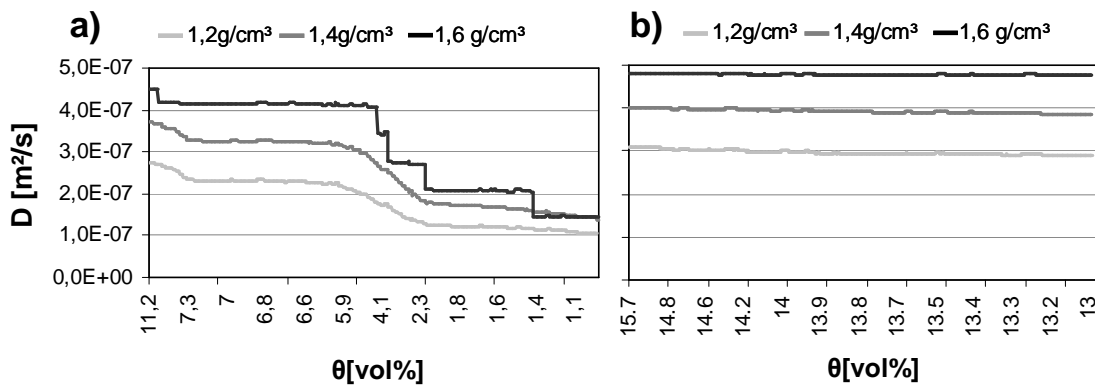


Figure 4-8 Thermal diffusivity (D) of homogenized samples calculated for a bulk density of $d_B= 1,2\text{g}/\text{cm}^3$ and measured at two depths: a) 2,5cm and b) 4,5cm.

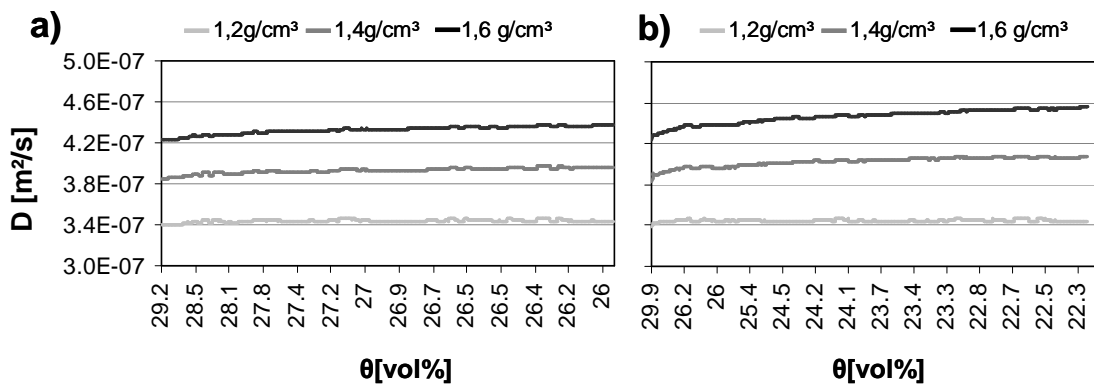


Figure 4-9 Thermal diffusivity (D) of homogenized samples calculated for a bulk density of $d_B = 1,6\text{g}/\text{cm}^3$ and measured at two depths: a) 2,5cm and b) 4,5cm

4.1.1.1.3.4 Thermal diffusivity calculated with the damping depth method

The same data as for physical-statistical model were also used to calculate the thermal diffusivity with the damping depth method but for the sake of some limitations and conditions, which have to be satisfied, it could be calculated only for a few depths and days. Results from these calculations together with damping depths calculated with the amplitude ratio and phase shift are presented in Table 4-1 for $d_B = 1,2\text{g}/\text{cm}^3$ and in Table 4-2 for $d_B = 1,6\text{g}/\text{cm}^3$. Damping depths of the soil obtained by the two methods are in good agreement; therefore, D can be calculated. The average value of damping depths for both samples is in the range of 10cm. Values of the thermal diffusivity for $1,2\text{g}/\text{cm}^3$ are about $4,41\text{-}6,62 \cdot 10^{-7}\text{m}^2/\text{s}$ and for $1,6\text{g}/\text{cm}^3$ $3\text{-}7,09 \cdot 10^{-7}\text{m}^2/\text{s}$, respectively.

Table 4-1 Thermal diffusivity values calculated from the amplitude ratio and the phase shift damping depths. Calculations made for homogenized soil sample prepared with bulk density of 1,2g/cm³.

Amplitude ratio	Phase shift	Diffusivity
[cm]	[cm]	[m ² /s]
11,91	12,1	6,62 *10 ⁻⁷
11,51	12,92	6,42*10 ⁻⁷
9,05	9,87	5,04*10 ⁻⁷
8,17	12,2	4,7*10 ⁻⁷
11,57	9,6	5,14*10 ⁻⁷
10,0	10,26	4,41*10 ⁻⁷
9,66	9,87	5,37*10 ⁻⁷

Table 4-2 Thermal diffusivity values calculated from the amplitude ratio and the phase shift damping depths. Calculations made for homogenized soil sample prepared with bulk density of 1,6g/cm³.

Amplitude ratio	Phase shift	Diffusivity
[cm]	[cm]	[m ² /s]
6,64	9,6	3,0 *10 ⁻⁷
12,58	9,87	5,5*10 ⁻⁷
11,09	12,1	6,2*10 ⁻⁷
9,73	12,2	7,09*10 ⁻⁷
8,5	12,1	4,9*10 ⁻⁷

The thermal diffusivity is affected by water content. Figure 4-10 presents the relationship between θ and D calculated by the damping depth method for bulk densities of 1,2g/cm³ and 1,6g/cm³. In the sample with a d_B value of 1,2g/cm³, the water content varied between 0-10vol%, while in the sample with $d_B=1,6g/cm^3$ it varies between 25-30vol%, resulting in thermal diffusivity values which increase with water content.

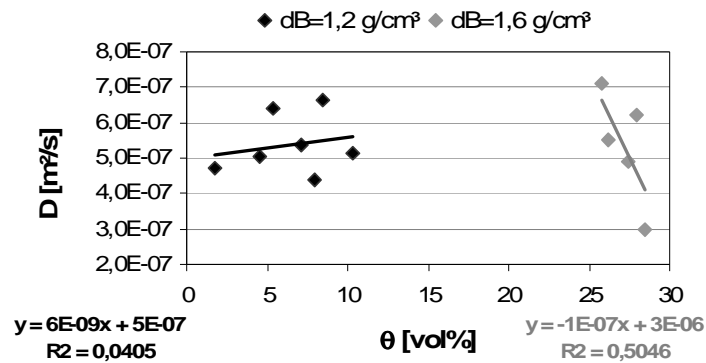


Figure 4-10 Thermal diffusivities calculated with damping depth method for homogenized soil samples prepared with bulk densities of $1,2\text{g/cm}^3$ and $1,6\text{g/cm}^3$.

However, the thermal diffusivity calculated with damping depth method (Figure 4-10 and Table 4-1, Table 4-2) gave higher values than those, calculated with the statistical-physical model (Figure 4-8, Figure 4-9).

4.1.1.2 Undisturbed soil samples

4.1.1.2.1 Soil temperature profile

Soil temperature profiles presented below show that the highest changes happened at the soil surface and decrease with increasing depth. No important differences between sampled depths: 0-30cm (Figure 4-11 a) and 30-60cm (Figure 4-11 b) can be observed. The temperature amplitude at the first depth is 10°C and 8°C and at the last 5°C and 7°C for both: warming and cooling phase in samples taken from 0-30cm and 30-60cm, respectively. The first six hours correspond to the warming and the next 21 to the cooling phase. After this time samples reach the initial conditions (room temperature $\approx 20^\circ\text{C}$).

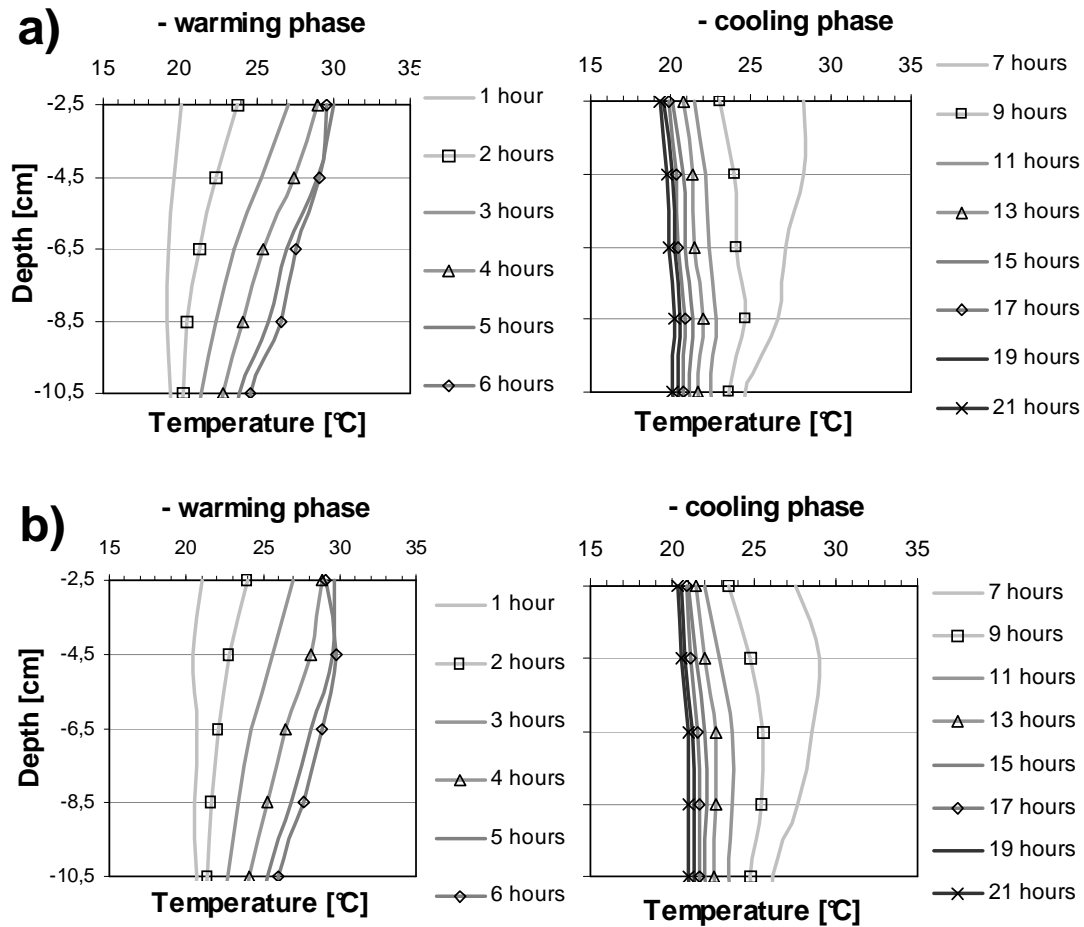


Figure 4-11 Soil temperature profiles from simulation of the daily temperature oscillation for samples taken from the uncompacted conventional tillage treatment; depth a) 0-30cm, b) 30-60cm. First six hours describe the warming phase and the next 21 the cooling phase.

4.1.1.2.2 Thermal properties

4.1.1.2.2.1 Uncompacted plots

Investigated tillage treatments before wheeling indicated some differences between plots and especially between sampled depths. In the „Mulch“ plots greater initial and maximal values of θ , λ and C_v were observed in the topsoil, while in the „Plough“ plot the inverse situation was observed with higher values in a samples taken from 30-60cm (Table 4-3). D for both tillage treatments reaches greater values for samples taken from the deeper soil horizon. The

intensity of evaporation, maximal temperatures as well as calculated (λ , C_v , D) properties, however, show a higher increase/decrease during the measurement in samples taken from 0-30cm (independent of the treatment). The temperature amplitude decreases with soil depth (M: $T=14$ and 11°C ; P: $T=12$ and 9°C for 0-30 and 30-60cm respectively) and reaches greater values for „Mulch“.

The results obtained show that the differences between the sampled depths were observed not only for single treatments but also between them. Trends indicate that the presented properties (except T and D) in the topsoil are greater for „Mulch“, while, in deeper depths (except T) the „Plough“ plot shows greater values for θ , C_v and λ (see also Table 4-8).

If only treatments are considered, the conservational system has a higher θ value at a given matric potential and, corresponding, λ and C_v reach higher values as well (statistically not significant as shows Table 4-8). The conventional system indicated greater T and D .

Table 4-3 Measured (T and θ) and calculated (λ , C_v , D) properties for uncompacted samples taken from „Mulch“ and „Plough“ and depths of 0-30cm and 30-60cm.

Property	„Mulch“		„Plough“	
	0 - 30	30 - 60	0 - 30	30 - 60
Depth [cm]				
T [$^\circ\text{C}$]	19- 32	19- 30	21- 33	21- 30
θ [vol%]	40 - 28	35 - 28	33 -26	39 -23
λ [W/mK]	1,04 -0,96	1,03 -0,95	1,00 -0,93	1,065 -0,95
C_v [$\text{J}/\text{m}^3\text{K}\cdot 10^6$]	2,85 -2,38	2,6 -2,3	2,6 -2,25	2,85 -2,15
D [$\text{m}^2/\text{s}\cdot 10^{-7}$]	3,65 -4,1	3,92 -4,18	3,9 -4,2	3,78 -4,4

4.1.1.2.2 Compacted plots

Results summed up in Table 4-4 show that plots after wheeling considered as single treatments show similar trends with the unwheeled ones. In „Mulch“ the

investigated properties (except D) are greater in samples taken from the topsoil. In „Plough“ the similar behaviour is shown for θ and C_v , whereas λ and D were higher in the samples taken from 30-60cm depth. The difference between the initial and the final value of the investigated properties was greater in the samples collected from 0-30cm. The initial temperature was higher in P, however, the amplitude does not show important differences and is approximately 14°C for both treatments.

If only treatments are considered it is visible that the properties: λ and C_v are greater in „Mulch“ (Table 4-8). These differences are statistically significant (statistic was not made for D and depth of 30-60cm - see comment to Table 4-8).

Table 4-4 Measured (T and θ) and calculated (λ , C_v , D) properties for compacted samples taken from „Mulch“ and „Plough“ and depths of 0-30cm and 30-60cm.

Property	„Mulch“		„Plough“	
	0 - 30	30 - 60	0 - 30	30 - 60
Depth [cm]				
T [°C]	22- 34	22- 34	20- 35	20- 34
θ [vol%]	42,5 -28	35 -25	40 -25	37,5 -18
λ [W/mK]	1,075 -0,96	1,025 -0,98	1,05 -0,97	1,075 -0,91
C_v [J/m ³ K*10 ⁶]	2,9 -2,3	2,65 -2,2	2,9 -2,22	2,8 -2,0
D [m ² /s*10 ⁻⁷]	3,6 -4,2	3,85 -4,4	3,65 -4,2	3,85 -4,6

The influence of soil compaction on the investigated soil properties summarized in Table 4-3 and Table 4-4 show that both: measured (T , θ) as well as calculated (λ , C_v , D) properties were greater in samples after wheeling, regardless of treatments and sampled depth.

4.1.1.2.2.3 Effect of water content on thermal properties of investigated soils.

Thermal conductivity and the volumetric heat capacity for both sampled depths (0-30cm; Figure 4-12 and 30-60cm Figure 4-13) decrease with decreasing θ as well. Regression parameters ($y=ax+b$) of the relationship between volumetric water content and the thermal conductivity are summed up in Table 4-5 (λ), Table 4-6 (C_v) and Table 4-7 (D). The greatest and the smallest differences between slopes of relationship between water content and thermal properties for different treatments were observed in conductivity and capacity, respectively.

Thermal conductivity calculated for undisturbed samples (M_{uc} , M_c , P_{uc} , P_c) is similar with those ones of the homogenized material with a $d_B=1,6g/cm^3$. Samples with $d_B=1,2g/cm^3$ (Appendix C) show a much steeper increase of λ . The intercept, however, is lower (start from the smaller values of λ but the reaction on θ changes is quicker).

The slope of C_v increases (Figure 4-12 b), Figure 4-13b) and Table 4-6) but the data do not show differences between the treatments and for the disturbed samples. Similar was observed for D with respect to the increase with θ . The direction of these changes, however, was inverse in the homogenized samples and $d_B=1,2g/cm^3$ (Appendix C, c).

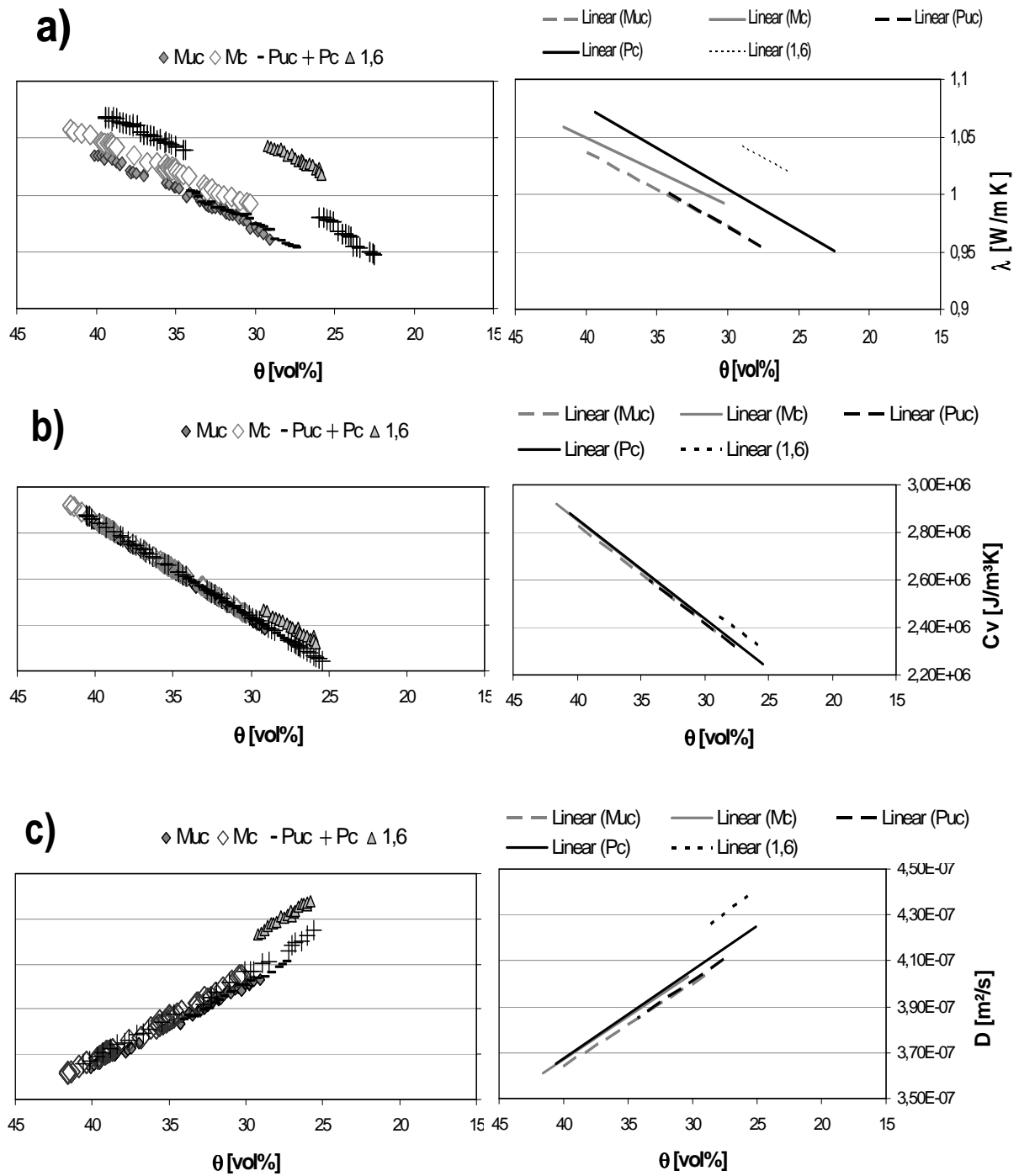


Figure 4-12 a) Thermal conductivity (λ), b) volumetric heat capacity (C_v) and c) thermal diffusivity (D) as a function of water content (θ) for samples taken from 0-30cm depth.

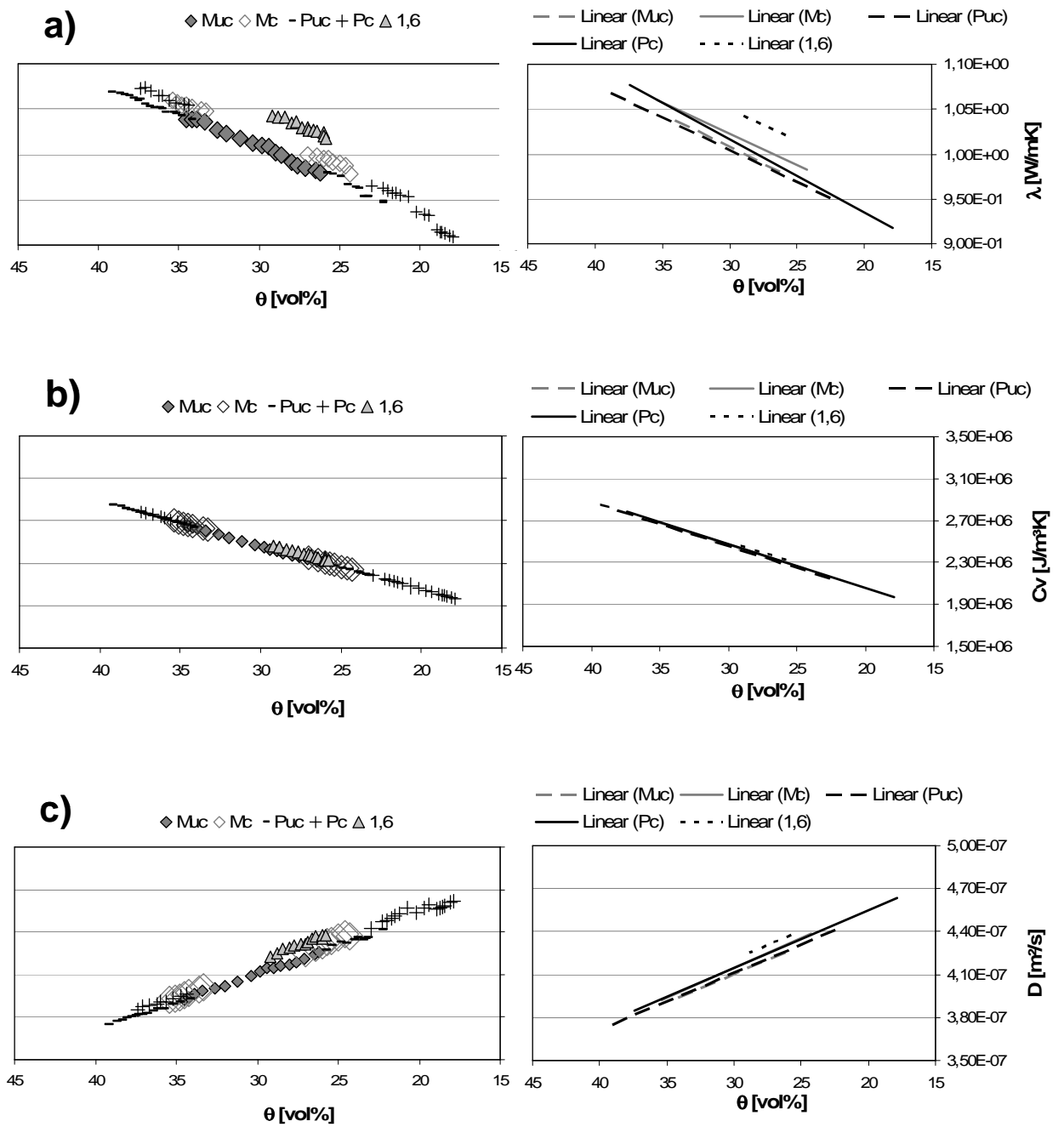


Figure 4-13 a) Thermal conductivity (λ), b) volumetric heat capacity (C_v) and c) thermal diffusivity (D) as a function of water content (θ) for samples taken from 30-60cm depth.

Table 4-5 Regression parameters ($y=ax+b$) of the relationship between volumetric water content and thermal conductivity in „Mulch“ (M) and „Plough“ (P) before (uc) and after (c) compaction. In addition homogenized samples with $d_B=1,2$ and $1,6\text{g/cm}^3$ were analysed.

Depth [cm]	0-30cm			30-60cm		
Plot	Slope	Intercept	R ²	Slope	Intercept	R ²
Muc	0,0067	0,771	0,986	0,0074	0,7869	0,964
Mc	0,0062	0,803	0,987	0,007	0,8123	0,996
Puc	0,0069	0,764	0,966	0,0072	0,7882	0,996
Pc	0,0072	0,788	0,996	0,0008	0,7771	0,992
1,2 [g/cm ³]	0,0295	0,0738	0,995	0,0295	0,0738	0,995
1,6 [g/cm ³]	0,0075	0,826	0,951	0,0075	0,826	0,951

Table 4-6 Regression parameters ($y=ax+b$) of the relationship between volumetric water content and heat capacity in „Mulch“ (M) and „Plough“ (P) before (uc) and after (c) compaction. In addition homogenized samples with $d_B=1,2$ and $1,6\text{g/cm}^3$ were analysed.

Depth [cm]	0-30cm			30-60cm		
Plot	Slope	Intercept	R ²	Slope	Intercept	R ²
Muc	$0,0417 \cdot 10^6$	$1,0 \cdot 10^6$	0,999	$0,0415 \cdot 10^6$	$1,0 \cdot 10^6$	0,999
Mc	$0,042 \cdot 10^6$	$1,0 \cdot 10^6$	0,999	$0,0416 \cdot 10^6$	$1,0 \cdot 10^6$	0,999
Puc	$0,042 \cdot 10^6$	$1,0 \cdot 10^6$	0,999	$0,0418 \cdot 10^6$	$1,0 \cdot 10^6$	0,999
Pc	$0,0418 \cdot 10^6$	$1,0 \cdot 10^6$	0,999	$0,0418 \cdot 10^6$	$1,0 \cdot 10^6$	0,999
1,2 [g/cm ³]	$0,0418 \cdot 10^6$	$9,34 \cdot 10^4$	0,999	$0,0418 \cdot 10^6$	$9,34 \cdot 10^5$	0,999
1,6 [g/cm ³]	$0,0415 \cdot 10^6$	$1,0 \cdot 10^6$	0,984	$0,0417 \cdot 10^6$	$1,0 \cdot 10^6$	0,99

Table 4-7 Regression parameters ($y=ax+b$) of the relationship between volumetric water content and thermal diffusivity in „Mulch“ (M) and „Plough“ (P) before (uc) and after (c) compaction. In addition homogenized samples with $d_B=1,2$ and $1,6\text{g/cm}^3$ were analysed.

Depth [cm]	0-30cm			30-60cm		
	Slope	Intercept	R ²	Slope	Intercept	R ²
Muc	$-4,0 \cdot 10^{-9}$	$5,0 \cdot 10^{-7}$	0,993	$-4,0 \cdot 10^{-9}$	$5,0 \cdot 10^{-7}$	0,979
Mc	$-4,0 \cdot 10^{-9}$	$5,0 \cdot 10^{-7}$	0,994	$-4,0 \cdot 10^{-9}$	$5,0 \cdot 10^{-7}$	0,998
Puc	$-4,0 \cdot 10^{-9}$	$5,0 \cdot 10^{-7}$	0,987	$-4,0 \cdot 10^{-9}$	$5,0 \cdot 10^{-7}$	0,998
Pc	$-4,0 \cdot 10^{-9}$	$5,0 \cdot 10^{-7}$	0,997	$-4,0 \cdot 10^{-9}$	$5,0 \cdot 10^{-7}$	0,997
1,2 [g/cm ³]	$2,0 \cdot 10^8$	$9,0 \cdot 10^{-8}$	0,978	$2,0 \cdot 10^{-8}$	$9,0 \cdot 10^{-8}$	0,978
1,6 [g/cm ³]	$-4,0 \cdot 10^{-9}$	$6,0 \cdot 10^{-7}$	0,977	$-4,0 \cdot 10^{-9}$	$6,0 \cdot 10^{-7}$	0,977

A statistical analysis requires identical conditions for the investigated properties. However, the analyzed data were collected, when the water content was about 28vol%, which was not fulfilled for the samples from 30-60cm. The thermal diffusivity was calculated from the relationship between λ and C_v , and was therefore, excluded from a detailed statistics analysis. Results presented in Table 4-8 show higher values for λ as well as for C_v for the compacted plots. Significant differences were founded for M, while, in P no significant differences between these plots were observed in C_v .

Table 4-8 Thermal conductivity (λ) and volumetric heat capacity (C_v) in „Mulch“ (M) and „Plough“ (P), plots before (uc) and after (c) compaction at 0-30cm depth (the cardinal letters mean the difference between uc and c plots, and small letters differences between treatments by significant level of $p<0,05$).

Property	λ [W/mK]		C_v [J/m ³ K]	
	uc	c	uc	c
„Mulch“	1,001 Ba	1,041 Aa	$2,59 \cdot 10^6$ Ba	$2,64 \cdot 10^6$ Aa
„Plough“	1,00 Ba	1,014 Ab	$2,59 \cdot 10^6$ Aa	$2,6 \cdot 10^6$ Ab

As summarized in Table 4-9 wheeled plots show higher bulk density (although M does not show statistical differences) and a smaller amount of coarse pores (Table 4-10).

Table 4-9 Bulk density for „Mulch“ and „Plough“ calculated from the WRC of samples taken from 12-16cm (the cardinal letters mean the difference between uncompacted (uc) and compacted (c) plots, and small letters the differences between treatments by significant level of $p < 0,05$) (data taken from Fazekas, 2005).

Plot	uc	c
„Mulch“	1,56 Aa	1,58 Aa
„Plough“	1,50 Ba	1,57 Aa

Table 4-10 Distribution of coarse pores for „Mulch“ and „Plough“ calculated from the WRC of samples taken from 12-16cm (the cardinal letters mean the difference between uncompacted (uc) and compacted (c) plots, the small letters define differences between treatments by significant level of $p < 0,05$) (data taken from Fazekas, 2005).

Pore	$\text{Ø} < 50\mu\text{m}$		$\text{Ø} 0,2-50\mu\text{m}$	
	uc	c	uc	c
„Mulch“	3,32 Ab	1,64 Ba	22,4 Aa	22,9 Aa
„Plough“	5,53 Aa	1,99 Ba	22,3 Aa	22,3 Aa

4.1.1.2.2.4 Thermal diffusivity calculated with the damping depth method

In order to assess the accuracy of this method, Figure 4-14 shows the relationship between the phase shift and the amplitude ratio damping depths (d) calculated for uncompacted and compacted plots from 0-30cm and 30-60cm. Both tillage treatments and depths show a good fit with the 1:1 line. Values of damping depths calculated for samples taken from 0-30cm are more concentrated in the middle part of the solid line, while for 30-60cm the data are more spread along the cross line. Differences in d are observed between the sampled depths and the plots. Damping depth reaches greater values for samples taken from 30-60cm and plots before compaction. Compacted samples

show higher values of d_{\min} and lower d_{\max} (for uc samples from depth 0-30cm $d=5-20$ cm and from 30-60cm $d=6,5-22,5$ cm; c samples show 6,5-17cm and 9-21,5cm respectively). Values are related to the phase shift damping depths.

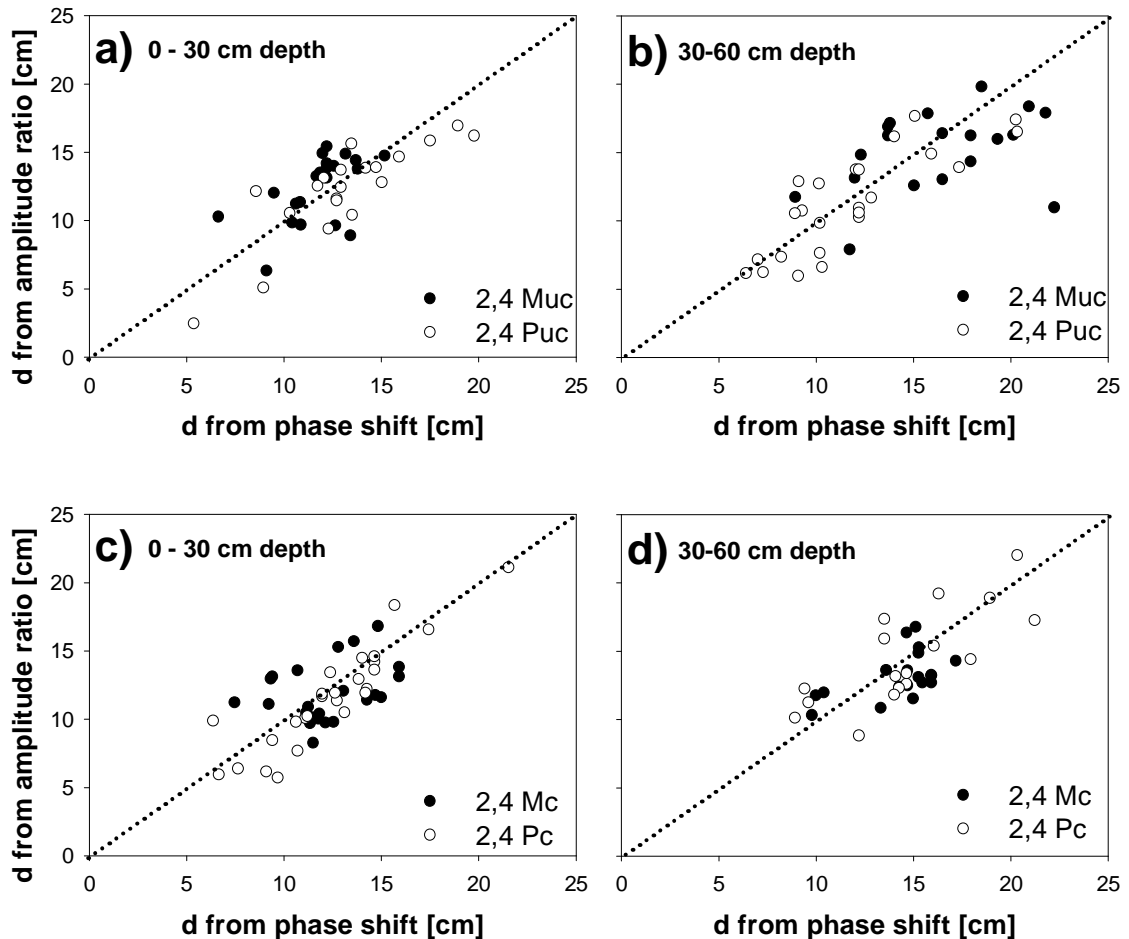


Figure 4-14 Relationship between damping depths (d) calculated from the phase shift and the amplitude ratio for: a) uncompact (Muc, Puc), c) compacted (Mc, Pc) plots from 0-30cm, and b) uncompact, d) compacted plots from 30-60cm.

From calculations of D (with damping depth method for uncompact plots, Figure 4-15 a) it can be seen that the thermal diffusivity for all depths and treatments shows a very weak decreasing tendency with increasing water content ($R^2= 0,02-0,25$). The range of the D ($0,1-1,7 \cdot 10^{-6} \text{m}^2/\text{s}$) for soil samples collected from the topsoil is greater for „Plough“ than for „Mulch“ ($0,3-1,0 \cdot 10^{-6} \text{m}^2/\text{s}$), considering that both investigated treatments (also depths) present similar water content.

Samples taken from deeper horizons (Figure 4-15 b) do not differ between the investigated treatments. However, if we compare the results with those for 0-30cm ($D=0,1-1,7 \cdot 10^{-6} \text{m}^2/\text{s}$), D (especially for M), reaches higher values and the range is $0,2-2,9 \cdot 10^{-6} \text{m}^2/\text{s}$.

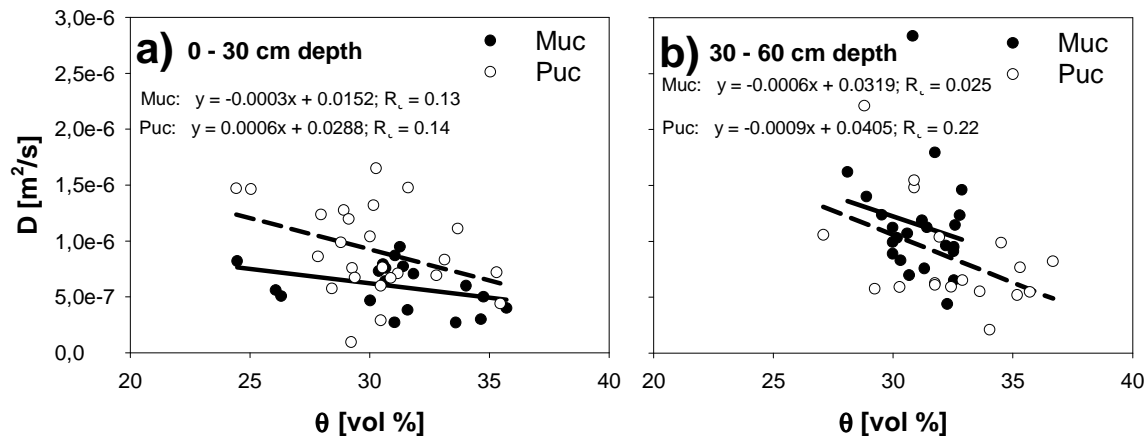


Figure 4-15 Thermal diffusivity calculated with damping depth method for samples taken from Muc, Puc and depth of a) 0-30cm, b) 30-60cm.

In the compacted plots the dependency between depth and treatment shows the same trend as those in the uncompacted plots. In samples taken from 30-60cm depth (Figure 4-16 b) D reaches higher values ($0,01-2,2 \cdot 10^{-6} \text{m}^2/\text{s}$) than those from 0-30cm ($0,03-1,2 \cdot 10^{-6} \text{m}^2/\text{s}$ for M and $0,04-1,5 \cdot 10^{-6} \text{m}^2/\text{s}$ for P) (Figure 4-16 a), where „Plough“ reaches higher values than „Mulch“. D shows a very weak decrease with increasing θ ($R^2 = 0,06-0,25$) (Figure 4-16 a, b).

No important differences were noticed between plots before and after wheeling.

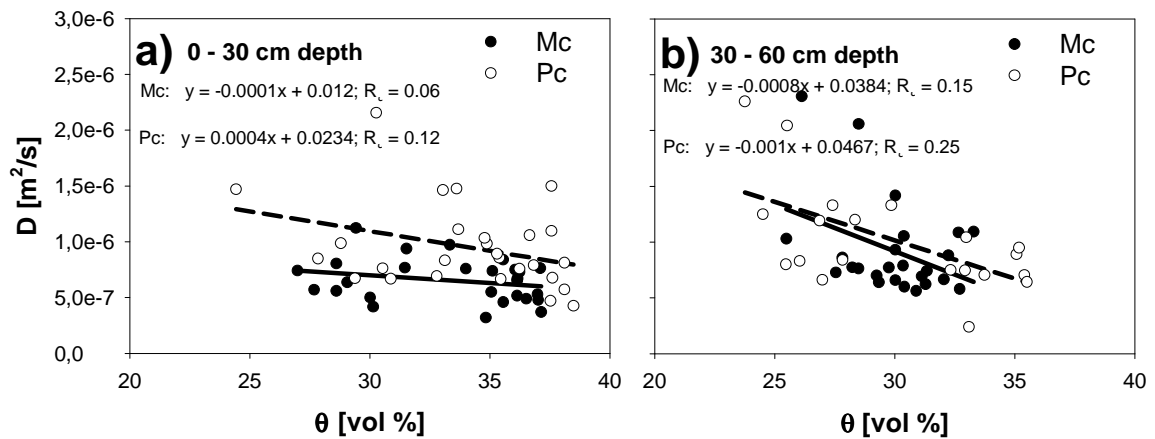


Figure 4-16 Thermal diffusivity calculated with damping depth method for samples taken from Mc, Pc and depth of a) 0-30cm, b) 30-60cm.

The thermal diffusivity values calculated with the damping depth method (Figure 4-15, Figure 4-16) are smaller than those calculated with physical-statistical model, if the treatments before and after compaction are compared (Table 4-3, Table 4-4). This is opposite to those results obtained for the homogenized material (Figure 4-8, Figure 4-9 and Figure 4-10), where D generally reaches the highest values. Calculations from both methods show greater values of D for samples taken from 30-60cm depth.

4.1.2 Field data

4.1.2.1 Soil temperature and thermal properties

In situ temperature was measured at 5 and 15cm depths, in the years: 1995, 1997-2000 from April to September. Shortage of data from October-March is caused by the necessity of removing the equipment during harvesting and winter. In 1996 the equipment was not installed in the soils.

Figure 4-17 informs about the hourly field temperature development in the „Mulch“ plot in 1995. During the day time, the intense solar radiation is absorbed by the soil which warms the ground surface more than the layers beneath. Higher temperature variations (lower T_{\min} and higher T_{\max}) occur at shallow depth (Appendix A). The temperature in 5cm ranged from 3,6 up to

24,9°C in the M-plot during April-September (1995). The average amplitude is 12-19°C and 1,3-2,4°C (Appendix A) at 5 and 15cm, respectively.

Characteristics of the remaining years (1997-2000), are summed up in Appendix A and underline that the temperature development has a similar character - days with the highest temperature (“warm months”) maintained for a longer time appear at the end of May and hold till end of June. Under conventional tillage (P), higher temperature values were measured at 5cm depth (except 1997). At 15cm depth no important differences in the temperature (except 1995 and 2000) between treatments were assessed. Independent of the treatments and depths lower temperature differences were observed in T_{\min} (0,05-1,1°C) than in T_{\max} (0,1-2,5°C). The maximum as well as the average amplitude decreases with increasing depth. “Warm months” show very high differences in amplitudes between investigated depths in 1997, 1998 and 2000, and months with average temperature in 1995.

If the daily average values are considered, T_{\max} as well as T_{\min} reach lower values. The observed (Figure 4-17) time shift in the temperature wave with depth ranges between 4-6 hours.

Temperature development (in 1995) for „Plough“ presented in Appendix B is very similar, however, in June and July T_{\max} it is slightly higher.

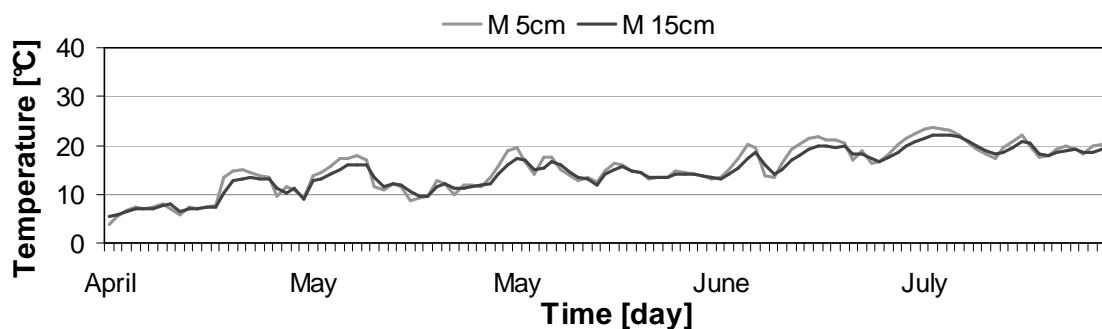


Figure 4-17 Temperature at 5 and 15cm depth under „Mulch“ treatment from April to July 1995.

In order to characterize the relationship between the thermal properties and the water content during the investigated period (1995, 1997-2000), the latter was

simulated, since these data were not available. The results for M and P in 1995 at 5 (M/P5) and 15cm (M/P15) depth are presented in Figure 4-18 as an example. Values of thermal properties and water contents of the remaining years are presented in Table 4-11. It is visible, that in „Mulch“ no differences in θ between depths were observed. This phenomenon can be explained with the pore size distribution which does not show differences between M5 and M15 (data taken from Fazekas, 2005). The observed θ loss is higher for „Mulch“ (46,15vol%) than for „Plough“ for both investigated depths (P5 loss 33,33vol% and P15- 32,25vol%). These changes directly affected the following thermal properties.

The soil thermal properties of the remaining years (summarized in Table 4-11) prove that the conservation tillage treatment in 5cm depth shows higher θ than in P. Average decrease of θ for M is 19,6vol%, whereas for P- 12,3vol%. Also fluctuations of θ during the investigated time period are greater under „Mulch“.

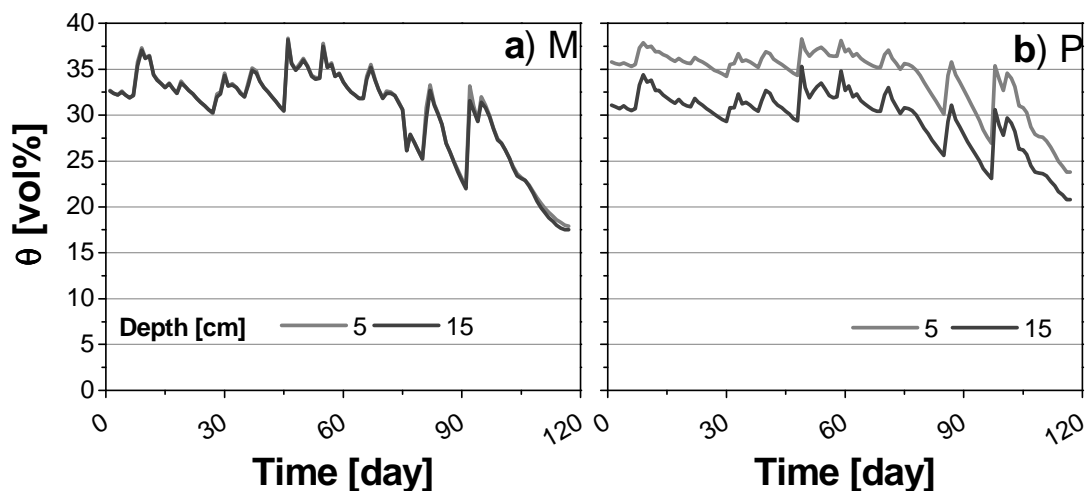


Figure 4-18 Water content development in the field from April to September 1995, for a) „Mulch“ (M) and b) „Plough“ (P) at depths of 5cm and 15cm.

Table 4-11 Maximal and minimal values of volumetric water content (θ), thermal conductivity (λ), volumetric heat capacity (C_v) and thermal diffusivity (D) calculated from field data (average daily values), measured for „Mulch“ and „Plough“ at 5 and 15cm during April- July 1995,1997-2000.

Year	Till. treat., depth [cm]	θ [vol%]	λ [W/mK]	C_v 10^6 [J/m ³ K]	D 10^{-7} [m ² /s]
1995	M5,15	38,4- 17,9	1,023- 0,853	2,77- 1,91	4,45- 3,69
	P5	38,3- 23,8	1,025- 0,924	2,76- 2,16	4,28- 3,7
	P15	35,3- 20,8	1,008- 0,894	2,64- 2,03	4,39- 3,81
1997	M5,15	38,5- 19,5	1,026- 0,874	2,77- 1,98	4,4- 3,69
	P5	38,3- 25	1,027- 0,936	2,76- 2,21	4,23- 3,71
	P15	35,4- 21,7	1,009- 0,906	2,67- 2,07	4,36- 3,79
1998	M5, 15	39,4- 18	1,029- 0,853	2,81- 1,92	4,44- 3,65
	P5	38,7- 21,4	1,028- 0,9	2,78- 2,06	4,36- 3,69
	P15	36,3- 19,2	1,014- 0,872	2,68- 1,96	4,42- 3,78
1999	M5, 15	39,5- 18,9	1,028- 0,859	2,81- 1,95	4,38- 3,64
	P5	38- 34,1	1,023- 0,998	2,59- 2,75	3,85- 3,7
	P15	34,7- 29,2	1,0- 0,96	2,61- 2,38	3,81- 4,04
2000	M5, 15	39,3- 23	1,029- 0,911	2,81- 2,12	4,27- 3,66
	P5	38,6- 27,5	1,026- 0,953	2,78- 2,38	4,11- 3,68
	P15	36,1- 23,6	1,011- 0,917	2,67- 2,15	4,25- 3,77

Figure 4-19, Figure 4-20 and Figure 4-21 show the λ , C_v and D development in 1995 at 5 and 15cm, respectively. Changes of these properties depend on θ changes. C_v and λ take the same and D the inverse direction as water content changes.

Values of thermal properties for the other investigated years (Table 4-11) also show that changes of these properties coincide with those of θ . Values of C_v and λ in 1995 and 1997 do not differ between each other and are for the

remaining years greater than in „Mulch“. Furthermore the D increases with decreasing θ . The highest D values are related to the lowest soil moisture and vice versa (by $\theta=17,9\text{vol}\%$; $D=4,45\cdot 10^{-7}\text{m}^2/\text{s}$ and by $\theta=39,5\text{vol}\%$; $D=3,64\cdot 10^{-7}\text{m}^2/\text{s}$).

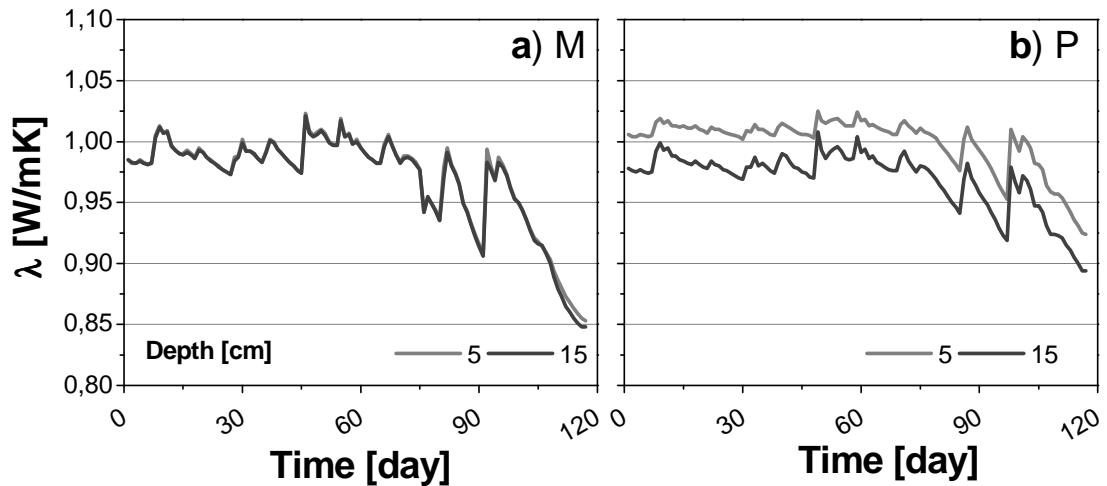


Figure 4-19 Thermal conductivity calculated for the field data from April to September 1995; a) „Mulch“ (M) and b) „Plough“ (P).

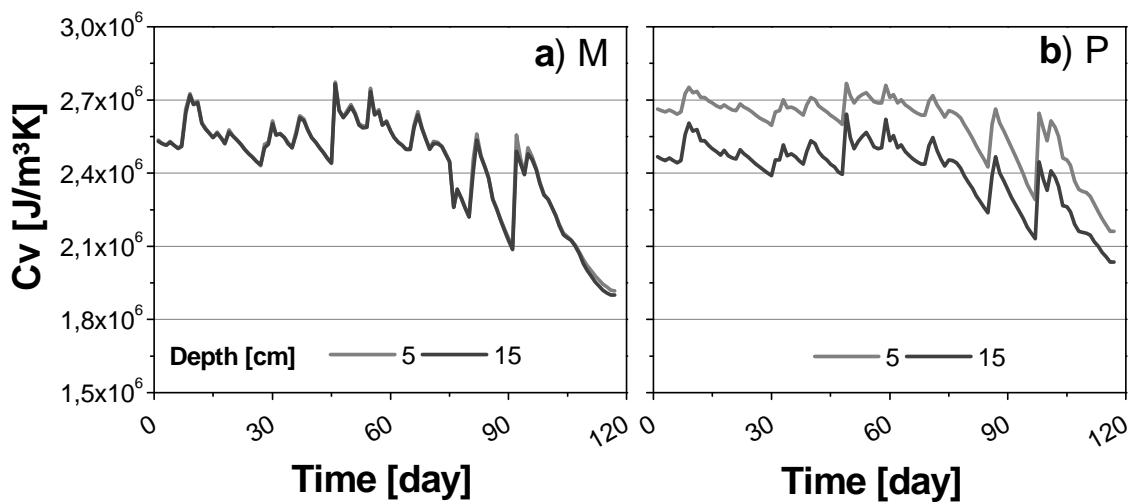


Figure 4-20 Volumetric heat capacity calculated from the field data from April to September 1995; a) „Mulch“ (M) and b) „Plough“ (P).

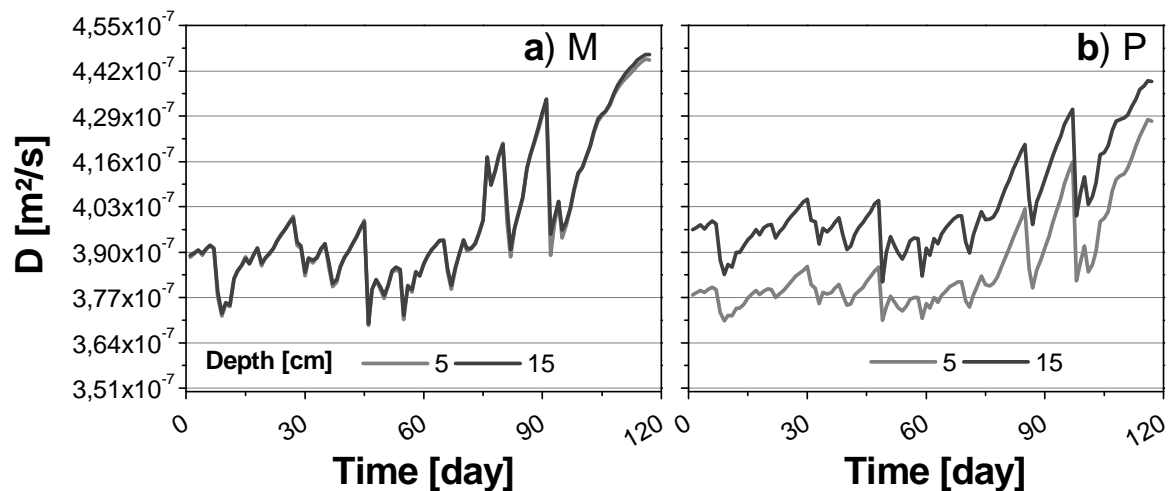


Figure 4-21 Thermal diffusivity calculated from the field data from April to September 1995; a) „Mulch“ (M) and b) „Plough“ (P).

To compare the thermal properties calculated from measurements carried out in the laboratory (soil samples Muc and Puc from 0-30cm) and under field conditions, soil samples and years with similar θ were chosen. It can be seen that, by similar θ thermal properties (except thermal diffusivity for M) as well as the water content show greater values under laboratory conditions.

Generally, however, θ as well as λ , D and C_v in P reach greater values under field conditions.

4.1.2.1.1 Calculations with the damping depth method

The relationship between damping depths (d) calculated from the phase shift and from the amplitude ratio method in 1995 and 1997-2000 (Figure 4-22) is close to the 1:1 line for both tillage treatments. Except 1995 and 1999 no important differences between d_{\min} and d_{\max} for M and P were observed. Minimum damping depths are 5-6,5cm and maximum 9,5cm (in 1995 d_{\max} for P=10,5cm and for M=13,5cm; in 1999 12,8 and 13,8cm, respectively). Damping depths in 2000 were greater than in other years (9-19cm) as a result of very small differences in time at which the two investigated depths reach their T_{\max} . In 1999 and 2000 d calculated with the phase shift method resulted in identical

values ($d=12,73\text{cm}$), because the maximal temperature was measured at the same time in the identical depths.

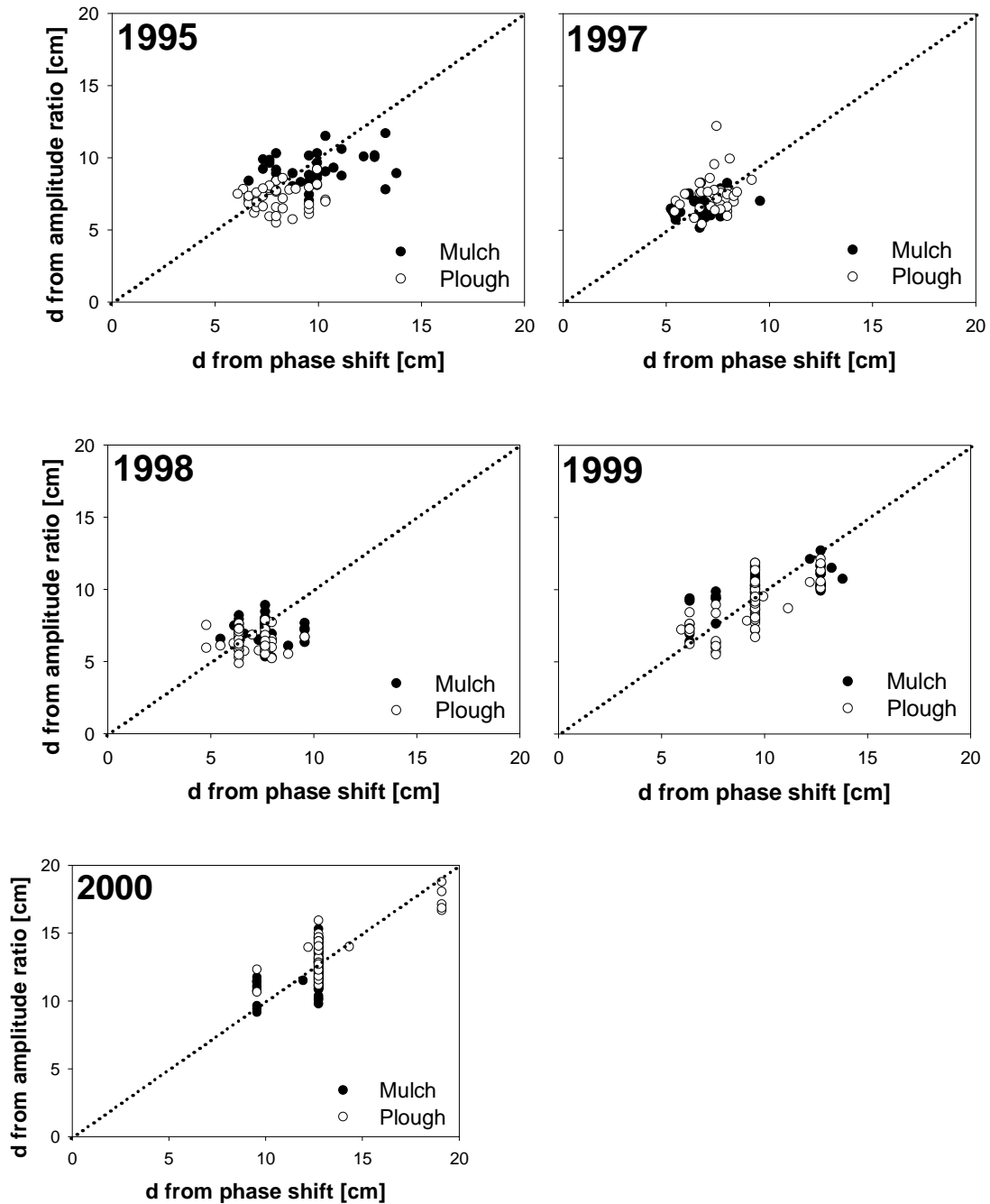


Figure 4-22 Correlation between damping depths (d) calculated from phase shift and amplitude ratio for „Mulch“ and „Plough“ in 1995 and 1997-2000.

Thermal diffusivity D calculated with damping depth method for „Mulch“ and „Plough“ in 1995 and 1997-2000 shows always a slight decrease with

increasing water content except for „Plough“ in 1997 (Figure 4-23). The values of thermal diffusivity for both tillage treatments as a function of θ are mostly identical for the years 1997-2000. In 1995 M shows higher values and in 2000 the range of D is greater (smaller min values) than under „Plough“ for the same values of θ . Similar dependencies were also observed in the temperature development (Appendix A) which can indicate the influence of T on D .

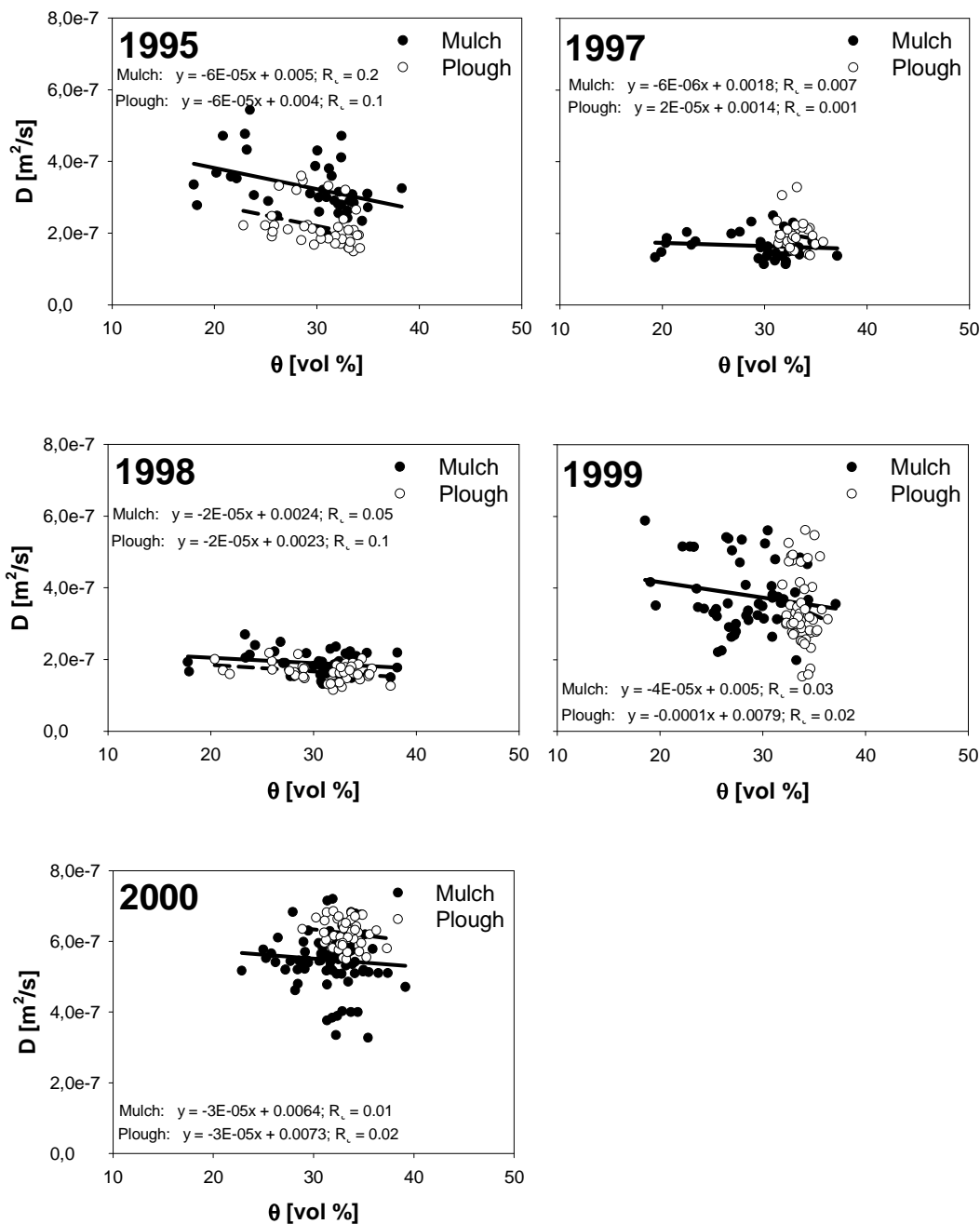


Figure 4-23 Thermal diffusivity calculated with the damping depth method for „Mulch“ and „Plough“ in 1995 and 1997-2000.

Differences in values of D between the two methods are much smaller than those calculated from laboratory measurements. Under field conditions, temperature oscillation is a natural phenomenon, however, because of exceeding the error limit by the damping depth (d) calculations, not all data could be used. In the years 1997 and 1998 („Mulch“) D calculated with the damping depth method is higher while in 1995, 1997 and 2000 („Plough“) is lower if compared with those values calculated with the statistical-physical method.

Thermal diffusivity calculated with this method for soil samples measured under laboratory and under in situ conditions show higher values for the former measurements.

4.2 Hydraulic properties

4.2.1 Pore volume and pore size distribution

The pore size distribution was determined from the water retention curve nominated on samples prepared from homogenized material and different bulk densities (Table 4-12). The soil samples (a particle density of $2,60\text{g/cm}^3$ was assumed to determine the total porosity) do not reach complete saturation. The difference between TP and θ_s becomes smaller with increasing bulk density. With increasing bulk density (in „Mulch“ and „Plough“) the amounts of wide (wCP) and narrow coarse pores (nCP) decrease and those of fine pores increases. The greatest changes were observed for the wide coarse pores ($\varnothing > 50\mu\text{m}$). „Mulch“ samples have a higher field capacity (nWP + MP) and a smaller amount of fine pores than those from „Plough“.

Table 4-12 Bulk density, total porosity (TP), water content at saturation (θ_s) and pore size distribution (PSD) determined from the water retention curve for “Mulch” (M) and “Plough” (P).

Bulk density [g/cm^3]	1,2		1,4		1,6	
Tillage treatment	2 M	2 P	2 M	2 P	2 M	2 P
TP [vol%]	54,4	57,0	47,1	49,4	39,4	38,9
θ_s [vol%]	47,7	50,1	41,5	41,2	34,6	34,9
PSD [vol%]						
> 50 μm (wCP)	14,26	15,07	8,08	8,37	1,22	0,51
50 -10 μm (nCP)	7,64	7,34	8,34	4,21	4,61	2,53
10 - 0,2 μm (MP)	10,75	9,68	7,63	7,33	8,83	6,26
> 0,2 μm (FP)	14,98	18,02	17,39	21,23	19,93	25,28

4.2.2 Hydraulic conductivity

4.2.2.1 Saturated hydraulic conductivity

With increasing bulk density k_f decreases exponentially (Figure 4-24). For each d_B , „Mulch“ presents higher or almost the same k_f value than the „Plough“ plot.

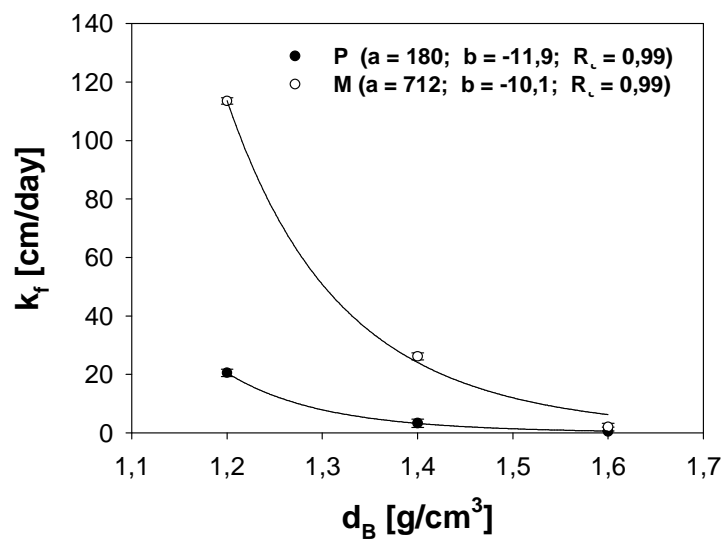


Figure 4-24 Saturated hydraulic conductivity (k_f) for three bulk density (d_B) values (1,2-1,4-1,6g/cm³) for „Mulch“ (M) and „Plough“ (P).

4.2.2.2 Unsaturated hydraulic conductivity

The unsaturated hydraulic conductivity decreases for both “Plough” and “Mulch”, but with lower intensity in samples prepared with $d_B=1,6\text{g/cm}^3$ (Figure 4-25).

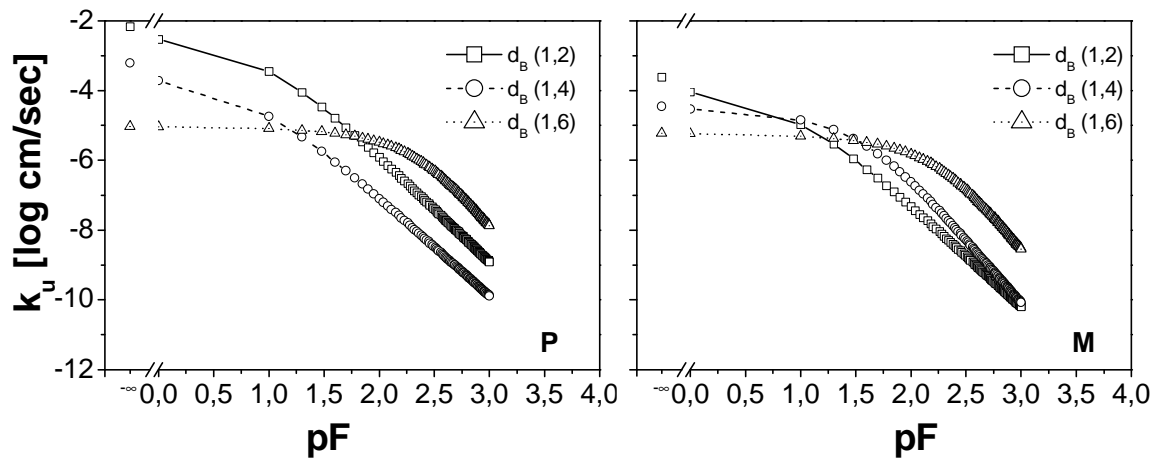


Figure 4-25 Simulated unsaturated hydraulic conductivity (k_u) for three bulk densities for a) „Plough“ (P); b) „Mulch“ (M).

Differences in k_u observed in P at pF 3,0 reach almost one order of magnitude depending on d_B , while for „Mulch“ this situation was not observed as a result of the faster decrease of k_u at $d_B=1,4$ than at $1,2\text{g/cm}^3$.

4.2.2.3 Air conductivity measurements

4.2.2.3.1 Air conductivity

In P the air conductivity is greater than in M, both at -60 and -150hPa (Figure 4-26 a and b). Values for M are homogeneous in the total soil profile, in contrast with k_l for P. The air conductivity for P presents the highest values at 2,5cm depth and then decreasing with increasing depth. As the soil drains, the volume of air-filled pores increases, and consequently also the air conductivity.

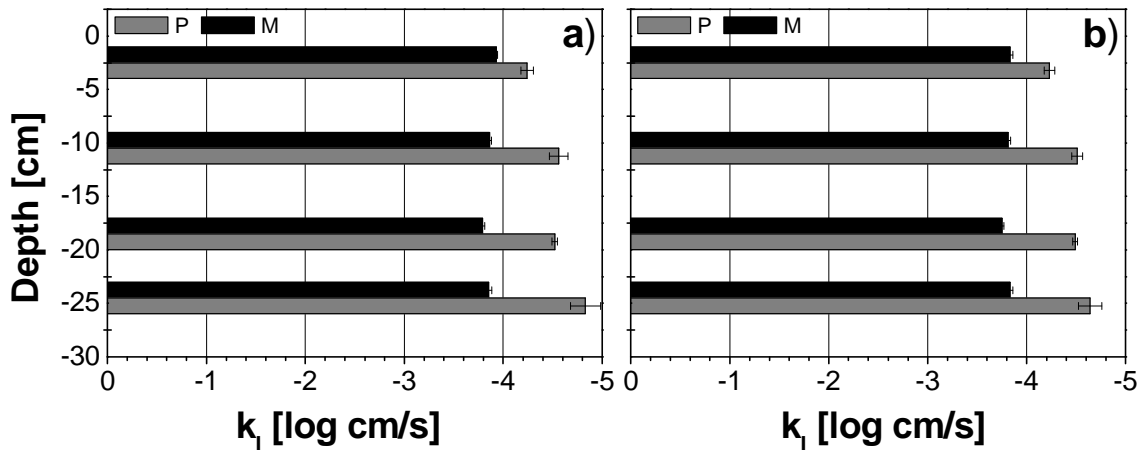


Figure 4-26 Air conductivity (k_l) for samples taken at different depths from „Mulch“ (M) and „Plough“ (P); k_l at a) -60hPa and b) -150hPa. Samples were collected from big cylinders (850 cm^3) with an initial bulk density of $1,4 \text{ g/cm}^3$.

For M, k_l increases at -500hPa (Figure 4-27). In addition, in P (at -60 and -150hPa) and M (at -500hPa) k_l decreases with increasing depth.

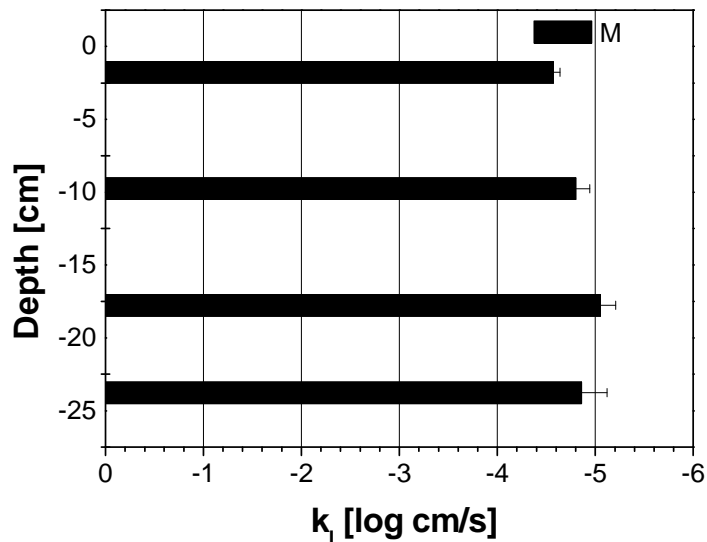


Figure 4-27 Air conductivity (k_l) measured at -500hPa. Samples taken at different depths from „Mulch“ (M) were collected from big cylinders (850 cm^3) with an initial bulk density of $1,4 \text{ g/cm}^3$.

Air conductivity (k_l) decreases exponentially with increasing bulk density. With increasing d_B , differences in k_l depending on water tension become smaller and are represented by the parameters of the exponential regression (Figure 4-28).

The relationship between d_B and k_i was fitted with an exponential model ($y=ax^b$). Parameters and regression coefficients are presented in Table 4-13

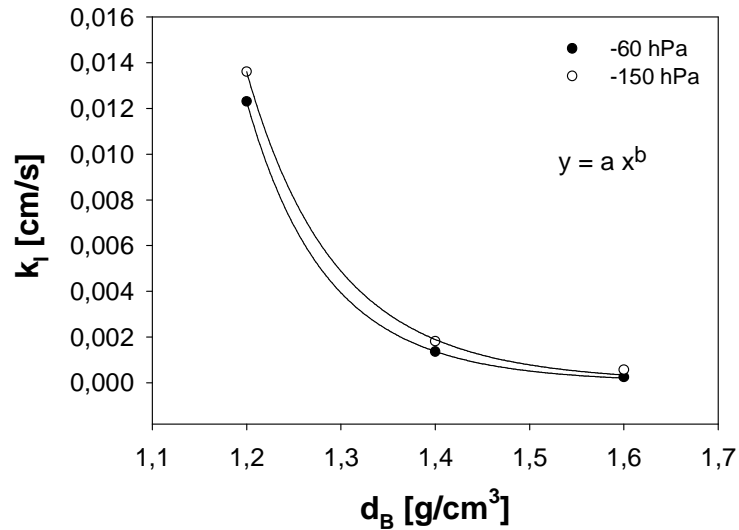


Figure 4-28 Air conductivity (k_i) of homogenized material depending on bulk density (d_B) and matric potential.

Table 4-13 Regression parameters and coefficients for the relationship between air conductivity (k_i) and bulk density (d_B).

Water tension	a	b	R ²
[hPa]	[-]	[-]	[-]
- 60	0,17	-14,2	0,99
- 150	0,14	-12,8	0,99

4.2.2.3.2 Relationship between air permeability and air-filled porosity

Changes in the geometry of the pore system depending on d_B , continuity parameters were derived from the relationship between ε_a and k_a .

Table 4-14 K_1 -value (k_a/ε_a) determined at -60hPa for „Mulch“ and „Plough“.

Depth [cm]	M K_1 [$\mu\text{m}^2 \cdot 10^2$]	P K_1 [$\mu\text{m}^2 \cdot 10^2$]
2,5	2,15	4,42
8,5	1,67	6,56
18,5	1,59	10,72
24,5	0,69	6,58

K_1 in P increases with increasing depth till depth of 18,5cm. The opposite was observed in M. At the same matric potential (-60hPa), the capacity of the soil to conduct air is higher in P than in M (Table 4-14 and Figure 4-26 a) and b)).

Table 4-15 presents K_1 for air permeabilities measured at different bulk densities and matric potentials. For $d_B=1,2\text{g/cm}^3$, the continuity parameter K_1 does not change (average value $\sim 7,3\mu\text{m}^2 \cdot 10^2$) depending on the air-filled porosity. This situation, however, was not observed at $d_B = 1,4$ and $1,6\text{g/cm}^3$, since quite high values were measured at matric potentials of -150 and -60hPa at $d_B=1,4$ and $1,6\text{g/cm}^3$, respectively.

Table 4-15 K_1 (k_a/ε_a) depending on bulk density and matric potential.

Maric potential [hPa]	K_1 ($d_B=1,2\text{g/cm}^3$)	K_1 ($d_B=1,4\text{g/cm}^3$)	K_1 ($d_B=1,6\text{g/cm}^3$)
	[$\mu\text{m}^2 \cdot 10^2$]	[$\mu\text{m}^2 \cdot 10^2$]	[$\mu\text{m}^2 \cdot 10^2$]
-60	7.82	1.83	5.58
-150	6.89	7.09	1.19
-300	6.78	1.45	0.74
-500	7.62	1.38	1.09

The relationship between ε_a and k_a was fitted with an equation proposed by Ball et al., (1988) (Figure 4-29). The regression parameters and blocked porosities (ε_b) at different bulk densities are presented in Table 4-16.

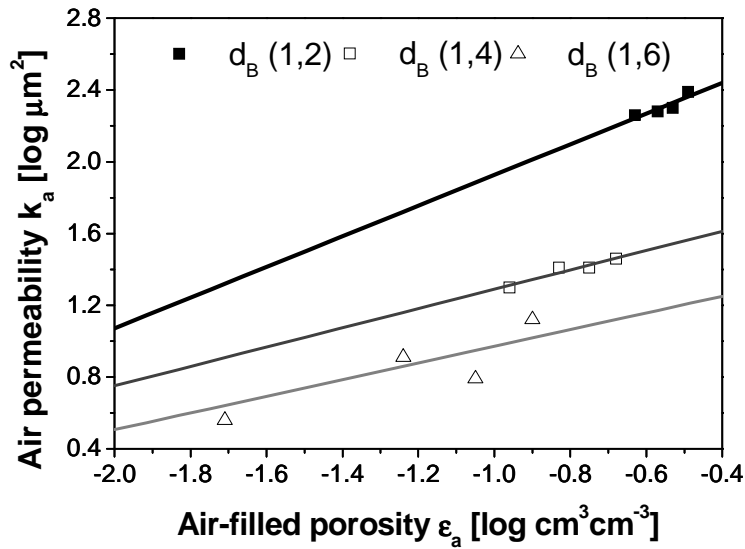


Figure 4-29 Relationship between air permeability (k_a) and air-filled porosity (ε_a) depending on the bulk density for samples taken from „Plough“.

Table 4-16 Regression parameters and blocked porosities (ε_b) depending on bulk density (d_B).

d_B [g/cm ³]	Log M [-]	N [-]	R ² [-]	ε_b [vol%]
1,2	2.78	0.85	0.79	0.05
1,4	1.82	0.53	0.92	0.04
1,6	1.55	0.58	0.78	0.21

Since the volume of air-filled pores decreases with increasing bulk density, the air permeability decreases as well. The effect of the bulk density on the air permeability is represented by the slope of the regressions (N) and the blocked porosities (ε_b). With increasing bulk density N tends to decrease. Greater differences are observed in the volume of blocked pores, since by $d_B=1,6\text{g/cm}^3$ ε_b reaches 0,21%. This shows that a large volume of air-filled pores does not take part in air transport by convection.

4.2.3 Shrinkage

4.2.3.1 Development of shrinkage curves

Shrinkage curves of disturbed soil samples (homogenized material) as a function of bulk density (1,2; 1,4; 1,6g/cm³) are shown in Figure 4-30 for „Mulch“ and „Plough“. For all densities and tillage treatments only a minimal shrinkage was determined. The curves do not start at the 1:1 line showing that the samples have not reached a complete saturation. Generally, with increasing d_B the void ratio (e) and the moisture ratio (ϑ) at saturation both decrease. Additionally, with increasing d_B the shrinkage curves become shorter and flatter. Samples prepared from „Plough “ (Figure 4-30 a) and „Mulch“ (Figure 4-30 b) at $d_B=1,2\text{g/cm}^3$ show a nearly normal shrinkage close to saturated conditions, i.e.: the volume decrease equals the water loss. A residual shrinkage predominates in all investigated samples. For the homogenized samples with an initial bulk density $d_B=1,4$ and $1,6\text{g/cm}^3$, only residual shrinkage was observed. This implies that the release of water is higher than the volume change as the soil drains.

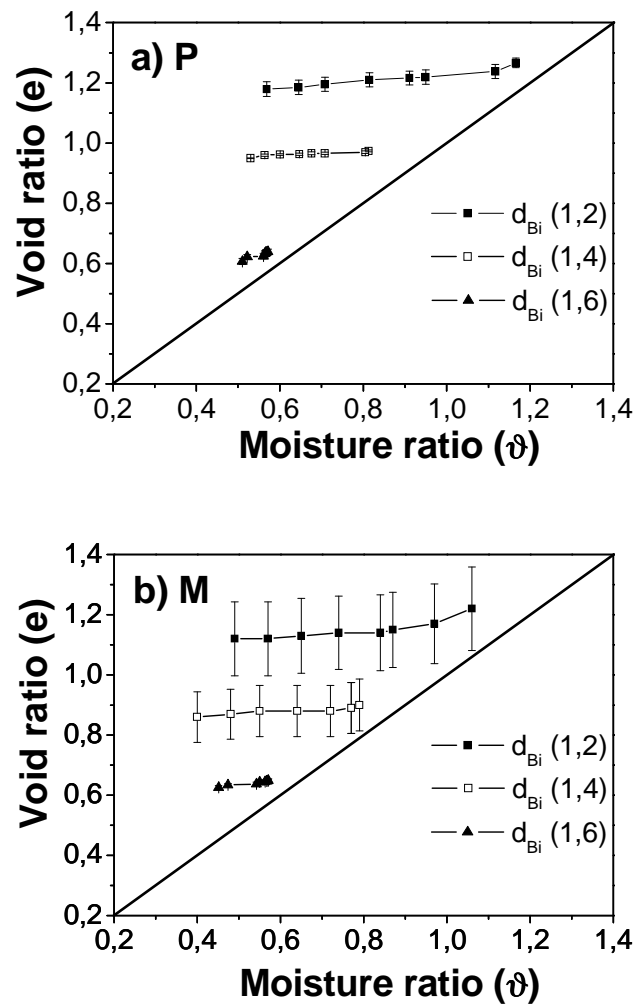


Figure 4-30 Shrinkage curves for disturbed samples from a) „Plough“ (P) and b) „Mulch“ (M) for three bulk densities (d_{Bi}) of 1,2; 1,4 and 1,6g/cm³. The error bars show the standard error (n=4).

4.2.3.2 Shrinkage capacity

The shrinkage capacity is defined as the difference between maximum (at saturated conditions) and minimum (at -500hPa) void ratio. Figure 4-31 shows that the shrinkage capacity decreases exponentially with increasing bulk density. This decrease in the shrinkage capacity is greater in „Mulch“ than in „Plough“ derived from the slope of the regression.

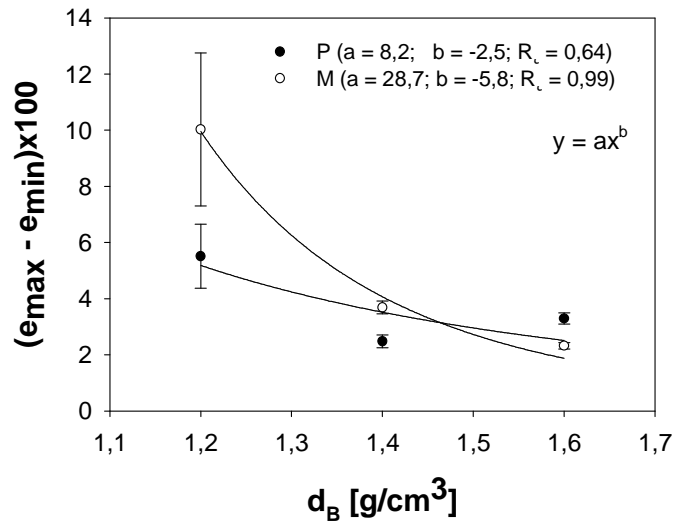


Figure 4-31 Shrinkage capacity for homogenized samples prepared from „Plough“ (P) and „Mulch“ (M) for three bulk densities (d_B): 1,2; 1,4; 1,6g/cm³.

4.2.3.3 Effect of shrinkage on the volumetric water content

Figure 4-32 presents the effect of shrinkage on volumetric water content for samples prepared from homogenized soil material, three different bulk densities (1,2; 1,4; 1,6g/cm³), and two tillage treatments: „Mulch“ (Figure 4-32 a) and „Plough“ (Figure 4-32 b). As the soil drains some structural changes take place. These changes can be expressed as differences in water content ($d\theta$) with and without consideration of shrinkage in relation to the volumetric water content at saturation (equation 4-1). The dashed line represents the situation for the soil assumed as a rigid body, when no changes in the volumetric water content due to shrinkage taking place.

$$d\theta = ((\theta_{rs} - \theta_{dh}) / \theta_s) * 100$$

Equation 4-1

where:

θ_{rs} = water content (vol) of rigid soil [vol%]

θ_{dh} = water content (vol) corrected by shrinkage [vol%]

θ_s = water content (vol) at saturation [vol%]

With decreasing bulk density, $d\theta$ increases showing that the structural changes due to shrinkage are larger. Samples prepared from „Mulch“ are more susceptible to shrinkage than those from „Plough“ at $d_B=1,2\text{g/cm}^3$. Additionally with d_B increase the curves are flatter and deviations of the volumetric water content (θ) from the dashed line appear later.

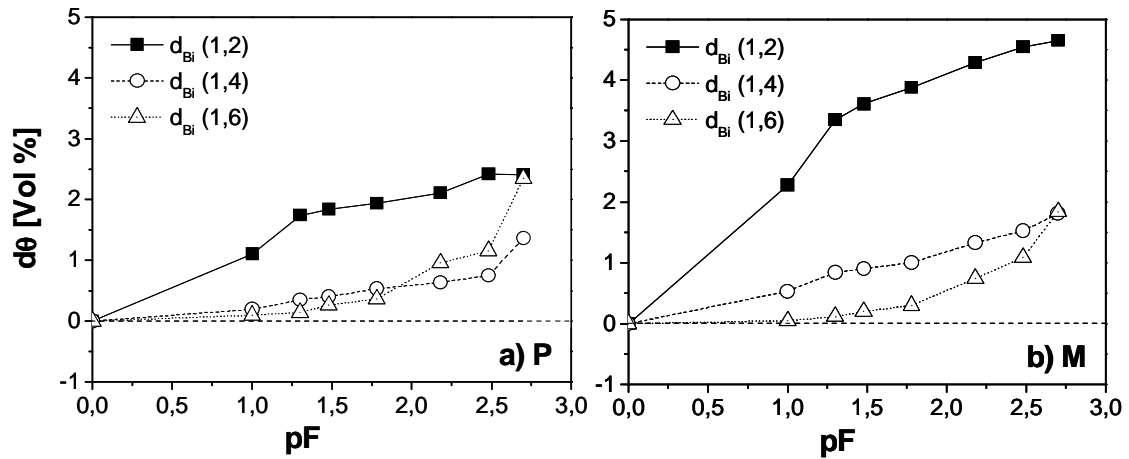


Figure 4-32 Effect of shrinkage on volumetric water content. a) „Plough“ (P) and b) „Mulch“ (M) at three bulk densities (1,2; 1,4; 1,6g/cm³). The dashed line represents the situation for a soil assumed as a rigid body.

5 Discussion

5.1 Effect of aggregate formation on thermal properties

Thermal properties of structured and homogenized soils are influenced by the number of contact points among particles and the degree of saturation at a given pore water pressure through the changes in the number of particles per aggregate volume and variations in the particle arrangement. The existing particle-particle connections between aggregates on account of their rearrangement in time lead to the cementation of these connections (Dexter et al., 1988). It is well known, that the first aggregation process is due to soil shrinkage resulting firstly in vertically orientated cracks forming a prismatic structure. Repeated wetting and drying cycles creates smaller aggregates through a rectangular crack propagation followed by shear-induced formation of blocky and subangular-blocky structure (Horn, 1994). As a result of swelling and shrinkage processes, the single aggregates become denser initially with a higher bulk density and strength increasing the particle contact area being the path for heat conduction. However, as mentioned by Horn (1993), with increasing wetting and drying cycles, the bulk density of soil aggregates may be reduced while the strength at the same time increases affecting, consequently, the heat conductivity in the soil. Since the soil is not a rigid body, we can expect that structural changes induced by swelling and shrinkage may affect not only hydraulic but also thermal properties as well, playing, consequently, an important role in the movement of water and heat in soils.

In the presented work, results derived from calculated thermal properties for different values of bulk density at a constant water content (samples prepared from homogenized material) show that the transfer of heat increases as the bulk density of the soil increases as was also described by Abu-Hamdeh and Redder (2000). However, the heat conductance in the soil depends not only on the continuity of contact points, but also on its water content, because at a low water content the distribution and geometry of water menisci play an important

role on heat conduction. Thus, each contraction of particles and the formation of new aggregates changes both the number of contact points but also the contact area which again alters the heat conduction, since aggregates with different forms and sizes affect the movement of water in soils and, consequently, their thermal properties. Regarding the ability to form water films around the soil particles the contact area between them is enlarged and the cross-sectional area which conducts the heat increased (Hanks and Ashcroft, 1980; de Vries, 1996). Heat conductivity and soil thermal diffusivity increase rapidly (Kaune et al., 1993), as soon as dry soil particles are surrounded by water films. Therefore, changes in water content due to the development of soil structure can affect the heat conduction and soil thermal diffusivity. Horn et al., (1994) investigated changes in soil thermal properties caused by various soil structures. They pointed out higher λ and D in structured than in disturbed loess as a function of water content. Similar, Arshad and Azooz (1996) assessed a greater thermal conductivity in undisturbed soils, apparently due to the different distribution and geometry of water menisci. Also Kaune et al., (1993) investigated the effect of aggregate formation on thermal properties and assessed higher λ in lysimeters with structured than in those with disturbed soil. Results from these papers are in agreement with some of those estimated in the presented work if homogenized and compacted samples with similar water content and bulk density are compared. However, investigations made by Ghuman (1985), showed lower λ for a gravelly soil measured under in situ conditions than those ones of homogenized material under laboratory conditions. This phenomenon was related to the heterogeneity of the soil profile and especially to the presence of stones.

Also the soil temperature itself is affected by the number of contact points between particles. Higher T_{\max} can be expected with increasing d_B , which is in agreement with the temperature development in undisturbed samples from the compacted plots which resulted in higher maximal temperatures than in the uncompacted ones. However, not only the total bulk density but also the arrangement of particles inside single aggregates defines their thermal properties. The measured temperature in the topsoil (5cm depth) under field

conditions as well as in some of the undisturbed samples show lower T_{\max} in „Mulch“, whereas the inverse was observed in the annually disturbed „Plough“. These findings are also in agreement with those of Burrows and Larson (1962), Al-Darby and Lowery (1987), Kovar et al., (1991), Raimbault (1993) and Drury et al., (1999) who also reported lower soil temperature under no-tillage treatment due to uneven i.e.: interrupted physical conditions (e.g.: surface crop residue which has a high solar reflectivity and acts as an insulating layer) than in the ploughed layer and at the soil surface compared to conventional tillage. Radke (1982), investigated relations between soil water and temperature, and observed lower temperature by higher soil moisture. He said that the soil warming under wet conditions is impeded due to greater soil heat capacity and more energy being used for water evaporation than warming the soil.

5.2 Effect of soil management on soil thermal properties

Different soil management systems (e.g.: conventional or conservation, zero tillage or ecological farming, presence or lack of crop residue on the soil surface), affect their physical, hydraulic and, consequently, thermal properties. Crop residue has a major impact on soil thermal conductivity and heat capacity (Walczak and Usowicz, 1994) regarding their ability to reflect soil radiation, reduction of evaporation (van Wijk et al., 1959) and also affect the net heat exchange (Hanks et al., 1961; Hay et al., 1978), the temperature gradient and the heat transfer. Also the different structure formation affected by tillage management alters the soil temperature and the thermal properties of soils. Without ploughing the soil will stay always dense, and, therefore, it can be expected that the soil temperature under the conservation tillage is higher than under conventional one. This effect, however, can be diminished when straw or plant material remains at the soil surface reflecting the solar radiation. These effects, influencing the rate of the water losses from the soil through evaporation (or evapotranspiration if plants are present), differ for bare soil and these one with the plant cover and, consequently, differences in the soil temperature are to be expected (Horton et al., 1994).

Thermal conductivity and volumetric heat capacity are also affected by the tillage practices (Allmaras et al., 1977; Abu-Hamdeh, 2000; Tyson et al., 2001) because of the tillage-induced soil compaction, which increases the bulk density and the penetration resistance but creates a platy structure, which affects the water movement in the first centimeters of soil. Furthermore, measured (T , θ) and calculated (C_v , λ , D) properties are affected by changes in soil organic matter, aggregate size distribution, and water retention which vary for „Mulch“ and „Plough“ (Azooz and Arshad, 1995). Loosening of soil by tillage decreases the amount of organic matter, but destroys the aggregate stability and alters the heat flux through a changed surface roughness (Potter et al., 1987). This, in turn changes the area of the soil surface which is in contact with the atmosphere and, consequently, decreases heat conductivity and thermal diffusivity (Johnson and Lowery, 1985; Noborio and McInnes, 1993; Arshad and Azooz, 1996; Nidal et al., 2000). Soil disturbance due to tillage can also shift or change the air to soil particles volume by creating additional air pockets (Licht and Al-Kaisi, 2005) that can be responsible for reducing the heat capacity of the tilled zone.

The contact area between soil particles or aggregates affected by tillage-induced homogenization of the soil changes their thermal properties as well. Because soils shrink and swell, their thermal properties change temporarily especially immediately after soil tillage due to structure reformation. The intensity of these changes depends on the characteristics of the soil management and soil material.

Since soil structure is more stable under conservation tillage, leading to enhanced particle contacts, thermal conductivity in the presented study is slightly greater under this treatment than under the conventional one. Thermal conductivity values reported here range between 1,05 and 0,95W/mK for Mulch uncompacted and between 1,0-0,93W/mK for Plough uncompacted. These data are much higher than those presented by other authors like e.g.: Nidal et al., (2000) who determined 0,78-0,45W/mK and 0,72-0,33W/mK for no-tillage, and ploughed plots, respectively (compacted plots show the same

dependencies). These differences, however, are caused by the higher water content in this study, which, as reported by Hopmans and Dane (1986), Azooz and Arshad (1995), de Vries (1996) and Hillel (1998), is the most important factor affecting this property. The heat conductivity decreases with the tillage intensity, which was detected also in the presented dataset for samples taken from the topsoil before and after compaction for both tillage treatments. These results agree with those of Nidal et al., (2000) who investigated clay loam and loam soil and estimated the highest heat conductivity for no-tillage and the smallest for rotary tillage.

The estimated values of heat capacity in the present analysis show the same dependencies between treatments as for heat conductivity. Under unwheeled conservation tillage treatment C_v ranged between $2,85-2,38 \cdot 10^6 \text{ J/m}^3\text{K}$ and under unwheeled conventional between $2,6-2,25 \cdot 10^6 \text{ J/m}^3\text{K}$. Regarding the relations between the volumetric heat capacity and water content, it can be concluded that these differences are caused mainly by the magnitude of θ in the investigated treatments. This agrees with results presented by Johnson et al., (1985) who also assessed the higher values of C_v in no-tillage than in conventional (moldboard) tillage and explained this with reference to the effect of the water content.

Soil thermal diffusivity is also affected by the tillage treatment and as reported by Johnsons et al., (1985), Anandakumar et al., (2001) it depends on the volumetric water content in the soil. This is in agreement with our results, as soil water content can be amended by tillage, which in turn can influence thermal conductivity, volumetric heat capacity and, consequently, the soil thermal diffusivity. In our study, similar to that of Arshad and Azooz (1996) lower thermal diffusivity was observed in uncompacted „Mulch“ (with higher θ). This was probably caused by a proportionally greater value of C_v to smaller λ what results in smaller thermal diffusivity being the factor of these properties. Results from sampled depth of 30-60cm and uncompacted plots show lower water content in „Mulch“ than in „Plough“, which results in higher values of D under conservational tillage treatment. At this depth, however, the bulk density was

higher than in the topsoil and leads to increase of thermal diffusivity. Johnsons et al., (1985) also investigated the influence of tillage treatment on thermal diffusivity and contrary to Arshad and Azooz (1996) assessed higher values in no-tillage system.

It is also to be mentioned that for the interpretation of estimated results not only physical properties, but also factors like sampling depth have to be regarded. Anandakumar et al., (2001) said that the soil layer can be regarded as homogenous since its thickness is only 10cm. In deeper parts, soil thermal properties, due to differences in the composition of the soil and change in water content, can differ from those at the top layer. For example, Flint and Childs (1987) assessed higher λ in deeper soil layers which was related in this case to the greater rock fragment percentage in the subsoil. Kovar et al., (1991) concluded that the influence of tillage practises on root distribution, soil temperature and soil water content reaches at least a depth of 30cm (if the ploughing depth is 25cm).

5.3 Effect of soil structure of water retention, hydraulic conductivity and rigidity as the basic for thermal properties

The soil as a porous media consists of the solid, liquid and gaseous phases. The proportion of these phases changes continuously, and is affected by climate, vegetation and soil management (Hillel, 1998). When the structural changes due to tillage (e.g.: soil compaction) take place an increase in bulk density and the change of the proportion of these phases take place. Thus soil physical properties due to internal (wetting and drying) and external (soil compaction) forces changes and, consequently, transport processes in soils, the biological activity and plant growth are affected as well. These aspects are reported by many authors (Ehlers, 1973; Parker, 1982; Wierenga et al., 1982; Nimmo and Akstin, 1988; Ahuja et al., 1998; Hartge and Horn, 1999; Richard et al., 2001; Landefeld et al., 2003; Sillona et al., 2003; Dörner, 2005). Soil compaction induces therefore not only a rearranging of soil grains to decrease

pore void space, change the pore size distribution, thereby increasing the d_B (Hartge and Horn, 1999; Horn and Baumgartl, 1999; Defosse et al., 2002), but leads also to changes in space variability of soil properties (Shein, 2000), which transfer the movement of matter in soil cover and change the soil functions in the biosphere (e.g.: water cycle). Since not only changes in the volume and the distribution of pores in the soil but also in the pore functions occur, it is to be expected that the thermal behaviour is affected as well. With increasing bulk density increase the number of contact points between particles (Hartge und Horn, 1999) affecting the capacity of soil to transport water and air since the continuity of the pore system is damaged as well (Chapter 4.1.2.3. and 4.2.1.1.). The change of the proportion of phases (water and air) with increasing bulk density and in pore continuity affects therefore also the thermal properties of the soil since their own properties govern the transfer of heat meaning that hydraulic and thermal processes in soils are linked.

The presented results indicate that soil compaction due to an increase in d_B leads to a decrease of structural pores reducing the saturated and unsaturated hydraulic conductivity (the last one in the pF range near saturation). This, in fact, results in a retarded warming or longer cooling process as far as the movement of water in soils became slower. Consequently, the soil thermal regime depends on soil moisture and its state in the soil which results in the urgent need to include the hydraulic properties if thermal properties have to be studied as carried out by many authors (Hopmans and Dane, 1986; Peth, 2004). Under saturated conditions soils are good heat conductors, based on the high ability of water to lead the heat. As the soil dries the air-filled pores increase and the unsaturated hydraulic conductivity decreases affecting the governing processes included in heat transport since the heat will be conducted mostly through the contact points between soil particles or aggregates. It is to be expected that the slower movement of water under unsaturated conditions together with entrapped air will retard the heat transport in soils (Marczewski and Usowicz, 2005).

From our results we observed that, during the daily temperature oscillation (warming and cooling phases) water evaporates from the samples with different intensity for the single investigated depths. Therefore, as a consequence of a more intense shrinkage (including crack formation) at the soil surface, air permeability decreases with depth which due to an increased amount of air-filled pores increases the air conductivity. Similar results were also reported by Ball et al., (1988). The increased air flow in the soil also affects their thermal properties regarding their very small heat conductivity and volumetric heat capacity of the air playing the role of a time dependent and induced-isolation. The increase of the air-filled pores may create some areas acting as isolation for the heat flow. The magnitude of the isolation will depend on the saturation degree and on the continuity of the pores because of its relevance in the rate of opening of air-conducting pores (Ball et al., 1988, see chapter 4.2.1.3.2.). Regarding the thermal conditions which are needed for seed germination the magnitude of the soil temperature is especially important for the topsoil where the highest decline of saturated hydraulic conductivity and air permeability are observed (Fazekas, 2005).

Investigations about the influence of compaction on unsaturated hydraulic conductivity amongst others were made by Sillona et al., (2003). Similarly to the presented results they also pointed out higher k_u conductivity in the compacted plot than in the tilled plots in a calcareous soil (Rendzina). Froehlich and McNabb (cited in McNabb et al., 2001) detected a tillage-induced increase in bulk density which caused an increase in soil strength but a decrease in air-filled porosity, infiltration rate and hydraulic conductivity (Ankeny et al., 1995). This phenomenon was also observed by Fazekas (2005), who analyzed the same soil types. She assessed for both investigated treatments („Plough“ and „Mulch“) a sharp decrease of k_f after a single wheeling. The temporal and tillage-induced changes on pore functions will affect the thermal behavior of the soil as mentioned previously showing that the thermal properties are time dependent as well.

The shrinkage and the crack formation influence the temperature and water content distribution as assessed by Selim and Kirkham (1970). Under controlled laboratory conditions they investigated samples with artificial cracks, and, pointed out that temperature in soil with cracks after 4 days of wind drying decreases approximately 1-2°C and under radiation it increases by about 5-10°C. Evaporation through crack walls caused lateral movement of water and can increase in the range of 12-30% depending on the crack width.

From our results we assessed that the changes in water content induced variations of the soil volume since water menisci are formed (see chapter 4.2.3.). Soil shrinkage implies that soil particles become closer and consequently the contact area becomes larger as well. On the other hand as the soil shrinks, the volumetric water content increases inside single aggregates, which may not affect the crack volume, but causes heterogeneous heat transport. This fact reveals that the thermal properties of the soil change as soon as structure formation takes place.

5.4 Critical ideas about the methods applied

5.4.1 Interpretation of data made by repacked soil samples

In data interpretation it should be considered that in spite of preparation of samples with a frame compression device, some discrepancies from homogeneity in the soil sample may occur, which in such an investigation can not be neglected, if we try to assess the effect of the bulk density and soil structure on soil physical properties. Oliviera et al., (1996) mentioned that the value of bulk density in repacked samples differs in soil samples showing greater values near the surface of the sample. Ripple et al., (1973), Nimmo et al., (1988) and Schiegg (1990) stated that it is difficult to achieve a homogenous and consistent repacked porous media even with a media having a narrow particle-size distribution. However, the method used to prepare the repacked material allows us to get samples with a high homogeneity, which is also proved

by the low dispersion of the data (especially for the saturated hydraulic conductivity).

5.4.2 Determination of thermal diffusivity

In order to describe the thermal behavior of the soils studied, two methods were used and compared: damping depth and statistical-physical method. The problem of comparing different results by using various methods is not new and was already discussed by Horton and Wierenga (1983) and Ghuman and Lal (1985). The data show that the calculated thermal diffusivity differs between the methods used. Thermal diffusivity calculated with the damping-depth method in almost all cases was higher than those estimated with the statistical-physical model.

The damping depth method was already used by Horton and Wierenga (1983), Chacko and Renuka (2002), and Peth (2004). This method does not always give good results, since some conditions, which have to be satisfied, are difficult to reach under laboratory conditions (i.e.: the values of damping depth calculated by the phase shift and the amplitude ratio of the temperature wave must be close). Van Wijk (1963) pointed out that this method is valid for a homogenous soil of infinite depth. Wierenga et al., (1969, 1982) assessed that when the water content changes considerably with depth, or when the surface temperature wave is not a periodic function (method main establishment) this method can not be used. Under laboratory conditions, where the simulation of daily oscillation was created manually (taking 21 hours), it was very difficult to reach a pure harmonic temperature wave. Such harmonic temperature development, however, is also difficult to estimate under field conditions, since the soil temperature depends on the processes in the surrounding environment (e.g.: days with clouds, rain or even strong wind). Furthermore, the interaction of temperature on the soil surface, and consequently the evaporation causes continuous changes of water content over time under field as well as under laboratory conditions. The problems in reaching the boundary conditions and the continuous changes on the water content have to be considered in such an

approach being determinant in the estimation of results. Peth (2004) and Wierenga et al., (1969, 1982) pointed out that in many cases the differences between values of damping depth estimated from phase and ratio relations were too large.

The second approach used for calculations of thermal diffusivity as well as for other thermal properties is the statistical-physical model of thermal conductivity described by Usowicz (1991, 1992) and used by Walczak and Usowicz (1994), Marczewski and Usowicz (2005). The advantage of this method is that no corrections are needed for deviations from periodicity of the temperature wave of the investigated soil depths and changing water content does not constitute a limitation of this method. Besides, boundary conditions are easier to discharge than the damping depth method. Thus this method can be used to calculate thermal properties for every soil (with defined texture, amount of mineral and organic matter, and noted development of temperature and water content during measurement) under laboratory and field conditions. This method, however, does not include the soil structure as an important factor for the interpretation of the results.

The discussion above shows that both methods present advantages and limitations which have to be considered in future investigations if the thermal properties of the soil at different scales (in labor or on the field) have to be investigated.

6 Conclusions

The most important conclusions and observations derived from the presented work are:

- Formation of aggregates as a result of shrinkage and swelling processes result in an increase of contact points between them, an increase of the particle contact area, being the pathway for the heat flow.
- Water through formation of water films around the soil particles enlarges the contact area between them and the cross-sectional area which conducts the heat increases. Since aggregates with different forms and sizes may be formed, they affect the movement of water in soils and, consequently, their thermal properties
- The tillage treatments affect the soil thermal regime as follows:
 1. soil roughness and its loosening in conventional treatment is the reason for a decreasing amount of organic matter, aggregate stability, higher evaporation and smaller soil surface area which remains in contact with the atmosphere which in fact decreases heat conductivity and diffusivity,
 2. conservation tillage treatment presents higher water content, as the main factor which decides the magnitude of soil ability to transport and conduct heat, as well as plant and root distribution, their growth, presence and intensity of biological activity in the soil,
 3. if the soil structure in „Mulch“ is not annually destroyed, the macropores formed by earthworms and plant roots may provide pathways for water flow. Also the capillary pores persist and the capacity of soil to store the water is higher than in „Plough“, affecting, consequently its thermal behaviour.

- Soil structure influences its hydraulic and thermal properties. Different distribution and geometry of water menisci cause higher thermal conductivity in structured than in homogenized soil samples. Also an increase in bulk density increases the amount and number of grain contacts between soil particles which leads to higher thermal properties as well. This, however, causes a decrease of structural pores and of pore continuity which results in a retarded warming and longer cooling process as far as the movement of water content in soil becomes slower.
- Increase the air flow and of the air-filled pores in disturbed soils may create some air areas, which retain a very low heat capacity and conductivity of the air and act as isolation for the heat flow.
- Soil thermal properties depend on internal (wetting-drying processes, changes in k_i , k_u , k_f) and external (solar radiation, compaction) factors which influence their magnitude and which define them as time-dependant processes.
- Values of thermal diffusivity calculated with two methods differ from each other. This phenomenon, however, is not new and appears if various methods with different boundary conditions are used for calculations of defined properties.

7 Summary

Soil temperature is one of the most important factors governing the exchange of energy and mass between the soil and the atmosphere as well as evaporation and aeration. Biological processes, like uptake of water and nutrients by roots, decomposition of organic matter by microbes, germination, seedling emergence and plant growth strongly depend on soil temperature and its thermal properties. These processes as well as the soil thermal regime depend also on soil texture, structure, and further physical and chemical properties. An increase in use of large machines in agriculture increases the total weight and the axle loads applied to the soil and, consequently, the risk of soil compaction leading to its degradation is greater as well. The result of increasing soil compaction through the increase in bulk density improves its thermal properties. On the other hand, however, soil compaction causes a disruption of the soil pore connectivities and flow processes of soil solutions and gas diffusion is affected as well. In recent years discussion about global climate changes has increased, contributing at the same time to an increasing interest in the influence of temperature on different factors not only in the area of biological science but also in agricultural and geological sciences and industry as well. In order to investigate the thermal properties of soils, the aim of this research was (i) to assess if there are changes in soil hydraulic and thermal properties caused by different tillage systems (conventional and conservation system) and soil compaction, (ii) to compare thermal properties of undisturbed and disturbed soil samples prepared by different bulk densities and determined by two different methods (damping depth and statistical-physical model) and (iii) to determine the effect of bulk density on soil shrinkage and pore functions (k_f , k_u , k_l) relating them to soil thermal properties.

To determine the thermal behaviour of these soils, undisturbed and disturbed soil samples were taken at two depths of a Stagnic Luvisol derived from loess: 0-30cm and 30-60cm before and directly after wheeling. With the disturbed samples, soil volumes repacked by 2(3) bulk densities were prepared with the

Load Frame device. Additionally, temperature data measured at two depths on the field were used. These data were measured by the Sugar Beet Institute in Göttingen. Changes in soil thermal properties appearing as a result of different soil management as well as caused by soil compaction (uncompacted and compacted plots) were measured for both tillage treatments and plots. To calculate thermal properties of the soil, the development of volumetric water content (with TDR needles) and temperature (with pT 100 thermistors) during the simulation of the daily fluctuation of temperature were registered in laboratory and then the thermal conductivity, volumetric heat capacity and heat diffusivity were calculated following the damping depth method and the statistical-physical model. Since soil thermal properties depend on the water-air relationship, hydraulic properties such as pore volume and size distribution, soil shrinkage, air permeability and saturated hydraulic conductivity were measured in soil samples prepared from homogenized material and different bulk densities.

Estimated results show that different tillage systems as well as compaction influenced soil thermal as well as hydraulic properties. Conventional tillage treatment of annually disturbed soil surface decreases the amount of organic matter and aggregate stability and alters the heat flux through changes in soil roughness, which changes the area of the soil surface in contact with the atmosphere and in turn decreases heat conductivity. Conservational tillage treatment with more stable and better developed soil structure at a depth of 0-30cm which represents ploughing depth and decides differences between soil management presents higher water content as the main factor deciding soil thermal properties. According to the magnitude of volumetric water content conservational treatment presents greater values of thermal conductivity and volumetric heat capacity. Thermal diffusivity, however, is lower than under the conventional tillage treatment. From the latter we can conclude that under conservation tillage treatment the soil can store more heat, but at the same time and as a result of the lower thermal diffusivity, the atmospheric variations do not affect the soil thermal regime strongly. The rate of soil warming is worse compared with the conventional treatment, however, with increasing bulk

density, thermal properties increase as well. As a result of tillage practises bulk density increases leading to a decrease in the pore size distribution which in turn leads to a decrease in the shrinkage behaviour of the soil. This means that the water and air flow in the soil is retarded decreasing the heat flow in soils especially if air pockets, acting as isolators, are formed. These changes in thermal properties influence biological processes in soils affecting plant growth, microbiological activity and decomposition of organic matter.

Zusammenfassung

Die Bodentemperatur ist eine der wichtigsten Kenngrößen, die den Energie- und Massenfluss zwischen Boden und Atmosphäre steuern. Biologische Prozesse wie die Wasser- und Nährstoffaufnahme durch Pflanzen, die Mineralisation von organischer Substanz durch Mikroorganismen, Keimung, und Pflanzenwachstum sind stark von Bodentemperatur und thermischen Eigenschaften abhängig. Sowohl diese Prozesse als auch der Tagesgang der Temperatur wird durch die Korngrößenverteilung, Bodenstruktur, Porenvolumen, Porengrößenverteilung und Porenfunktionen beeinflusst. Durch die zunehmende Nutzung schwerer Maschinen in der Landwirtschaft sind die auf den Boden aufgetragenen Gesamtgewichte und Radlasten gestiegen, was zu einer zunehmenden Gefahr durch Bodendegradation insbesondere als Folge von Bodenverdichtung führt. Einerseits werden durch die Steigerung der Lagerungsdichte im Zuge der Bodenverdichtung die thermischen Eigenschaften des Bodens verbessert, andererseits führt die mechanische Störung des Bodens zu einer Verschlechterung von Porenkontinuität und Transportprozessen in Böden. In den letzten Jahren hat die Diskussion über „Global Climate Change“ zugenommen. Infolgedessen ist das Interesse an der Bedeutung der Bodentemperatur für verschiedene Bodeneigenschaften in der Landwirtschaft gestiegen. Gegenstand dieser Arbeit war die Untersuchung von thermischen Bodeneigenschaften mit dem Ziel (i) den Effekt von Bewirtschaftungssystemen (konventionell und konservierende Bodenbearbeitung) auf hydraulische und thermische Eigenschaften zu quantifizieren, (ii) die thermischen Eigenschaften (bestimmt durch 2 Methoden; „damping depth und statistical-physical Modell“) in gestörten und ungestörten Bodenproben bei verschiedenen Lagerungsdichten zu vergleichen und (iii) den Effekt der Lagerungsdichte auf das Schrumpfungsverhalten und Porenfunktionen des Bodens zu untersuchen und diese Vorgänge in Beziehung zu den thermischen Eigenschaften zu setzen.

Um die thermischen Eigenschaften des Bodens unter verschiedenen Bodenbearbeitungsvarianten und Lagerungsdichten bestimmen zu können,

wurden gestörte und ungestörte Proben aus 2 Bodentiefen einer Pseudogley-Parabraunerde aus Löss entnommen (0-30cm und 30-60cm vor und nach Befahrung). Anhand eines „Lastrahmens“ wurde gestörtes Bodenmaterial auf verschiedenen Lagerungsdichten vorverdichtet. Zusätzlich wurden aus dem Gelände gemessene Temperaturdaten (Institut für Zuckerrübenforschung in Göttingen) benutzt, um den Tagesgang der Bodentemperatur zu beschreiben, woraus thermische Eigenschaften insitu abgeleitet werden konnten. Für die Erfassung der Bodentemperatur und des Wassergehaltes im Labor wurden Temperaturfühler (pT 100 Thermistoren) und TDR Nadeln benutzt. Aus den gemessenen Daten wurde die Wärmeleitfähigkeit, Wärmekapazität und thermische Diffusivität bestimmt als Funktion des Wassergehaltes.

Die Ergebnisse lassen erkennen, dass Bodenbewirtschaftung und Lagerungsdichte die hydraulischen und infolgedessen auch die thermischen Eigenschaften des Bodens beeinflussen. Konventionelle Bearbeitung führt zu einer Abnahme der organischen Substanz, einer Verringerung der Aggregatstabilität und zu einer Unterbrechung des Wärmeflusses durch die Veränderung der Bodenrauigkeit an der Grenzfläche Boden-Atmosphäre. Konservierende Bodenbearbeitung verbessert und stabilisiert die Bodenstruktur und infolgedessen auch die Konduktivität und Wärmekapazität steigen. Die thermische Diffusivität hingegen wird kleiner und ist außerdem geringer als bei konventioneller Bodenbearbeitung. Daraus lässt sich schließen, dass unter konservierender Bodenbearbeitung einerseits die Böden mehr Wärme speichern können und andererseits atmosphärische Temperaturschwankungen sich aufgrund der geringen thermischen Diffusivität weniger stark auf den Wärmehaushalt im Boden auswirken. Die Erwärmungsgeschwindigkeit ist im Vergleich zur konventionellen Bodenbearbeitung gering, allerdings nehmen mit steigender Lagerungsdichte die thermischen Eigenschaften zu. Mit zunehmender Lagerungsdichte und je nach Bodenbearbeitung verändern sich außerdem die Porengrößenverteilung und das Schrumpfungsverhalten. Folglich wurde festgestellt, dass Wasser- als auch die Luftströmung verzögert und neu entstandene Lufträume hemmen, was zusätzlich den Wärmefluss hemmt.

Podsumowanie

Temperatura gleby jest jednym z najważniejszych czynników kontrolujących wymianę energii i masy pomiędzy glebą i atmosferą jak również ewaporację i napowietrzenie gleby. Procesy biologiczne jak pobieranie wody i nawozów przez korzenie roślin, rozkład materii mineralnej przez mikroby, kiełkowanie i wzrost roślin silnie zależy od temperatury gleby i jej termicznych właściwości. Te procesy, jak również termiczny stan gleby zależy również zarówno od jej tekstury, struktury jak i fizycznych i hydraulicznych właściwości. Wzrost stosowania dużych maszyn w rolnictwie zwiększa całkowitą wagę jak i również obciążenie osi kol których nacisk jest podawany do gleby i konsekwentnie, ryzyko obciążenia gleby prowadzące do jej degradacji jest także zwiększone. Skutkiem zwiększenia obciążenia gleby poprzez wzrost jej gęstości poprawia jej właściwości termiczne. Z drugiej strony jednak, powoduje przerwanie połączeń między porami co wpływa również na procesy przepływu substancji rozpuszczonych w wodzie jak i dyfuzję gazu. W ciągu ostatnich lat wzrosła dyskusja nad globalnymi zmianami klimatu, prowadząc w tym samym czasie do wzrostu zainteresowania wpływem temperatury na różne czynniki nie tylko w kręgach naukowych zajmujących się biologią, ale również w rolnictwie, geologii i przemyśle. W celu zbadania właściwości cieplnych gleb, celem tych badań było (i) wykazanie czy istnieją zmiany w hydraulicznych i termicznych właściwościach powodowane przez różne systemy uprawy (orkowy i bezorkowy system) i obciążenie gleby, (ii) porównanie właściwości termicznych próbek glebowych z nienaruszoną strukturą i próbek przygotowanych ze zhomogenizowanej gleby i różnych wartości gęstości objętościowej przy zastosowaniu dwóch różnych metod obliczeń (damping depth i modelu fizyczno-statycznego) jak i (iii) wyznaczenie efektu gęstości objętościowej na kurczenie się gleby i funkcje porów (k_f , k_u , k_i) i odniesienie ich do właściwości termicznych gleb.

W celu określenia zachowania termicznego tych gleb, przygotowano próbki z gleba zhomogenizowaną jak również próbki z nienaruszoną gleba były pobrane z dwóch głębokości: 0-30cm i 30-60cm ze Stagnic Luvisol pochodzącego z lesu

przed i bezpośrednio po przejechaniu parcel sprzętem żniwnym. Próbki ze zhomogenizowaną glebą z dwoma gęstościami objętościowymi przygotowane były za pomocą urządzenia Load Frame device. Dodatkowo, temperatura mierzona w warunkach polowych na dwóch głębokościach była także uwzględniona. Dane udostępnione były przez Instytut Buraków Cukrowych w Göttingen. Zmiany właściwości termicznych pojawiające się jako rezultat różnych upraw gleb jak również spowodowane poprzez obciążenie gleby (nieobciążone i obciążone parcele) były mierzone dla dwóch typów upraw i parceli. W celu obliczenia właściwości cieplnych gleby, przebieg objętościowej zawartości wody (igłami TDR) i temperatury (termistorami pT 100) podczas symulacji dziennych fluktuacji temperatury były rejestrowane w warunkach laboratoryjnych, a następnie objętość cieplna, dyfuzyjność cieplna i konduktywność cieplna były obliczone za pomocą metody damping depth method i statystyczno-fizycznego modelu. Od kiedy termiczne właściwości gleby zależą od stosunków wodno-powietrznych, właściwości hydrauliczne jak objętość porów i rozkład ich wielkości, kurczenie gleby, przepuszczalność powietrzna i nasycona przepuszczalność hydrauliczna były pomierzone na próbkach przygotowanych ze zhomogenizowanego materiału i różnych gęstości objętościowych.

Otrzymane wyniki wykazały, że zarówno różne typy upraw jak i obciążenie gleby wpływa na termiczne jak i hydrauliczne właściwości gleb. Uprawa orkowa ze względu na niszczone każdego roku powierzchnie gleby obniża ilość materii organicznej, stabilność agregatów i wpływa na przepływ strumienia ciepła poprzez zmiany w chropowatości gleby, co zmienia obszar powierzchni gleby będący w kontakcie z atmosferą i w rezultacie obniża konduktywność termiczną. Bezorkowa uprawa z bardziej stabilną i lepiej rozwiniętą strukturą gleby na głębokości 0-30cm która reprezentuje głębokość uprawy (plugowania) i decyduje o różnicach między uprawą gleby prezentując wyższą zawartość wody będącą głównym czynnikiem decydującym o termicznych właściwościach gleb. Odnosząc do wielkości θ , uprawa nieorkowa wykazuje większe wartości konduktywności cieplnej i objętości cieplnej. Dyfuzyjność cieplna jednakże, jest niższa niż pod uprawą orkową. Z tych zależności można wnioskować że gleby

pod uprawą nieorkową może gromadzić więcej ciepła, ale w tym samym czasie jako wynik niższej dyfuzyjności zmiany atmosferyczne mają tu mniejszy wpływ na wartości bilansu cieplnego. Szybkość ogrzewania się gleby jest gorsza niż w uprawie bezorkowej, jednakże ze wzrostem gęstości objętościowej właściwości termiczne wzrastają. Na skutek zabiegów agrotechnicznych i wzrastającej gęstości objętościowej, rozkład wielkości porów jak i kurczenie gleby maleje. To oznacza, że przepływ wody i powietrza jest utrudniony, prowadząc do zmniejszonego przepływu ciepła, szczególnie jeżeli formowane są przestrzenie wypełnione powietrzem, działające jako izolator dla przepływu ciepła. Te zmiany we właściwościach cieplnych wpływają na biologiczne procesy w glebie i w rezultacie na wzrost roślin, aktywność mikrobiologiczną i rozkład materii organicznej.

8 Literature

- Abu-Hamdeh, N. A. and R. C. Redder. (2000): Soil thermal conductivity: Effects of density, moisture, salt concentration and organic matter. *Soil. Sci. Soc. Am. J.* 64: 1285-1290.
- A G Boden. (1994): *Bodenkundliche Kartieranleitung*, 4. Aufl., Hannover.
- Ahuja, L. R., F. Fiedler., G. H. Dunn., J. G. Benjamin, and A. Garrison. (1998): Changes in soil retention curves due to tillage and natural reconsolidation. *Soil. Sci. Soc. Am. J.* 62: 1228-1233.
- Allen, R. G., Smith, M., Perrier, A. and Pereira, L. S. (1994): An update for definition of reference evapotranspiration. *ICID Bulletin* 43, No. 2: 1-34.
- Allmaras, R. R., W. W. Nelson and E. A. Hallauer (1972): Fall vs spring plowing and related heat balance in western Corn Belt. *Minn. Agric. Exp. Stn. Tech. Bull.* P 283.
- Allmaras, R. R., E. A. Hallauer, W. W. Nelson, and S. D. Evans. (1977): Surface energy balance and soil thermal property modifications by tillage induced soil structure. *Minn. Agric. Exp. Stn. Tech. Bull.* 306 P.
- Amoozegar., A. (1988): Preparing soil cores collected by a sampling probe for laboratory analysis of soil hydraulic properties. *Soil. Sci. Soc. Am. J.* 52: 1814-1816.
- Anandakumar. K., R. Venkatesan., and T. V. Prabha. (2001): Soil thermal properties at Kalkappan in coastal south India. *Proc. Indian Acad. Sci.*,110, No3: 239-245.
- Ankeny, M. D., T. C. Kaspar, and M. A. Prieksat. (1995): Traffic effects on water infiltration in chisel-plow and no-till systems. *Soil. Sci. Soc. Am. J.* 59: 200-204.
- Arshad, M. A. and R. H. Azzoz. (1996): Tillage effects on soil thermal roperties in a semiarid cold region. *Soil. Sci. Soc. Am. J.* 60: 561-567.
- Asrar, G. and E.T. Kanemasu. (1983): Estimating thermal diffusivity near the soil surface using Laplace transform: uniform initial conditions. *Soil. Sci. Soc. Am. J. Vol.* 47: 397-402.
- Azzoz, R. H. and Arshad, M. A. (1995): Tillage effect on thermal conductivity of two soils in Northern British Columbia. *Soil. Sci. Soc. Am. J.* 59: 1413-1423.
- Bachmann et al., J. (1997): Thermisches verhalten der Böden. In: Blume, H.P., Felix Henningsen, W. R. Fisher, H.-G. Frede, R. Horn and K.Stahr (Hrsg.): *Handbuch der Bodenkunde* , 2, Ecomed, Landsberg/Lech, 1-40.
- Ball, B. C., D. J. Campbell., J. T. Douglas., J. K. Henshall, and M. F. O'Sullivan. (1997): Soil structural quality, compaction and land management. *Eur. J. of Soil Sci.* 48: 593-601.

- Ball, B. C., O'Sullivan, M. F. and R. Hunter (1988): Gas diffusion, fluid flow and derived pore continuity indices in relation to vehicle traffic and tillage. *J. of Soil Sci.* 32: 327-339.
- Bohne, K. (2005): An introduction into applied soil hydrology. Lecture notes in Geo Ecology, Catena Verlag GMBH, 35447 Reiskirchen, Germany.
- Boivin, P., P. Garnier, , and Tessier, D. (2004): Relationship between clay content, clay type, and shrinkage properties of soil samples. *Soil. Sci. Soc. Am. J.* 68:1145-1153.
- Bristow, K. L., Gaylon. S. Campbell and Kees Callissendorf. (1993): Test of a heat-pulse probe for measuring changes in soil water content. *Soil Sci. Soc. Amer. J.* 57:930-934.
- Bristow, K. L., G.L. Kluitenberg and R. Horton (1994): Measurement of soil thermal properties with a dual –probe heat pulse technique. *Soil Sci. Soc. Amer. J.* 58: 1288-1294.
- Burrows, W. C., and W. E. Larson., (1962): Effect of amount of mulch on soil temperature and early growth of corn. *Agron. Journal.* 54:19-23.
- Cambell, G. S., C. Calissendorf and J. H. Williams. (1991): Probe for measuring soil specific heat using a heat- pulse method. *Soil Sci. Soc. Amer. J.* 55:291-293.
- Cambell, G. S. (1985): Soil physics with basic – transport models for soil–plant systems. Elsevier-Amsterdam.
- Chacko, T. and P. G. Renuka. (2002): Temperature mapping, thermal diffusivity and subsoil heat flux at Kariavattomof Kerala. *Proc. Indian Acad. Sci. (Earth Planet. Sci.)*, 111, No. 1, pp.79-85.
- Deutscher Verband für Wasserwirtschaft und Kulturbau e. V. (DVWK) (1996): Ermittlung der Verdunstung von Land- und Wasserflächen. Bearbeitet vom DVWK – Fachausschuss „Verdunstung“. Bonn. 135 P.
- De Vries, D. A. (1996): Thermal Properties of Soil. In: Van Wijk, W. R. (Hrsg.): *Physics of plant Environment*. North-Holland Publishing Company, Amsterdam: 210-235.,3.
- Dexter, A. R. (2004): Soil physical quality. Part I. Theory, effects of soil texture, density, and organic matter, and effect on root growth. *Geoderma* 120, 201-214.
- Dörner, J. (2005): Anisotropie von Bodenstrukturen und Porenfunktionen in Böden und deren Auswirkungen auf Transportprozesse im gesättigten und ungesättigten Zustand. Dissertation, Kiel, 182 P. ISSN 68.
- Ehlers, W. (1973): Gesamtporenvolumen und Porengrößenverteilung in unbearbeiteten und bearbeiteten Lösböden. *Zeitschrift für Pflanzenernährung und Bodenkunde* 134: 193-206.
- Elimoel, A. Elias, R. Cichota, H. H. Torriani and Q. de Jong van Lier. (2994): Analytical soil- temoperature model: Correction for temporal variation of daily amplitude. *Soil Sci. Soc. Amer. J.* 68:784-788.

- Fazekas, O. (2005): Bedeutung von Bodenstruktur und Wasserspannung als stabilisierende Kenngrößen gegen intensive mechanische Belastungen in einer Parabraunerde aus Löss unter Pflug- und „Mulch“saat. Dissertation, Kiel, 170 P. ISSN 67.
- Flint., A. L., S. W. Childs., (1986): Field procedure for estimating soil thermal environments. *Soil Sci. Soc. Amer. J.* 51:1326-1331.
- Fuhrer, O. (2000): Inverse Heat Conduction in Soils- A New Approach Towards Recovering Soil Moisture from Temperature Records. Diploma Thesis. ETH, Zurich, Dept. Physics
- Fuhrer, O. (2000): The effect of soil moisture on the thermal properties of soils.
- Ghuman, B. S., R. Lal., (1985): Thermal conductivity, thermal diffusivity, and thermal capacity of some nigerian soils. *Soil Science*. Vol.139, No.1: 74-80.
- Hadas, A. (1968): A comparison between two methods of determining the thermal diffusivity of a moist soil. *Soil. Sci. Soc. Am. Proc.* 32: 28-30.
- Hadas, A. (1977): Heat transfer in dry aggregated soil: I. Heat conduction. *Soil Sci. Soc. Am. J.* 41. 1055-1059.
- Hanks, R.J. and Ashcroft, G.L. (1980): *Applied Soil Physics*. Springer ISBN. Berlin, New York.
- Hanks, R. J., D. D. Austin and W.T. Ondrechen. (1971): Soil temperature estimation by a numerical method. *Sci. Soc. Am. J. Vol.* 35, 665-667.
- Hartge, K.H. (1984): Vergleich der Verteilungen der Wasserleitfähigkeit und des Porenvolumens von waagrecht und senkrecht entnommenen Stehcylinderproben. *Zeitschrift für Pflanzenernährung und Bodenkunde* 147: 316-323.
- Hartge, K.H. and R. Horn (1989): *Die physikalische Untersuchung von Böden*. Stuttgart, Enke, 177 P.
- Hartge, K. H. and R. Horn (1999): *Einführung in die Bodenphysik*. Enke, Stuttgart, 304 P.
- Hasan, K. Q., and P. J. Zinke. (1964): The influence of vegetation on soil thermal regime at the san dimas lysimeters. *Soil Sc. Soc. Proc. Division S-7*: 703-706.
- Hay, R. K. M., J. C. Holmes and E. A. Hunter (1978): The effect of tillage, direct drilling and nitrogen fertilizer on soil temperature under a barley crop. *J. Soil Sci.* 29: 174-183.
- Hill, R. L. (1990): Long-term conventional and no-tillage effect on selected soil physical properties. *Soil. Sci. Soc. Am. J.* 54: 161-166.
- Hillel, D. (1998): *Environmental Soil Physics*. Academic Press, London, 771 P.
- Hopmans, J. W., and J. H. Dane. (1986): Thermal conductivity of two porous media as a function of water content, temperature, and density. *Soil Science*. Vol. 142.

- Horn, R. (1993): Mechanical properties of structured unsaturated soils. *Soil Technology*, 6, 47-75.
- Horn, R. (1994): Effect of aggregation of soils on water, gas, and heat transport, in Schulze, E.D. (ed.): *Flux control in biological systems*. Academic Press, San Diego, CA, USA, pp. 335-364.
- Horn, R., H. Taubner., M. Wuttke., and T. Baumgartl. (1994): Soil physical properties related to soil structure. *Soil & Till. Research*. 30: 187-216.
- Horn, R., and T. Baumgartl. (1999): Dynamic properties n structured soils. p. A19-A51. In M. Sumner (ed.) *Handbook of soil science*. CRC Press, Boca Raton, FL.
- Horton, R., P. J. Wierenga. (1983): The effect of column wetting on soil thermal conductivity. *Soil Sci. Vol. 138, No.2:102-108*.
- Horton, R. (1989): Canopy shading effect on soil heat and water flow. *Soil Sci. Soc. Amer. J.* 53: 669-679.
- Horton, R., Bachmann et al., J.,T. Ren and R. R. van der Ploeg. 2001. Comparison of the thermal properties of four wettable and four water-repellent soils. . *Soil Sci. Soc. Amer. J.* 65:1675-1679.
- Jaeger, J. C. and J. H. Sass (1964): A line source method for measuring the thermal conductivity and diffusivity of cylindrical specimen of rock and other poor conductors. *Brit. J. Appl. Phys.* 15: 1187-1194.
- Janse, A. R. P. and G. Borel (1965): Measurement of thermal conductivity in situ in mixed materials, e.g., soils. *Neth. J. Agr. Sci.* 13: 57-62.
- Kaune, A., T. Türk and R. Horn (1993): Alteration of soil thermal properties by structure formation. *J. of Soil Sci.* 44, 231-248.
- Keith, A. Smith and Ch. E. Mullins (1991): *Soil analysis- physical methods*. 538 P. New York.
- Kmoh, H. G. und Hanus (1965): Vereinfachte Methodik und Auswertung der Permeabilitätsmessung des Bodens für Luft. *J. Plant Nutr. Soil Sci.* 111 (1): 1-10.
- Kohnke, H. (1968): *Soil physics*. McGraw-Hill, New York
- Kowalik, P. (1999): *Ochrona Środowiska Glebowego*. Wydanie Politechniki Gdańskiej. 72 P. ISBN 83-88007-07-6.
- Kowalik, S. (2004): *Zagadnienie z gleboznawstwa dla studentów inżynierii środowiska*. Uczelniane wydawnictwa naukowo-dydaktyczne, Kraków.120 P. ISSN 0239-6114.
- Licht, M. A., M. Al-Kaisi., (2005): Strip-tillage effect on seedbed soil temperature and other soil physical properties. *Soil & Tilage Research*. 80: 233-249.
- McNabb, D. H., A. D. Startsev, and H. Nguyen. (2001): Soil wetness and traffic effect levels on bulk density and air- field porosity of compacted boreal forest soils. *Soil. Sci. Soc. Am. J.* 65: 1238-1247.

- Malicki, M. A. (1996): Elektryczny pomiar wilgotności i zasolenia gleby z zastosowaniem techniki elektrometrycznej (TDR). Zeszyty problemowe postępow nauk rolniczych z. 429, 215-221.
- Marczewski, W., and B. Usowicz., (2005): Distribution of soil thermal properties in a field with black fallow and grass cover. *Acta Agrophysica*. Lublin, Vol. 5., No. 3: 745-757. ISSN 1234-4125.
- Nidal, H. Abu-Hamdeh., and R. C. Reeder. (2000): Soil thermal conductivity-effect of density, moisture, salt concentration, and organic matter. *Soil Sci. Soc. Am. J.* 64: 1285-1290.
- Nidal, H. Abu-Hamdeh. (2000): Effect of tillage treatments on soil thermal conductivity for some Jordanian clay loam and loam soils. *Soil and Tillage Research*, 56: 145-151.
- Nimmo, J. R. and K. C. Akstin (1988): Hydraulic conductivity of a sandy soil at low water content after compaction by various methods. *Soil Sci. Soc. Am. J.* 52: 303-310.
- Nofziger, D.L. and Wu. J (2002): Soil temperature variations with time and depth. Research Associate, Department of Plant and Soil Science, Oklahoma State University, Stillwater, OK 74078.
- Oliviera, I. B., A. H. Demond and A. Salehzadeh (1996): Packing of sands for the production of homogenous porous media. *Soil Sci. Soc. Am. J.* 60: 49-53.
- Parker, J. C., D. F. Amos and L. W. Zelazny. (1982): Water adsorption and swelling of clay minerals in soil system. *Soil Sci. Soc. Am. J.* 46: 450-456.
- Parker, J. C., D. F. Amos, and D. L. Kaster. (1977): An evaluation of several methods of estimating soil volume change. *Soil Sci. Soc. Amer. J.* 41: 1059-1064.
- Peng, X., R. Horn., A. Smucker and S. Peth (2005): Improving measurement of soil shrinkage in 2D with the aid of image analysis. *Catena*, in press.
- Peng, X. and Horn R. (2005): Modelling soil shrinkage curve across a wide range of soil types. *Soil Sci. Soc. Amer. J.* 69: 584-592.
- Peth, S. (2004): Bodenphysikalische Untersuchungen zur Trittbelastung von Böden bei der Rentierweidewirtschaft an borealen Wald- und subarktisch-alpinen Tundrenstandorten. Dissertation. Kiel, 160 P. ISSN 64.
- Philips, R. E., D. Kirkham., (1962): Soil compaction in the field and corn growth. *Agronom. Journal.* 54: 29-34.
- Potter, K. N., R. M. Cruse and R. Horton (1985): Tillage effect on soil thermal properties. *Soil Sci. Soc. Amer. J.* 49: 968-973.
- Radke, J. K., (1982): Managing early season soil temperatures in the northern corn belt using configured soil surfaces and mulches. *Soil. Sci. Soc. Amer. Journal.* 46: 1067-1071.

- Richard, G., Cousin, I., Sillon, J. F., Bruand, A., Guerif, J. (2001): Effect of compaction on the porosity of a silty soil: influence on unsaturated hydraulic properties. *Eur. J. Soil Sci.* 52, 49-58.
- Richard, G., Sillon, J. F., and O.Marloie. (2001): Comparison of inverse and direct evaporation methods for estimating soil hydraulic properties under different tillage practices. *Soil Sci. Soc. Amer. J.* 65: 215-224.
- Ripple, C. D., R. V. James, and J. Rubin (1973): Radial particle-size segregation during packing of particulates into cylindrical containers. *Powder Technol.* 8: 165-175.
- Scheffer/Schachtschabel (2002): *Lehrbuch der Bodenkunde*. Blume, H-P., G. W. Brümmer, U. Schwertmann, R. Horn, I. Kögel-Knabner, K. Stahr, K. Auerswald, L. Beyer, A. Hartmann, N. Litz, A. Scheinost, H. Stanjek, G. Welp and B.-M. Wilke. 15.Aufl., Spektrum Akademischer Verlag, Berlin, 593 P.
- Schiegg, H. O. (1990): Laboratory setup and results of experiments of two-dimensional multiphase flow in porous media. (Engl. Transl.). Rep. DE-AC06-76RLO1830. U. S. Dep. Of Energy, Washington, DC.
- Schäfer-Landefeld, L., R. Brandhuber., S. Fenner., H. J. Koch, and N. Stockfisch. (2004): Effect of agricultural machinery with high axle load on soil properties of normally managed fields. *Soil & Tillage Research*, 75: 75-86.
- Schulte im Walde, W., H. G. Frede and M. Meyer (1976): Wärme-Leitfähigkeits/Wassergehalts-Charakteristiken einer Griserde aus Würm-Löss and die Anwendung der WLF-Methode bei der kontinuierlichen Verfolgung infiltrativer und eveporativer Wassergehaltsänder. *Göttinger Bodenkundliche Berichte*. 44:53-130.
- Selim. H. M. and don Kirkham. (1970): Soil temperature and water content changes during drying as influenced by cracks: a labolatory experiment. *Soil Sci. Soc. Amer. J.* 565- 569.
- Šimůnek, J., M. Šenja und M. Th. van Genuchten (2003): *The Hydrus 2D Software Package for Simulating the Two – Dimensional Movement of Water, Heat, and Multiple Solutes in Variably – Saturated Media*. Version 2.102. U.S. Salinity Laboratory, U.S. Department of Agriculture, Agricultural Research Service, Riverside, California. 227 S.
- Tigges, U. (2000): Untersuchungen zum mehrdimensionalen Wassertransport unter besonderen Berücksichtigung der Anisotropie der hydraulischen Leitfähigkeit. Dissertation, Kiel. 145 P. ISSN 56.
- Tyson, E. Ochsner, R. Horton and Tusheng Ren. (2001): A new perspective on soil thermal properties. *Soil Sci. Soc. Amer. J.* 65: 1641-1647.
- Usovicz, B. (1991): Studies on the dependence of soil temperature on its moisture in field. Ph. D. Thesis (in Polish). Academy of agriculture, Lublin.

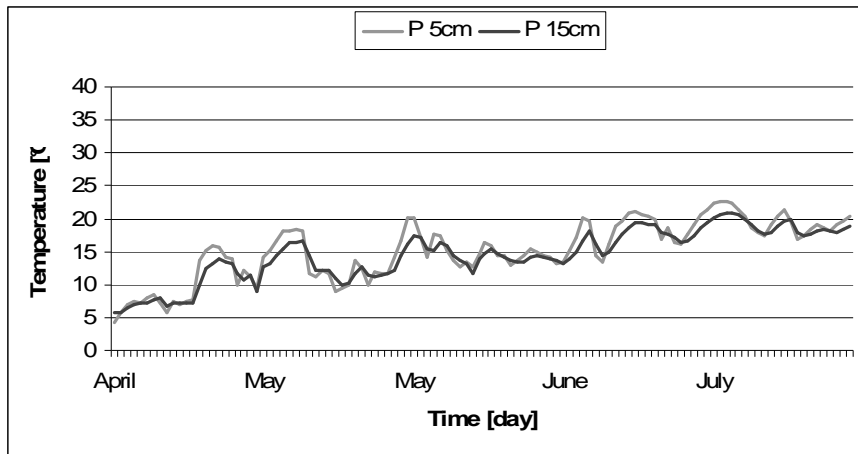
- Usovicz, B. (1992): Statistical-physical model of thermal conductivity in soil. Polish journal of soil Science. Vol.XXV/1. PL ISSN 0079-2985.
- Usovicz, B. (2000): Statystyczno – fizyczne modele przepływu masy i energii w osrodku porowatym. Lublin, Acta Agrophysica. ISSN 1234 – 4125.
- Usovicz, B. and L. Usovicz. (2001): Thermal conductivity of soils- comparison of experimental results and estimation methods. Acta Agrophysica, Lublin. 10 P.
- Usovicz, B. (2002): Szacowanie cieplnych właściwości gleby. Acta Agrophysica, Lublin. 72, 135-165.
- Usovicz, B. (2005): Rozkład właściwości cieplnych gleby na czarnym ugorze i pod murawą. Acta Agrophysica, Lublin. 11 P.
- Van Eimer, and H. Häckel. (1979): Wetter- und Klimakunde für Landwirte, Gärtner, Winzer und Landschaftspfläger. Ein Buch der Agrarmeteorologie. Eugen Ulmer, Stuttgart. 269 P.
- Van Genuchten, M.Th (1980): closed – form equation for predicting the hydraulic conductivity of unsaturated soils. Soil Sci. Soc. Amer. J. 44: 892-898.
- Van Genuchten, M.Th., F.J. Leij and S.R. Yates., (1991): The RETC Code for Quantifying the Hydraulic Functions of Unsaturated Soils. Version 6.0. US Salinity Laboratory, USDA, ARS. Riverside, California.
- Van Wijk, W.R. and W. J. Derksen (1996): Sinusoidal Temperature Variation in a Layered Soil. In: Van Wijk, W. R. (Hrsg.): Physics of plant Environment. North-Holland Publishing Company, Amsterdam: 171-207.
- Van Wijk, W.R. and D. A. De Vries (1996): Periodic Temperature Variations in a Homogenous Soil. In: Van Wijk, W. R. (Hrsg.): Physics of plant Environment. North-Holland Publishing Company, Amsterdam: 102-143.
- Van Wijk, W.R. and D. W. Scholte Ubing (1996): Radiation. In: Van Wijk, W. R. (Hrsg.): Physics of plant Environment. North-Holland Publishing Company, Amsterdam: 62-101.
- Walczak, R., and B. Usovicz., (1994): Variability of moisture, temperature and thermal properties in bare soils and in crop field. Intern. Agrophysics. Lublin, Vol. 8 (1), pp. 161-168.
- Wierenga, P. J., D.R. Nielsen and R.M. Hagan (1969): Thermal properties of a soil based upon field and laboratory measurements. Soil. Sci. Soc. A. Proc., Vol. 33.
- Zawadzki, S., B. Dobrzański., S. Kowaliński., T. Skawina., F. Kuźnicki., (1999): Gleboznawstwo. Podrecznik dla studentow. Wydanie IV poprawone i uzupelnione. Panstwowe Wydawnictwo Rolnicze i Lesne. Warszawa, 559 P. ISBN 830901703-0.

Appendix

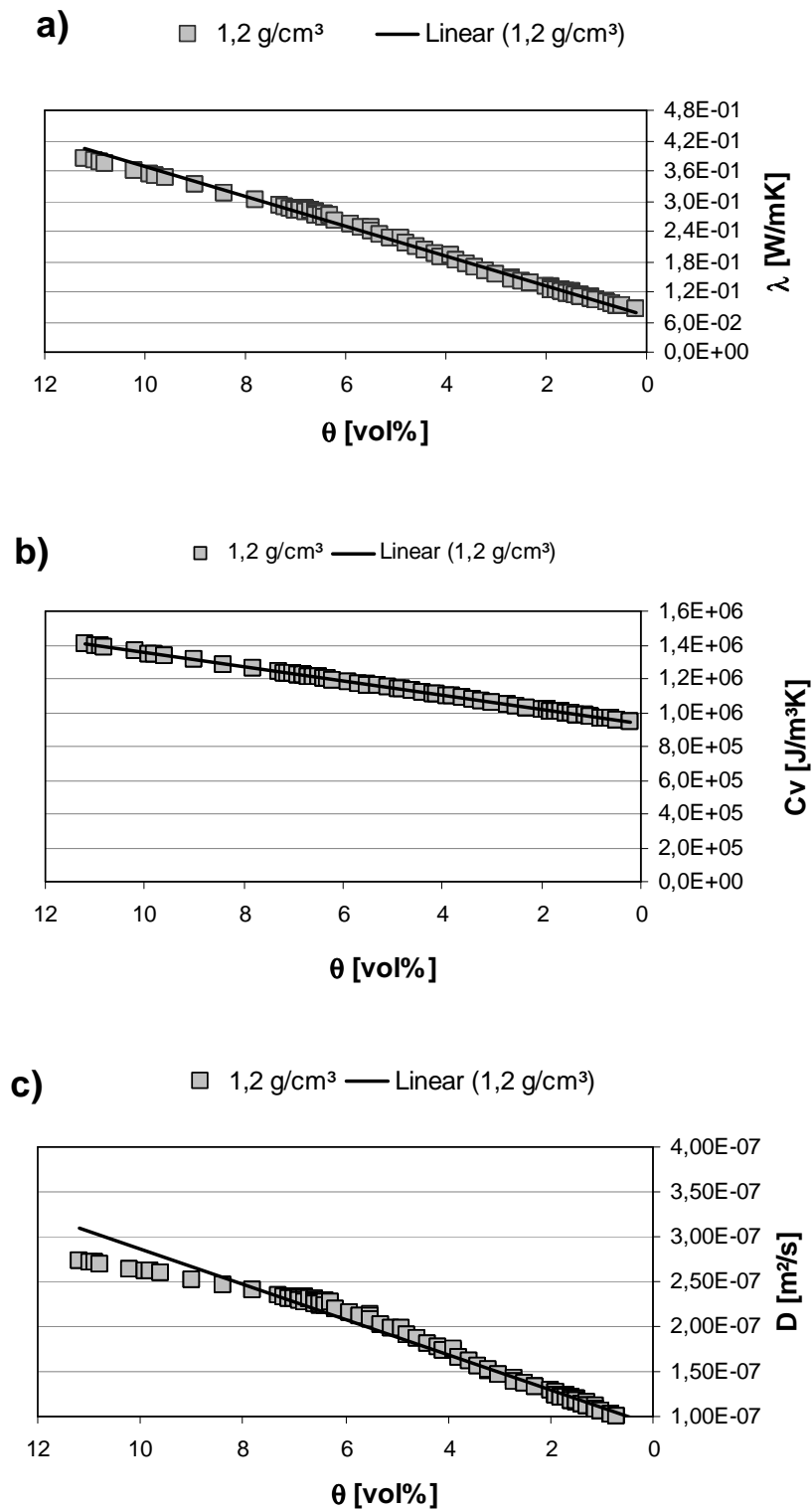
Appendix

Appendix A General minimum (T_{min}) and maximum (T_{max}) temperature, months with maximal temperature and amplitude in these periods ($Ampl_{max}$), average temperature (T_{av}) in the remaining period and average amplitude ($Ampl_{av}$) in this time period. Presented values are for years 1995, 1997-2000; in months April- August.

Year	Till. treat., depth [cm]	T_{min} [°C]	T_{max} [°C]	Month with T_{max}	$Ampl_{max}$ [°C]	T_{av} [°C]	$Ampl_{av}$ [°C]
1995	M5	3,6	29,4	VI, VII	6,5- 12	8,0- 22	12- 19
	P5	3,0	30,7	VI, VII	5,7- 11	8,7- 23,2	12,7- 19,6
	M15	7,8	23,6	VI, VII	2,2- 3,4	10- 16	1,3- 2,4
	P15	8,4	21,7	VI, VII	1,4- 2,2	9,6- 15	1,0- 1,5
1997	M5	0,2	36,7	V, VI	10- 17	14- 24	5,1- 7,7
	P5	0,5	32,6	V, VI	11- 12,3	15- 22	4,0- 6,6
	M15	4,7	22,4	V, VI	1,0- 2,7	16,4- 19,2	1,0- 1,6
	P15	5,5	22,6	V, VI	1,1- 2,7	16,6- 20	1,1- 1,3
1998	M5	1,15	29,6	V, VI	10- 11	13- 22	1,8- 4,5
	P5	1,5	32,1	V, VI	13- 17	13- 22	1,4- 4,1
	M15	5,25	19,8	V, VI	2,0- 2,4	13,8- 18,7	0,5- 0,7
	P15	5,65	19,7	V, VI	1,6- 3,5	13,8- 18,7	0,7- 0,9
1999	M5	2,95	31,3	V, VI	5,9- 16,6	16- 24	5,0- 7,0
	P5	1,85	32,6	V, VI	6,0- 18	15- 23	5,5- 7,0
	M15	5,35	23,35	V, VI	3,0- 5,0	16,5- 20	1,6- 2,6
	P15	5,3	23,55	V, VI	3,0- 5,0	16- 19	1,6- 2,6
2000	M5	4,1	30,8	V, VI	10,5- 16	12,5- 20,5	3,7- 5,0
	P5	3,25	32,2	V, VI	10,5-16	12- 20,5	3,7- 5,0
	M15	6,2	24,55	V, VI	3,7-7,8	14- 19	1,2- 1,9
	P15	5,75	25,6	V, VI	3,7-7,8	13,8- 18,8	1,2- 1,9



Appendix B Temperature at 5 and 15cm depth under „Mulch“ treatment from April to July 1995.



Appendix C a) Thermal conductivity (λ), b) volumetric heat capacity (C_v) and c) thermal diffusivity (D) as a function of water content (θ) for samples prepared from homogenized material and bulk density 1,2g/cm

Thanks

I would like to thank Prof. Dr. Rainer Horn for giving me the chance to realize this project in his Institute and for his invaluable assistance and support.

Panu Profesorowi Witoldowi Stępniewskiemu, dzięki któremu zainteresowałam się gleboznawstwem dziękuję za pomoc naukową i mile spędzony czas podczas jego wizyt w Kiel.

I'm grateful to all people from the Sugar Beet Institute in Göttingen for cooperation during the sampling time and especially to Dr. Heinz-Josef Koch.

I would also to give thanks to all workers and PhD students for the amiable atmosphere at work. Moreover I would like to thank to Dr. José Dörner, Dr. Orsolya Fazekas and Dr. Stephan Peth for their inestimable pieces of advice and suggestions toward my work.

Najserdeczniejsze i największe podziękowania kieruję w stronę moich rodziców i was Anetko, Sylwko i Grzesiu za waszą wiarę we mnie i nieustanne wsparcie w trudnych chwilach. Bez was nie poradziłabym sobie i nie wytrzymała do końca. Dziękuję!!!

My greatest thanks go to José, Orsi and Stefan and all Polish students I have meet in our institute. Conversations with you opened up new horizons to me, going beyond the "scientific" and make the time at work more pleasant. Special thanks are directed toward my P. M. (Asia, Justyna, Kasia) for your dear friendship, support and all crazy things we have done together it would have been difficult without you. I am happy to have met you. Te P. L. II. estoy agradecida por todo!!

Every scientific work is difficult to realize without financial support. Therefore, I would like to thank the Promotion of Scientific and Artist Young Researchers of Christian-Albrechts-University in Kiel for the financial support.

Curriculum vitae

Personal data:

Name: Dorota Agnieszka Dec
Date of birth: 04.03.1978
Place of birth: Nisko, Poland
Nationality: Polish
Marital status: single

School education:

1984-1992 Primary school in Leżajsk
1992-1996 B. Chrobry's Secondary school

Study:

1996-2002 Technical University of Lublin

Occupational activity:

2003-2006 Scientific assistant in the Institute for Plant
Nutrition and Soil Science at the Christian
Albrecht University in Kiel
2006 Promotion

